A SEDIMENTOLOGIC, SEQUENCE STRATIGRAPHIC, AND ICHNOLOGIC CHARACTERIZATION OF THE CRETACEOUS U AND M2 SANDSTONE MEMBERS, NAPO FORMATION, ORIENTE BASIN OF ECUADOR

A Thesis Submitted to the
College of Graduated and Postdoctoral Studies
In Partial Fulfillment of the Requirements
For the Degree of Master of Science
In the Department of Geological Sciences
University of Saskatchewan
Saskatoon

By

MAYRA ALEJANDRA ZUNIGA ALBUJA

PERMISSION TO USE

In presenting this thesis in partial fulfillment of the requirements for a Postgraduate degree from the University of Saskatchewan, I agree that the Libraries of this University may make it freely available for inspection. I further agree that permission for copying of this thesis in any manner, in whole or in part, for scholarly purposes may be granted by the professor or professors who supervised my thesis work or, in their absence, by the Head of the Department of the Dean of the College in which my thesis work was done. It is understood that any copying or publication or use of this thesis or parts thereof for financial gain shall not be allowed without my written permission. It is also understood that due recognition shall be given to me and to the University of Saskatchewan in any scholarly use which may be made of any material in my thesis.

Requests for permission to copy or to make other use of material in this thesis in whole or part should be addressed to:

Head

Department of Geological Sciences

University of Saskatchewan

114 Science Place

Saskatoon, Saskatchewan, S7H 5E2, Canada

Dean

College of Graduate and Postdoctoral Studies

University of Saskatchewan

116 Thorvaldson Building, 110 Science Place

Saskatoon, Saskatchewan, S7N 5C9, Canada

ABSTRACT

The Upper Cretaceous M2 and U Sandstone members of the Napo Formation are prolific hydrocarbon producers in the Oriente Basin, Ecuador. To understand the depositional origin of these reservoirs, a detailed sedimentologic, sequence-stratigraphic, and ichnologic study was performed, using 490 ft (ca. 149 m) of conventional core from six wells. Sedimentary facies, stratal stacking pattern, discontinuity surfaces, and trace fossils were documented. Nine lithofacies, two depositional sequences in each member, and depauperate and fully marine ichnofacies were identified. Both members present evidence of tidal (e.g. mudstone drapes on bedforms, double mudstone layers, flaser, wavy, and lenticular bedding, and thick-and- thin alternations of siltstone and claystone layers) and river (e.g. hyperpycnal flow deposits) influence. The shoreline was trending northeast-southwest within the study area and the predominant sediment source came from cratonic areas located to the east.

In the study area, the U Sandstone Member represents three main broad environments: fluvial, estuarine, and deltaic. The base of the U Sandstone Member marks the base of depositional sequence 1 (DSU1), representing a subaerial unconformity formed as a result of valley incision during a relative fall of sea level. DSU1 comprises the lower and middle intervals and the lower part of the upper interval. DSU1 consists of lowstand moderate-sinuosity fluvial deposits, followed by transgressive estuarine deposits and highstand mixed tide- and river-influenced deltaic deposits. A subaerial unconformity marks the base of depositional sequence 2 (DSU2), which was followed by renewed lowstand fluvial deposition within an incised valley in the more proximal areas and transgressive estuarine sedimentation. DSU2 is recorded in the upper part of the upper interval. Trace fossils in the U Sandstone Member are recorded in the estuarine and deltaic deposits; fluvial deposits present sparse bioturbation. The depauperate *Skolithos* and *Cruziana* ichnofacies are commonly present in the estuarine and deltaic deposits, recording brackish-water conditions.

The M2 Sandstone Member records sedimentation in a mixed tide- and river-influenced deltaic environment, encompassing delta front and prodeltaic subenvironments, as well as transgressive deposits signaling deltaic abandonment. Two depositional sequences have been recognized (DSM1 and DSM2). The underlying A Limestone Member, which pinches out towards the east, most likely represents the transgressive systems tract (TST) of

DSM1. Deposition may have been controlled by an interplay of eustatic changes, tectonism, and active volcanism. This member consists of discrete thickening- and coarsening-upward packages that may represent either parasequences or intervals recording delta lobe switching. The parasequence sets exhibit progradational-stacking (seaward) patterns and have clinoformal geometry that exhibit both vertical and lateral facies changes. Various degrees of biogenic reworking are recorded (BI 1-6), commonly in the sandstone-dominated facies, generally representing the depauperate *Cruziana* Ichnofacies, indicative of brackish-water conditions.

Integration of ichnology, sequence stratigraphy, and sedimentology was fundamental in order to provide detailed paleoenvironmental models for the U and M2 Sandstone members. This study represents the first detailed ichnologic study in Ecuador. It is expected that this research will encourage geoscientists in the country to adopt these conceptual and methodological tools in reservoir characterization.

ACKNOWLEDGEMENTS

I would like to thank my supervisor, Dr. Luis Buatois who gave me the opportunity to work with such an incredible team, and along with Dr. M. Gabriela Mángano, welcomed me to their home. Thanks for your patience, time, and for always being aware of your students no matter where in the world you are, or that the world is facing a pandemic. Thank you for sharing your knowledge and expertise with me. It has been years of professional growth without a doubt. In the same way, special thanks to my co-supervisor Dr. M. Gabriela Mángano, who has not only been an excellent professor but also a bird mom for all her work team. My sincere gratitude and admiration to both of you. I could not have asked for better mentors.

A special thanks to Dr. Joyce McBeth, and MSc. Kain Michaud for their insightful and thorough comments and recommendations that facilitated the development and writing of this thesis, and also for all the patience and sincere help they provided along the way.

Also, I would like to thank the University of Saskatchewan and the AAPG (American Association of Petroleum Geology) who were the sponsors of this project. It is important to acknowledge and thank Dr. Cristian Vallejo (Escuela Politécnica Nacional, Quito, Ecuador) and Petroamazonas E.P., whose knowledge and support with key information were fundamental during the development of this project.

Thanks also to all my fellow student and friends: Andrei, Brittany, Maxi, Romain, Neal, and Fernando. You guys have made the department of geology a nice place. Thanks also to everyone who has extended a hand during these last years.

My greatest gratitude is to my boyfriend, Mario, his family, and to my dad, my mom, and my brothers. There are no words that can express how thankful I am with all of you. Thank you for letting me dream high and helping me reach them. Thanks for being the push I need day by day and never letting me give up. Nothing would have even been possible without your presence in my life. You all will always be the secret behind the magic.

------To my wonderful mother, for her unconditional love and support-----

TABLE OF CONTENTS

LIST OF FIGURES

LIST OF ABBREVIATIONS

BI	Bioturbation Index
FSST	Falling Stage System Tract
HST	Highstand System Tract
LST	Lowstand System Tract
MFS	Maximum Flooding Surface
SB	Sequence Boundary
TS	Transgressive Surface
TST	Transgressive System Tract
WRS	Wave Ravinement Surface

CHAPTER 1

1. INTRODUCTION

The Cretaceous Napo Formation has been considered the source rock of almost all hydrocarbon accumulations discovered in Ecuador. In addition, reservoir rocks are present in the Napo Formation. However, a precise paleoenvironmental characterization of this unit is still lacking. The goal of this thesis is to characterize the ichnology, sedimentary facies, and sequence stratigraphy of the U and M2 Sandstone members of the Napo Formation. U Sandstone (early Cenomanian – middle Cenomanian) and M2 Sandstone (late Turonian – early Santonian) members are mainly composed of sandstone, wackestone, and mudstone. In addition to conventional facies analysis, trace-fossil analysis allows for refinement of sedimentologic descriptions and interpretations, particularly regarding paleoenvironmental characterization. Stratal stacking patterns and discontinuity surfaces are analyzed as well. Through the integration of these various lines of evidence, a more robust depositional model is proposed. This research has the potential to significantly impact the hydrocarbon industry in Ecuador. In addition, although a number of papers have characterized trace-fossil distribution in river-, wave- and tide-dominated deltas (e.g. Moslow & Pemberton, 1988; Gingras et al., 1998; MacEachern et al., 2005; Buatois et al., 2008; Carmona et al., 2009; Gani et al., 2009; Hansen & MacEachern, 2009; Buatois & Mángano, 2011; Buatois et al., 2012; Ayranci et al., 2014; Canale et al., 2016; Dasgupta et al., 2016), our knowledge of mixed systems is still quite patchy. The recognition of both fluvial and tidal processes in the U and M2 Sandstone members may allow us to enhance ichnologic characterization of mixed systems.

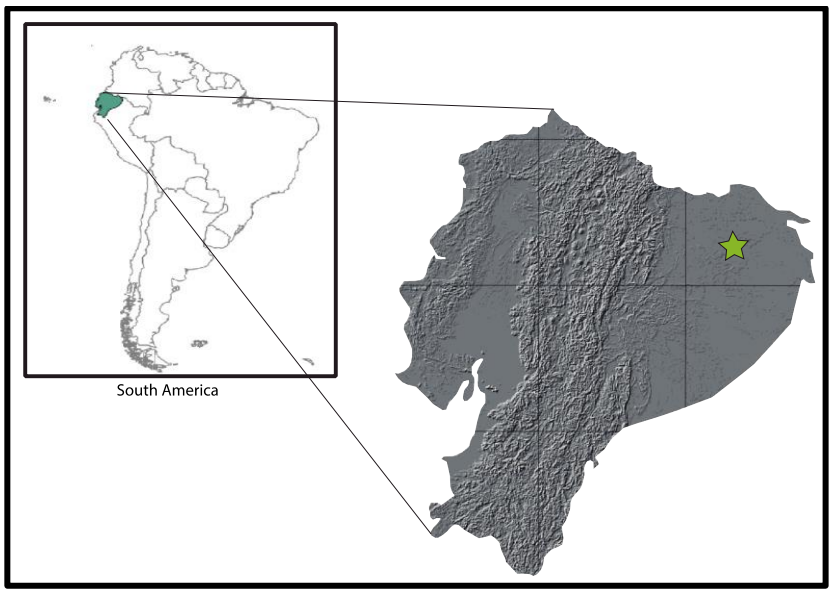

Figure 1.1. *Ecuador location in South America. The yellow star shows the location of the studied area (modified from Google Earth©).*

1.1. General Research Objective

The purpose of this thesis is to analyze and interpret the sedimentology, sequence stratigraphy, and ichnology of the U and M2 Sandstone members of the Napo Formation based on the study of six cores.

1.2. Specific Research Objectives

- To identify and interpret sedimentary facies for the U and M2 Sandstone members.
- To identify trace fossils, trace-fossil assemblages, and their paleoenvironmental implications.
- To establish paleoenvironments by integrating sedimentologic and ichnologic data.
- To propose a model of depositional evolution from a sequence-stratigraphic perspective.

1.3. **Research Scope**

This research will be of great interest to oil companies working in the Oriente Basin of Ecuador, since it integrates multiple datasets, such as sedimentology, ichnology, and sequence stratigraphy. The incorporation of these different lines of evidence will provide a more detailed paleoenvironmental model of the U and M2 Sandstone members. Furthermore, this study represents the first detailed ichnologic study of these units and arguably the first in the country. This novel research will hopefully motivate other scientists to propose new projects on this topic.

1.4. **Hypotheses**

In order to fulfil the aforementioned objectives, the following hypotheses are considered:

- The U and M2 Sandstone members can be distinguished in core by lithologic and ichnologic features, as well as by their inferred sequence-stratigraphic architecture.
- Environmental restriction affected ichnodiversity and degree of bioturbation in the U and M2 Sandstone members.
- Considering the flat topography of the basin during deposition of the U and M2 Sandstone members in the area, subsidence and sea-level changes are regarded as important allogenic controls on sedimentation.
- Tidal and fluvial processes were the main controls during deposition of the studied successions.

CHAPTER 2

2. LITERATURE REVIEW

Some of the best conventional hydrocarbon reservoirs are associated with depositional systems that concentrate large amounts of sand. Sandstone can display good reservoir qualities, such as lateral continuity, porosity, and permeability (e.g. Shepherd, 2009). Reservoir quality is defined by its oil/gas capacity and deliverability. In this context, river-mouth environments are prone to host good hydrocarbon reserves. Fluvial deposits have a moderate hydrocarbon potential, with reservoirs mainly represented by channel fills (Catuneanu, 2006). Moreover, tidal-dominated deposits host an important number of petroleum reservoirs (e.g., the McMurray Oil Sands, Alberta, Canada) (Dalrymple & Choi, 2007). Hence, detailed analyses of coastal depositional systems are necessary to estimate lithofacies spatial distribution. This might help to classify lithofacies according to petrophysical parameters. Lack of understanding of the spatial distribution and stratal stacking pattern may lead to an erroneous hydrocarbon exploration strategy. The study of sedimentary processes is essential to propose accurate and reliable paleoenvironmental interpretations.

2.1.Estuaries

According to Dalrymple's (2006) definition, estuaries are "transgressive coastal environments at the mouth of rivers, which receive sediments from both fluvial and marine sources, and that contain facies influenced by tides, waves, and fluvial processes. Estuaries are considered to extend from the landward limit of tidal facies at its head to the seaward limit of coastal facies at its mouth." Estuarine classification takes into account salinity and density distribution, circulation pattern, and the mixing processes. Dalrymple et al. (1992) defined two integradational estuary types, wave- and tide-dominated.

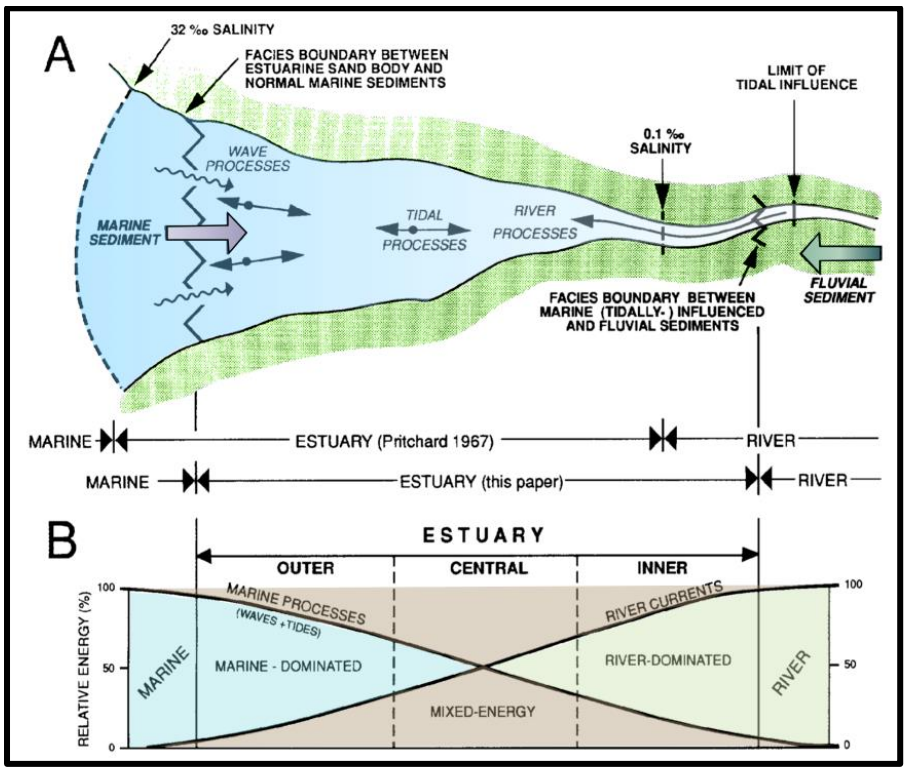

Figure 2.1. *Illustration showing subdivisions and depositional processes in an estuary (modified from Dalrymple et al., 1992).*

2.2.Process Framework

2.2.1. Physical processes

Three important physical processes must be considered when estuaries are analyzed: river currents, tidal currents, and waves. The importance of these processes varies through the river-to-marine transition. For the purposes of this review, tidal currents and waves are going to be considered.

2.2.1.1.Tidal currents

Tidal action influences the seaward part of estuaries, which in result produces an alternation of landward-directed (flood) and seaward-directed (ebb) tidal currents. Tidal ranges and tidal currents increase in a landward direction, because the incoming tidal wave is compressed into a progressively smaller cross-sectional area due to its funnel shape, until friction causes it to decrease toward the tidal limit. The tidal limit is best considered as a zone rather than a specific point. For estuaries, the maximum tidal-current speed occurs in the

middle section. This area is known as the tidal maximum (Dalrymple & Choi, 2007; Shchepetkina et al., 2019).

2.2.1.2.Wave action

Wave energy at the bed will increase landward from the shelf towards the shallower water at the coastline, reaching a maximum at the mouth of the estuary. Because of the funnel shape (open-mouth) of tide-dominated estuaries, wave energy penetrates into the estuary; however, frictional dissipation in shallow water causes the waves to decrease in a landward direction. As a result, the mouth of tide-dominated estuaries experiences more wave action than areas either seaward or landward (Dalrymple & Choi, 2007).

2.2.2. Chemical processes

The salinity increase from the river to the sea is caused by the mixing of fresh water and salt water, which is a fundamental characteristic in estuaries. The vertical gradient of salinity is dependent on the intensity of turbulence that increases as the strength of the river and tidal current increases within the zone of mixing. Hence, the fluvial-to-marine transition typically experiences brackish-water conditions.

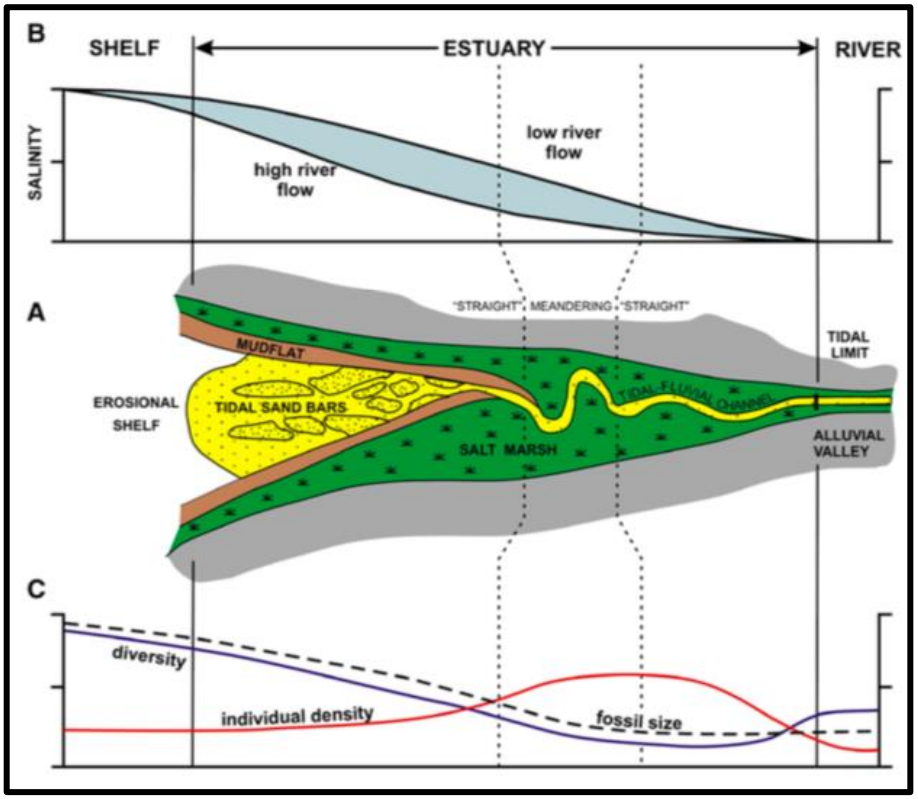

Figure 2.2. *(A) Schematic facies map of a tide-dominated estuary. (B) Longitudinal variation of salinity through a tide-dominated estuary: the salinity gradient migrates up estuary as the river discharge decreases and down estuary when the river discharge is higher. (C) Longitudinal variation of the diversity of benthic invertebrate organisms, burrows size, and the relative number of individuals per square meter (taken from Dalrymple & Choi, 2007).*

2.2.3. Biological processes

Due to the fluctuating nature of estuarine environments, there are few eukaryotic organisms that are able to adapt to estuaries. Diversity of organisms increases towards the sea (e.g. Buatois et al., 1997). Organisms that are able to live in these hostile conditions tend to be opportunistic (e.g. *Skolithos* Ichnofacies, Vossler & Pemberton, 1988). Also, monospecific assemblages characterize this environment. Furthermore, because of the stress conditions, these organisms tend to be smaller than their marine counterparts (Buatois & Mángano, 2011).

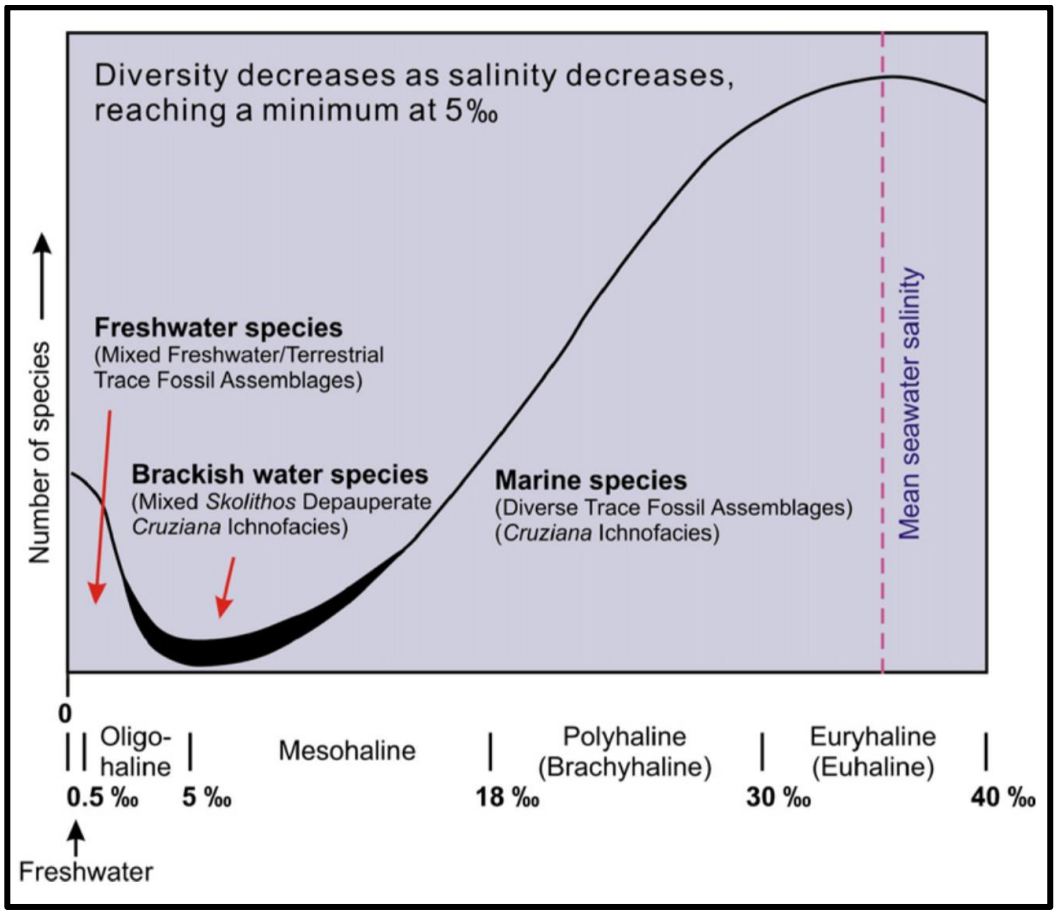

Figure 2.3. *Classification of salinity levels and variations of species diversity through the freshwater to seawater transition. Note that the brackish - water environments have low taxonomic diversity and are characterized by mixed* Skolithos-Cruziana *(taken from Dalrymple & Choi, 2007).*

2.3.Resultant Currents and Transport Directions

By virtue of determining the relative location at which a given deposit was formed in the estuarine-marine transition, all the above-mentioned processes need to be considered.

Depth-related variation of the physical, chemical, and biological processes can directly influence the nature of the deposits. The water movement in the seaward part of estuaries is typically dominated by tidal currents, whereas the inner part is dominated by river currents.

2.4.Tide-Dominated Estuaries

Tidal dominance in estuaries is produced either by the presence of large tidal range and/or by the presence of weak wave action in the coastal zone (Davis Jr & Hayes, 1984). Estuaries influenced by tides have a funnel shape; however, exceptions might exist (e.g. Changjiang Delta, Hori et al., 2002). A dominant characteristic of tide-dominated estuaries is their elongate sand bars, which are oriented perpendicular to the coastline and encompass broad sand flats that pass landward into a low-sinuosity single channel (Dalrymple et al., 1992).

If the estuary morphology and facies distribution is being analyzed, it is important to be aware that wave-generated barriers may be restricted or absent (Dalrymple & Choi, 2007). Due to the sand-bar distribution in tide-dominated estuaries, the central estuary basin will not be easily identified or may not be present at all. In tide-dominated estuaries, the tripartite morphosedimentary distribution is not as developed as in wave-dominated estuaries. The head zone of tide-dominated estuaries is still affected by fluvial processes but, in contrast, a bayhead delta is not always formed. However, the coarser sediments continue to be deposited by fluvial processes as in wave-dominated estuaries (Davis & Dalrymple, 2012).

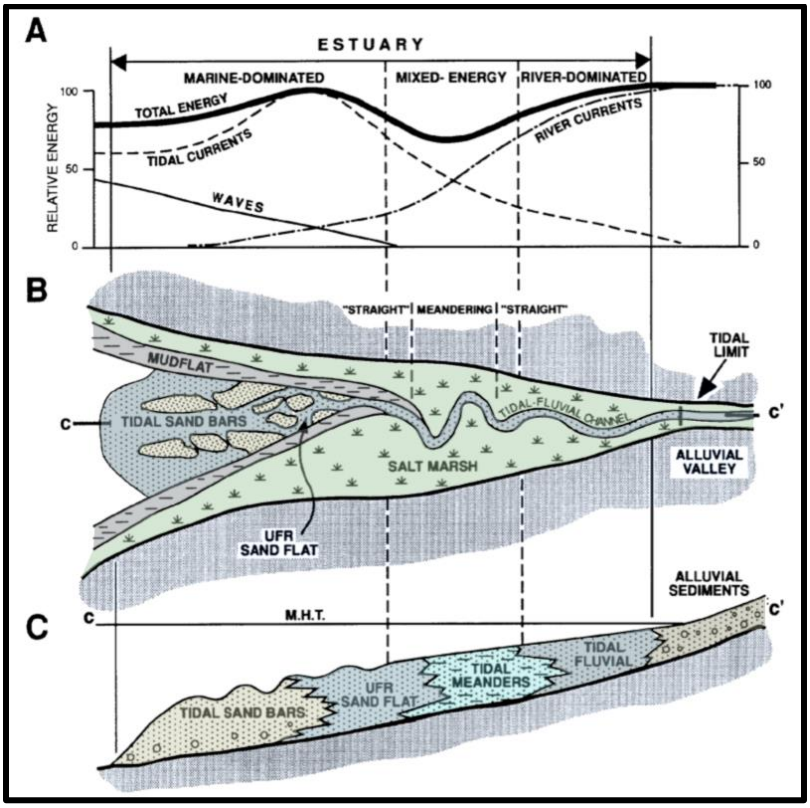

Figure 2.4. *Tide-dominated estuary model. The model includes: (A) energy gradient, (B) morphologic elements in plain view, (C) sedimentary facies in longitudinal section within an idealized tide-dominated estuary (modified from Dalrymple et al., 1992).*

In this type of environment, the sediments are forming sand bodies locally separated by areas with high mud content. Boyd et al. (2006) differentiated three main zones in a tide-dominated estuary: mud flat, tidal bars/channels and the sand flat. The reservoir facies tend to be restricted to the channels and tidal-bars and the non-reservoir facies or with poor quality reservoir correspond to the mud flat sediments. In addition, both environments dominated by waves or tides, are intermittently influenced by tidal cycles, and seasonal flooding during transgressive and regressive periods (Davis & Dalrymple, 2012).

2.5.Wave-Dominated Estuaries

Wave-dominated estuaries are divided into three zones, reflecting their energy gradients. These are (from distal to proximal): a marine sand body comprised of barriers, washover fan, tidal inlet and tidal delta deposits; the central basin of the estuary which is

generally mud-dominated; and the innermost part of the estuary the bayhead delta which can be tidal and/or salt-water influenced. In wave-dominated estuaries, river currents have high energy towards a landward direction. The central basin has minimum energy levels influenced by rivers and waves. Sediments are constantly moving perpendicular to the coast and onshore towards the mouth of the estuary, where a subaerial or slightly submerged bar (oriented parallel to the shoreline) is developed and deposited. The development of these bars in the outer part of the estuary protects the middle part of the estuary from incoming waves; for this reason, wave-dominated estuaries have a tripartite morphology. However, a number of few inlets in the outer bars may form allowing the entrance of waves (Dalrymple et al., 1992).

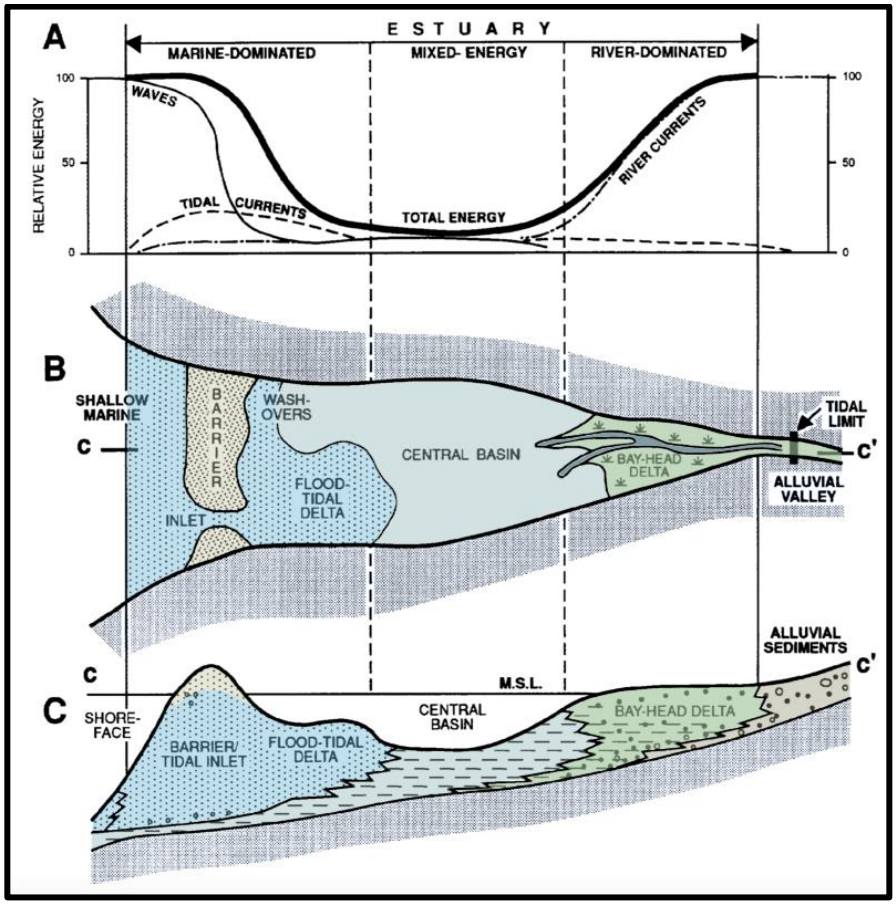

Figure 2.5. *Wave-dominated estuary model. (A) Energy gradient. (B) Morphologic components in plain view. (C) Sedimentary facies in longitudinal section within an idealized wave-dominated estuary. The shape of the estuary is schematic. The barrier/sand plug is shown here as headland attached, but on low-gradient coasts it may not be connected to the local interfluves and is separated from the mainland by a lagoon (modified from Dalrymple et al., 1992).*

2.6.Shoreline Trajectories

The interaction between sedimentation and accommodation results on depositional trends in response to changes in base level. Furthermore, the transgressive and regressive shoreline trajectories are influenced by this change. Hence, the types of shifts are essential to reconstruct specific stacking patterns, as revealed by sequence stratigraphic analysis (Catuneanu, 2006).

2.6.1. Transgression

A transgression is defined as the landward migration of the shoreline. As a result of this migration, the marine water close to the shoreline deepens. Transgressions result in retrogradational stacking patterns. Within the non-marine side of the basin, the transgression is commonly characterized by the presence of tidal-influenced structures in the fluvial succession (Catuneanu, 2006).

2.6.2. Regression

A regression, on the contrary, is the seaward migration of the shoreline. This migration results in shallowing close to the shoreline. Regressions result in progradational stacking patterns (Catuneanu, 2006).

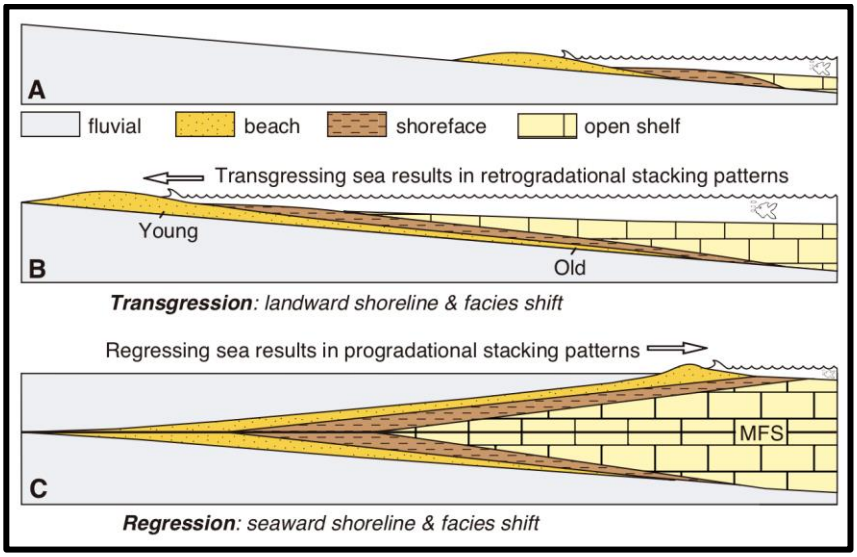

Figure 2.6. *Transgressions and regressions. Note the retrogradation and progradation (lateral shifts) of facies, as well as the surface that separates retrogradational from overlying progradational geometries (MFS or maximum flooding surface) (taken from Catuneanu, 2006).*

2.6.3. Normal regression

A normal regression occurs when sedimentation outpace the low rates of base-level rise at the shoreline. This scenario occurs during early and late stages of base-level rise. The new accommodation space created is totally consumed by sedimentation resulting in aggradational and progradational facies successions. Also, this seaward facies shift results in the formation of coarsening-upward shallow-marine successions in wave-dominated settings (Catuneanu, 2006).

2.6.4. Forced regression

A forced regression occurs when during the falling leg of the base level cycles, the accommodation is reduced (Posamentier et al., 1992). This reduction can be caused by external controls, which are mainly the interplay of subsidence and sea level-changes. As a result, the shoreline is forced to regress regardless of the sedimentation factor.

CHAPTER 3

3. GEOLOGIC FRAMEWORK

3.1. Tectonic Framework

The Oriente Basin was developed on the east side of the Andean front in Ecuador. It is an active retroarc foreland basin that was developed as result of flexural subsidence induced by Andean crustal thickening. This basin continues to the north in Colombia where is referred to as the Putumayo Basin, and to the south in Peru, where is known as the Marañon and Ucayali basins. The Oriente Basin accumulated products of the Andean denudation and from the gradual incorporation of new sourced regions during fold-thrust invasions. The western limit of the basin is represented by the overthrusting front of the Eastern Cordillera in Peru, Cordillera Real in Ecuador and Eastern Cordillera in Colombia, while to the east, it is bounded by the Amazon craton (Ruiz et al., 2007; Gombojav & Winkler, 2008; McGroder et al., 2015; Wolaver et al., 2015).

Three main stages characterize the evolution of the basin and can be distinguished as follows:

Extensional Stage (pre-rift and rift): this stage is represented by the development of grabens and semi-grabens during the Devonian-Late Jurassic. These structures are clearly visible in seismic (Baby et al., 2004). In this stage, the Subandean zone was uplifted and deformed, representing a magmatic arc during most of the Jurassic (Misahualli arc). This stage is represented by the pre-Jurassic Pumbuiza and Macuma, and the Late Triassic- Late Jurassic Santiago, Chapiza, and Misahualli formations.

Passive Margin Stage: this stage is characterized by the formation of a weakly subsiding, shallow-marine basin during the Cretaceous (Aptian-Campanian) (Canfield et al., 1982). Strata thin towards the west due to wedging and erosion. This stage is represented by the Hollin and Napo formations.

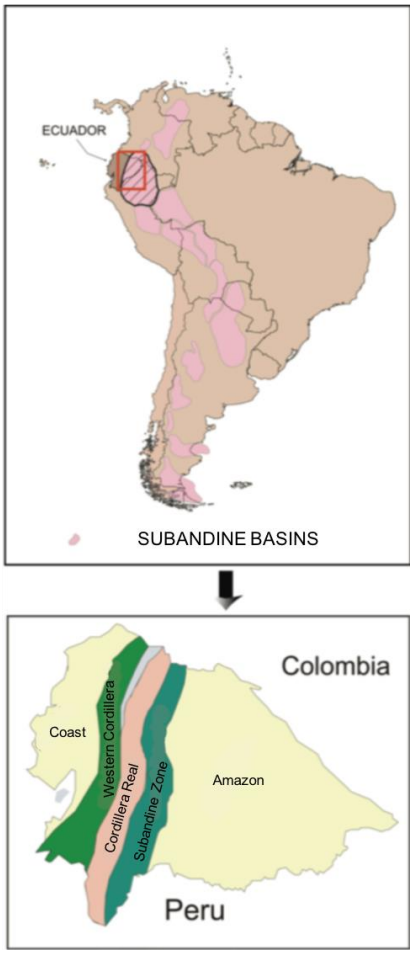

Figure 3.1. *Oriente Basin location within the framework of the Subandean basin geodynamics (modified from Baby et al., 1999; Christophoul, 1999).*

Foreland Stage: the Oriente Basin during this stage was located in a retro-arc foreland position related to the development of the Andean protocordillera. This final stage started at the end of the Late Cretaceous and spanned until the present. The units that represent this stage are composed of fluvial deposits, showing the influence of the Andean Cordillera in the Oriente Basin. This stage is represented by the Tena, Tiyuyacu, Orteguaza, Arajuno, Chambira, Mesa, and Mera formations (Baby et al., 2014).

The Oriente Basin is also characterized by three tectonic domains. Each of them has its own geometric and kinematic characteristics inherited from the pre-Cretaceous topography (Baby et al., 1999). The Eastern domain or Subandean system shows, from north to south, three morpho-structural zones.

- The Napo uplift, which belongs to a remarkably elongated dome. Its orientation is NNE-SSW and it is limited at the east and west by transpressional faults.
- The Pastaza Depression, where the faults become more overthrusted due to the contact of the Subandean Zone and Western Cordillera.
- The Cutucu uplift, characterized by a change in the orientation of the structures from N-S to NNW-SSE, and the occurrence of Triassic and Jurassic rocks (Santiago and Chapiza formations).

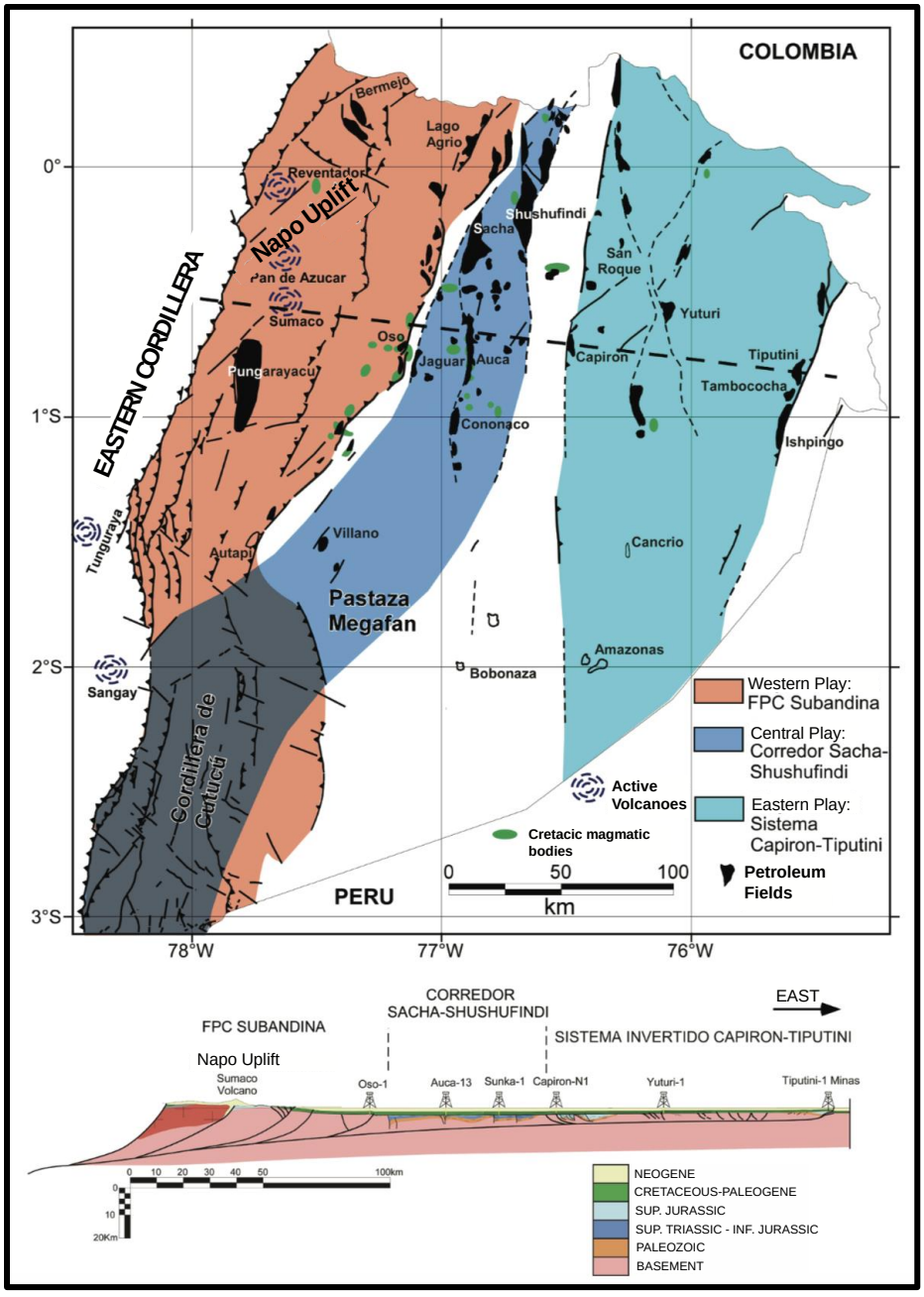

Figure 3.2. *Tectonic Map of the Ecuadorian Amazon Basin (modified from Baby et al., 1999).*

Exhumation of the narrow Andean orogen and subsidence of the Oriente Basin are the processes invoked to explain its structural and stratigraphic variability (e.g. Tschopp, 1953; Dashwood & Abbotts, 1990; Balkwill, 1995; Gombojav & Winkler, 2008; Baby et al., 2013). In Ecuador, the Mesozoic-Cenozoic depositional history of the Oriente Basin involved detrital input from the Amazonian craton, Andean magmatic arc, and Andean fold-thrust belt (Christophoul et al., 2002; Baby et al., 2004; Vallejo et al., 2006).

Formation of the Oriente Basin was mainly controlled by the early dynamics of the Northern Andes starting in the Jurassic (Spikings et al., 2015). Subsequently, the Oriente Basin was developed as an eastward-pinching foreland basin since the Maastrichtian (Gombojav & Winkler, 2008), and hosts ca. 4.5 km of mainly clastic deposits. Studies have shown that the Oriente Basin initiated approximately at 115-100 Ma. This occurred after a long period of extension between 145 and 120 Ma, which resulted in the formation of grabens and half-grabens during the extensional stage, leading to deposition of evaporites, continental debris flow sediments, and shallow-marine sediments during the Middle Jurassic (Diaz et al., 2004; Spikings et al., 2015). The Misahualli Formation, comprising basaltic pyroclastic deposits and rhyolitic lava flows, is present on the west side of the Oriente Basin, whereas the Chapiza Formation, formed by tuffaceous and nonmarine clastic deposits, occurs farther east (Romeuf et al., 1995). Extension was followed by a period of compression along the northern South American plate margin, also known as the passive margin stage, which closed a series of fore-, inter-, and back-arc basins (Guamote, Peltetec, Alao, and Upano basins) against the continent (Litherland et al., 1994; Spikings et al., 2015). In the Oriente Basin, this compression created an unconformity separating the pre-Cretaceous strata below from the Aptian to Albian Hollin Formation above, which is distinctly observed in the seismic lines (Balkwill, 1995). Earlier authors ascribed this deformational event (Peltetec event) to the collision of allochthonous terranes between ca. 120 and 110 Ma (e.g., Litherland et al., 1994; Spikings et al., 2015), creating a primordial Andean chain in the Eastern Cordillera located to the west of the basin (Ruiz et al., 2007; Gombojav & Winkler, 2008). The compression was followed by a period of punctuated thermal subsidence during the Cretaceous.

The Lower Cretaceous Hollin Formation comprises ca. 150 m of fluvial to marine tidal deposits of quartz sandstone and sporadic coal layers, the latter representing the onset of long-term marine conditions (Tschopp, 1953; Dashwood & Abbotts, 1990; Baby et al., 2004). This long-term transgression was driven by tectonic influence and relative sea-level rise across the new basin floor. Detrital sediment supply during deposition of the Hollin Formation was contributed from both the South American craton and from a primordial, Cretaceous Andean cordillera (Gombojav & Winkler, 2008).

A regional, erosional unconformity separating the Napo and Tena formations was produced during the foreland stage. This unconformity represents the erosion of the upper part of the Napo Formation and marks a significant lithologic change from shallow-marine deposits of the Napo Formation to overlying dominantly continental deposits of the Tena Formation. The latter is composed of ca. 750 m of fluvial red siltstone intercalated with silty sandstone (Tschopp, 1953; Dashwood & Abbotts, 1990; Jaillard, 1997; Alava-Toro & Jaillard, 2005; Gutierrez et al., 2019). Along the western border of the basin, the erosion level below the Tena Formation reaches the Turonian-Coniacian M2 limestone of the Napo Formation, whereas along the eastern border of the basin this unconformity separates the fluvial to coastal deposits of the Campanian M1 Sandstone from the red beds of the Tena Formation. During the Late Cretaceous, thick-skinned tectonics produced the inversion of pre-Cretaceous extensional, mainly northward-striking fault systems (Balkwill, 1995; Baby et al., 2013). The overthrusting Cretaceous sedimentary succession gave rise to the formation of N-S elongated folds, which comprises the main structural oil traps of the basin. This Late Cretaceous deformation event is likely related to the collision of fragments of the Caribbean Plateau against the continental margin of the Northern Andes (Luzieux et al., 2006; Vallejo et al., 2006). The establishment of prevailing continental depositional environments in the Oriente Basin occurred during the Maastrichtian, as evidenced by the fluvial sandstone and red beds of the Tena Formation (Tschopp, 1953; Canfield et al., 1982).

The Tena Formation is, in turn, overlain by the Paleocene to Eocene conglomerate of the Tiyuyacu Formation. The Tiyuyacu Formation is an approximately 200-800 m thick coarse-grained unit characterized by marked thickness variations and internal unconformities (Christophoul et al., 2002; Baby et al., 2013). Deposition of this unit depicts the accelerated

uplift of the Andean cordillera located to the west of the Oriente Basin (Gombojav & Winkler, 2008).

The Tiyuyacu Formation records fluvial channel-belt and possibly alluvial-fan deposition during eastward migration of thrusting. Shallow-marine deposits of the Oligocene Orteguaza Formation conformably overlie the Tiyuyacu Formation reaching only 250 m in thickness (Christophoul et al., 2002; Roddaz et al., 2010). It represents a period of limited sediment accumulation. Increased sediment accumulation was recorded by the Oligocene-lowermost Miocene Chalcana Formation, which corresponds to fluvial channel and floodplain deposits up to 450 m thick (Roddaz et al., 2010). Miocene deposits include the Arajuno Formation, an eastern marine equivalent of the Curaray Formation partially coeval with the Chambira Formation. The Arajuno Formation is an approximately 1000-1500 m thick unit containing sandy and gravelly fluvial channel deposits intercalated with rooted floodplain deposits (Burgos et al., 2005; Roddaz et al., 2010). The Pliocene-Quaternary Mesa and Mera formations consist of <200 m of thick gravel terraces representing proximal deposition within the Pastaza fluvial megafan (De Berc et al., 2005).

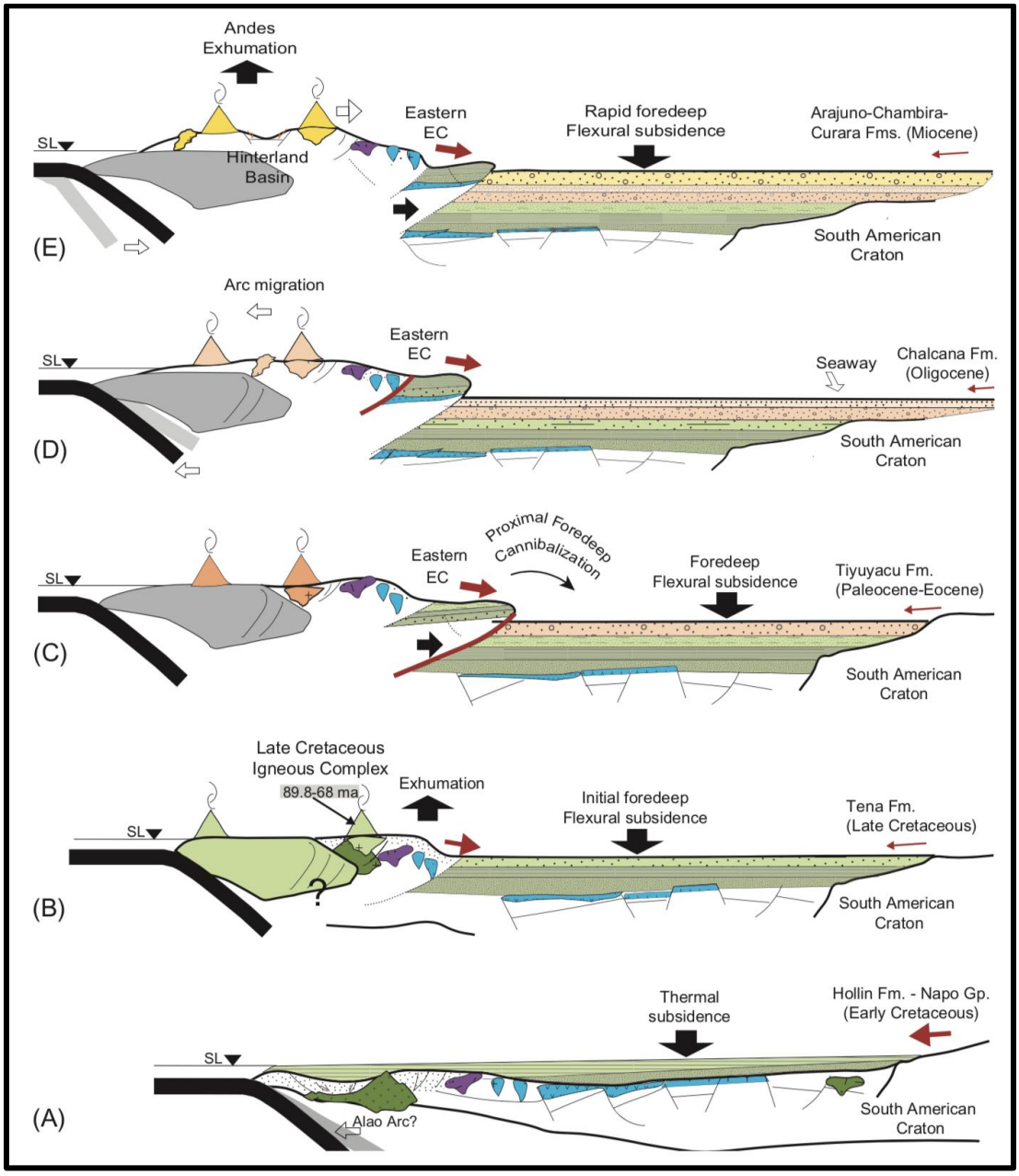

Figure 3.3. *Schematic cross section of the Ecuadorian margin emphasizing the evolution of sediment source regions during Cretaceous-Cenozoic basin development in the Subandean Zone and Oriente Basin. (A) Cretaceous post-extensional thermal subsidence (Hollin Formation, Napo Group). (B) Late Cretaceous onset of shortening flexure, and foreland basin sedimentation (Tena Formation). (C) Paleocene-Eocene shortening, thrust belt advance, and continued flexural subsidence (Tiyuyacu Formation). (D) Oligocene continued contributions from Andean sourced during diminished foreland accumulation (Chalcana Formation). (E) Miocene-Quaternary main phase of Andean shortening and rapid flexural subsidence in the Oriente foreland basin (Arajuno Formation, Mesa/Mera Formation), with detrital contributors from Andean basement and intrusive rocks (taken from Gutiérrez et al., 2019).*

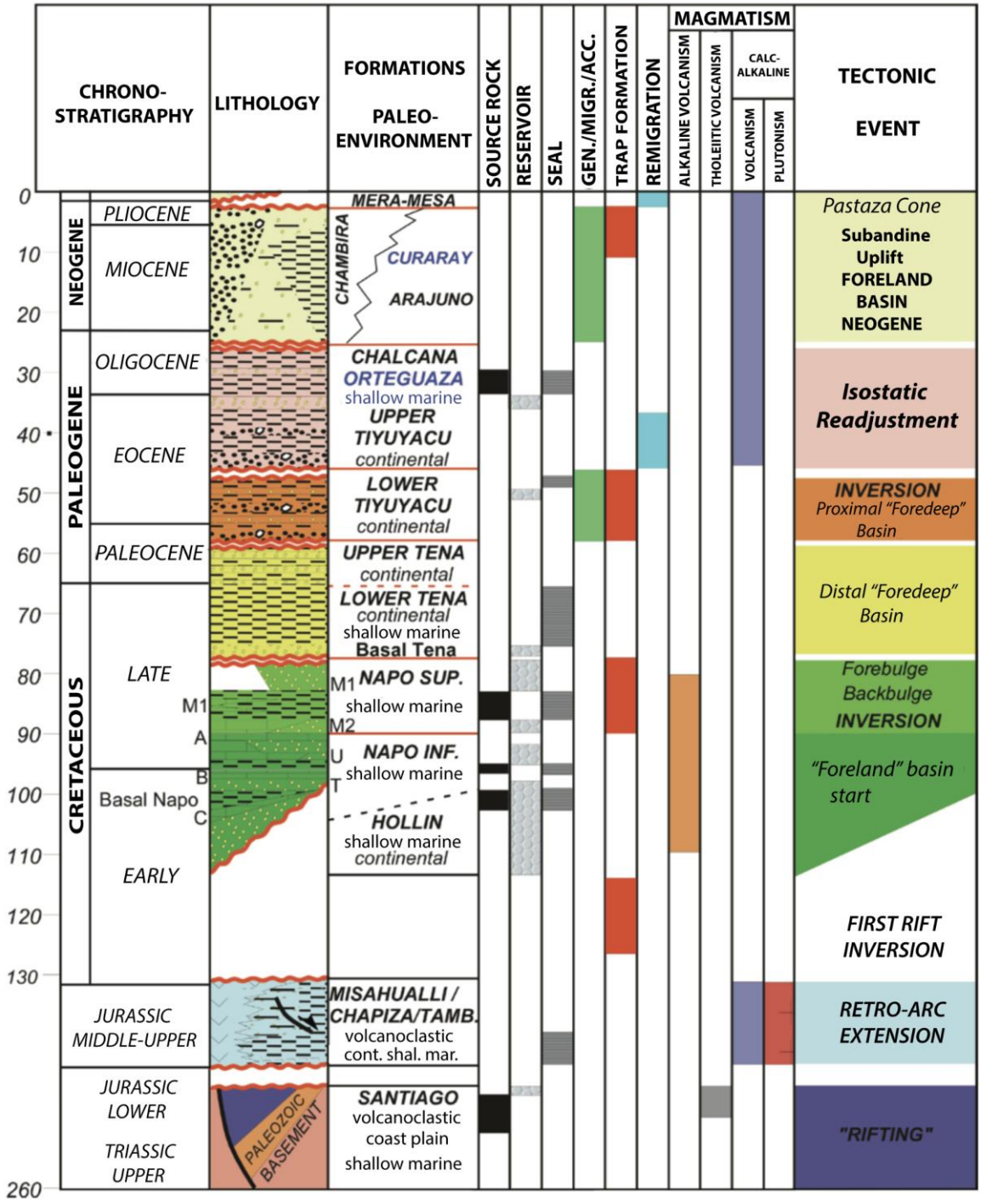

Figure 3.4. *Tectono-stratigraphic section and geodynamic events that controlled the development of the Oriente Basin and its petroleum systems (modified from Baby et al., 2014).*

3.2. Stratigraphic Framework

Sedimentation in the Oriente Basin is subdivided into five stages of relatively high sedimentation rates separated by times of reduced sedimentation or non-deposition. In a sequence-stratigraphic context, relative sea-level changes controlled the availability of accommodation space and distribution of sediments, particularly during deposition of the three first cycles of the continental pre-Andean Oriente craton margin. In particular, the beginning of the Andean compression played a major role in controlling sediment supply and accommodation space during the Turonian (90 Ma). The last two depositional cycles, which are restricted to the east side of the Oriente Basin, were condensed on the west side in the Subandean zone.

The Oriente Basin was very shallow and flat during the Cretaceous, showing very limited to no subsidence and low sedimentary input. Hence, the main geodynamic factor that controls deposition in the Oriente Basin during the Aptian – Maastrichtian interval were eustatic changes. A drop-in sea level resulted in the emergence of wide areas within the basin. Nearshore zones underwent progradation, while more distal zones underwent aggradation. In subaqueous zones, the proximal parts received a large amount of sediment. The sediments prograded until reaching the sea level, becoming exposed until the subsequent transgression (Baby et al., 2014).

Jaillard (1997) produced a detailed cross section of the Mesozoic and Cenozoic Ecuadorian Amazon. This author subdivided the Napo Formation into four units: Basal Napo (late – early Albian), Lower Napo (late Albian – late Cenomanian), Middle Napo (early – late Turonian) and Upper Napo (Coniacian – Campanian), noting that the Middle Napo displays a constant thickness in the sub Andean zone (78-91 m). Palynologic analyses allowed establishing accurate ages for the different members of the Napo Formation. The M2 Member contains *Coilopoceras* sp., *Mammites* aff. *barkeri,* and *Neoptychites* sp. (Tschopp, 1953).

The Napo Formation is a stratigraphic unit that includes at least five major stratigraphic sequences ranging from the Albian to the Campanian (White et al., 1995; Vallejo et al., 2002). The lower two stratigraphic sequences (T and U) were deposited during Albian and Cenomanian transgressions; they comprise successions that retrograde from fluvial to tide-

dominated estuarine, and then to open marine environments (Estupiñan et al., 2010). The basin was protected from large, open, oceanic waves and swells, by the presence of a partial topographic barrier to the west (Jaillard, 1997; Vallejo et al., 2002; Gombojav & Winkler, 2008). Consequently, the Oriente Basin appears to have been narrow and influenced mainly by river and tidal currents moving through the shallow Ecuadorian Cretaceous seaway (e.g. Jaillard, 1997).

Next, the M1 Shale and M1 Limestone members of the Napo Formation were deposited during the Santonian transgression (Ordoñez et al., 2006), and comprise mainly offshore and shelf shale and limestone. During the Santonian, the sea transgressed across the whole basin and the M1 Limestone and associated shale are considered to represent the maximum flooding interval of the Napo second-order stratigraphic cycle. The organic-rich Upper Napo Shale marks the top of the formation. In the westernmost part of the Oriente Basin, this member was deposited in a shallow-marine environment during the Campanian. Deposition of the overlying M1 Sandstone and Shale members is more complex and somewhat different from the underlying four stratigraphic sequences in the basin (Vallejo et al., 2017).

The sedimentary succession represented by the Hollin, Napo and Basal Tena formations records strong shoreline shifts. Additionally, these formations show vertical and lateral facies changes along the basin. Relative sea-level variations-controlled accommodation space. Hence, this factor affected regionally the distribution of sedimentary facies in the basin. The rapid progradation of fluvial and nearshore clastic sedimentary facies above shallow-marine platform facies, product of a sea-level drop, are clear examples of forced regressions (Posamentier et al., 1992).

In the Albian – Maastrichtian, multiple eustatic cycles are recognized. The megasequence Hollin – Napo – Basal Tena is described as a repetitive series of sandstone, limestone, and shale showing a cyclicity controlled by the eustatic sea-level fluctuations (White et al., 1995). The correlation of the base-level drop with the progradation of the sandstone bodies along the Oriente Basin shown in Figure 3.5 is supported by the biostratigraphic information available for each member of the Napo Formation (White et al., 1995).

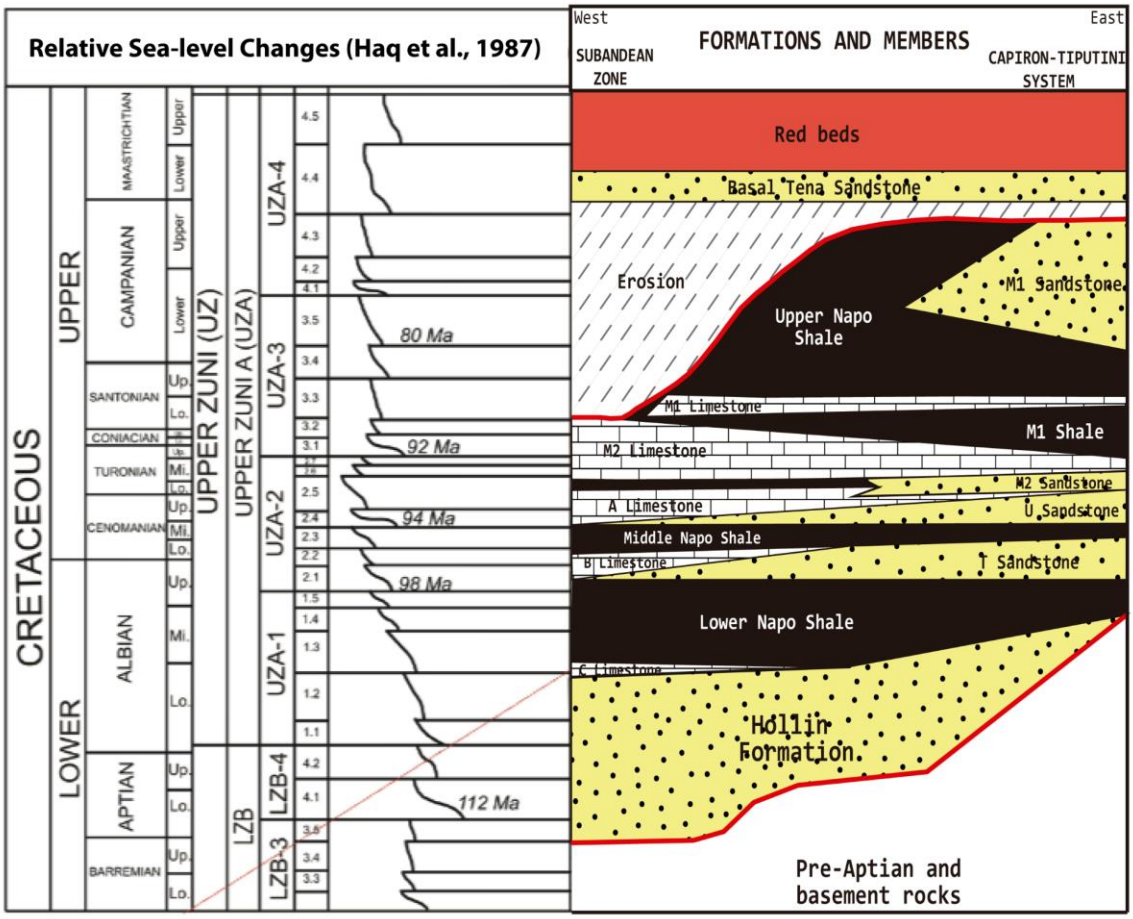

Figure 3.5. *Lithostratigraphic units, sedimentary cycles, and their relationship with the eustatic curve during the Cretaceous in the Oriente Basin (modified from Haq et al., 1987; Vallejo et al., 2017).*

This ideal sedimentary cycle shows the complete variation of the base level, and it is identified in each sequence of the Hollin – Napo – Basal Tena sedimentary succession. It starts with an erosive channelized fluvial deposition, sourced from the east-southeast. This fluvial system was locally deposited within incised valleys passing upwards into estuarine environments (LST-TST). The sea-level rise took place filling the estuary and a succession of shallow-marine deposits spilled over the margin of the incised valleys, which shows the transgression to the east side of the Oriente Basin (TST). Overlying thick limestone deposits represent the platform environment belonging to the highstand prism (HST) (Baby et al., 2014).

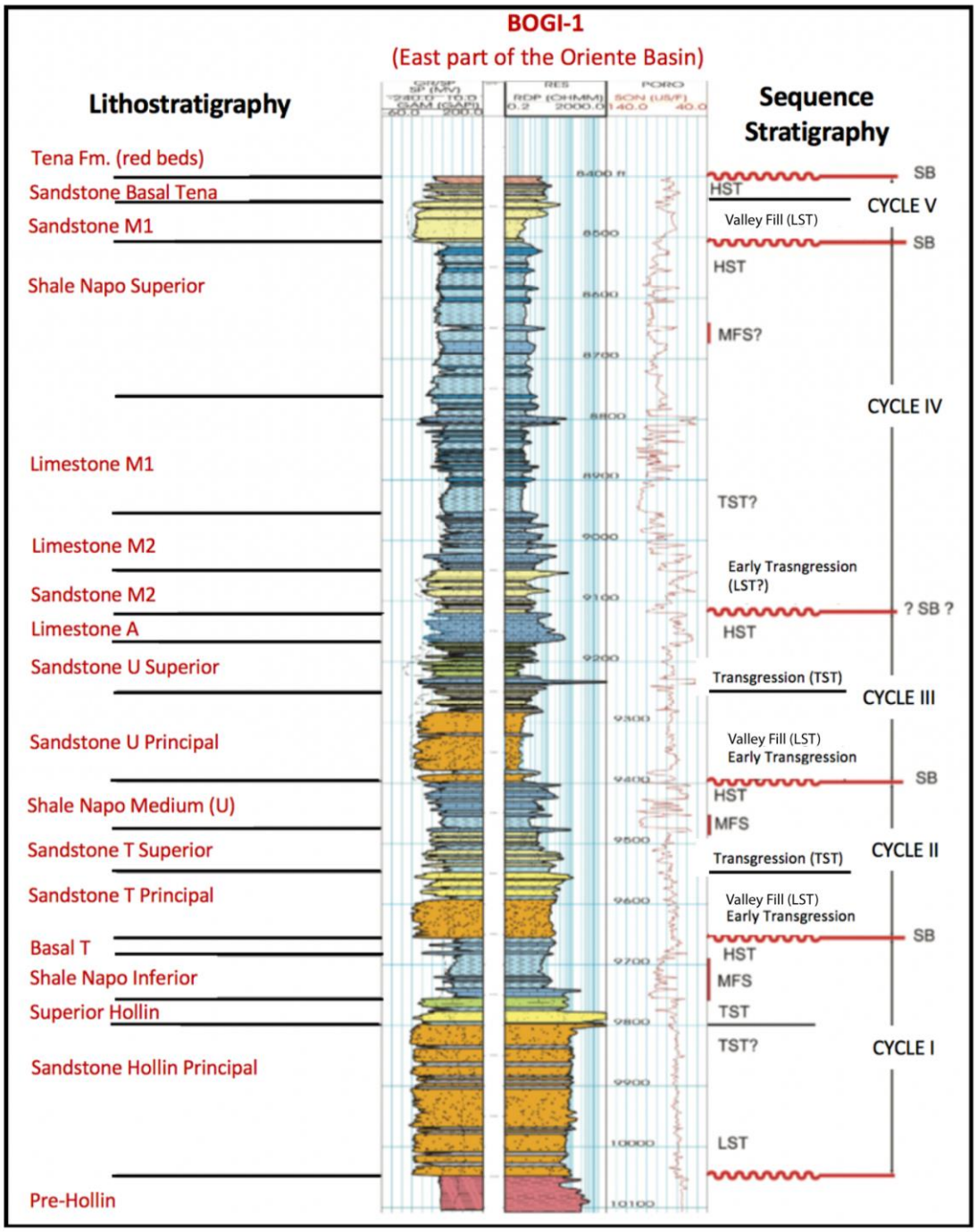

Figure 3.6. *Sedimentary cycles of the Oriente Basin during the Cretaceous, as defined for well Bogi-1 (modified from Baby et al., 2014).*

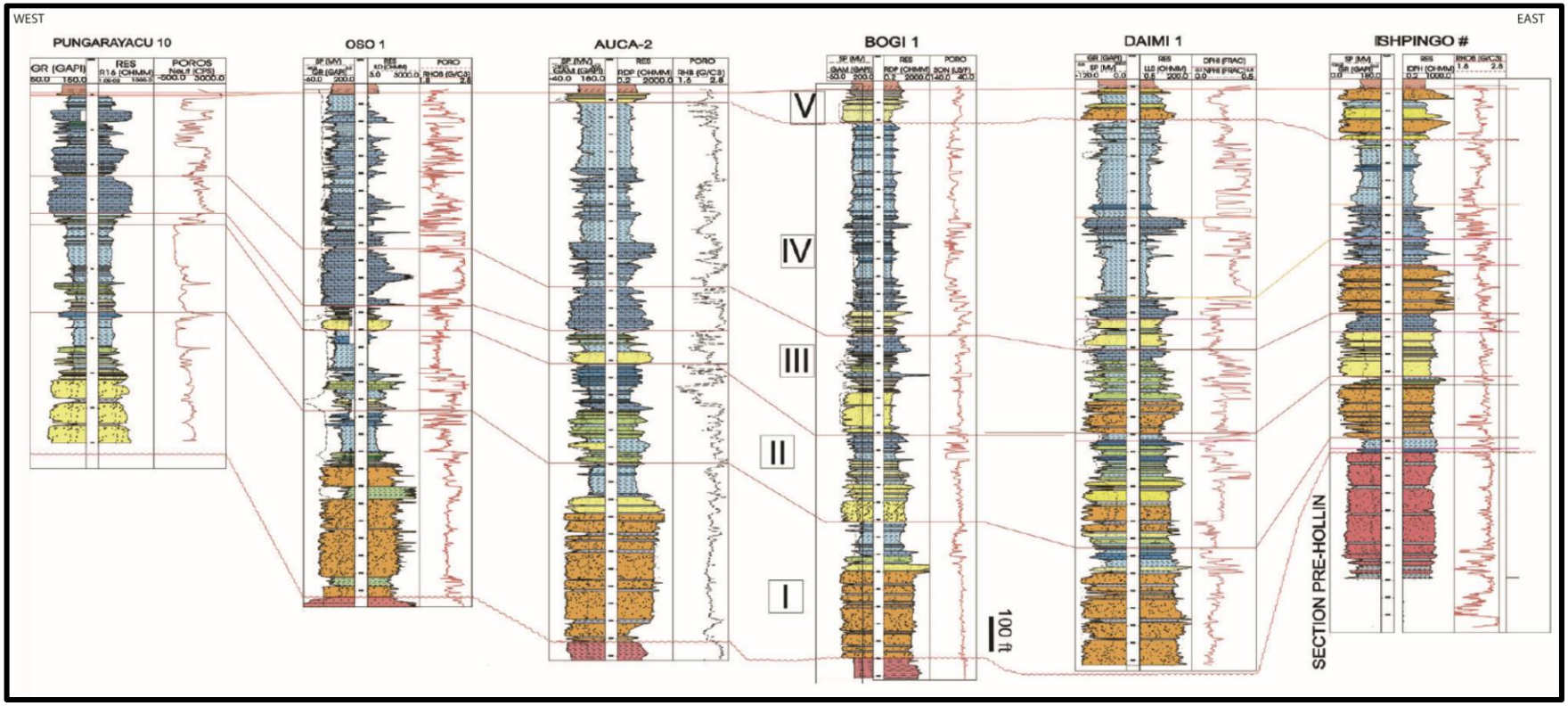

Figure 3.7. *E-W well correlation in the Oriente Basin showing Cretaceous sedimentary cycles (modified from Baby et al., 2014).*

A sedimentary model proposed that Late Cretaceous deposition in the Oriente Basin resulted from the interplay of very low subsidence and eustatic cycles (Raynaud et al., 1993). During sea-level falls, the basin emerged and erosion carved low-relief paleovalleys. During eustatic transgressions, the landward migration of the shoreline infilled the paleodepresions with sandy sediments derived from erosion of the basin platform. Sedimentation took place in open, shallow-marine environments towards the west and southwest, and fluvial to estuarine environments towards the east and northeast.

Dashwood & Abbotts (1990b) determined the limits of M2 Member deposition. The Napo M2 Sandstone is restricted to the east of the basin. During the Late Cretaceous and Paleogene, the onset of "Early Andean" compression from the west provided tectonic loading in the foredeep and caused significant Cretaceous oil generation. Freshwater influx, particularly from the east, caused early biodegradation of oil in shallow reservoirs. Haq et al. (1987) proposed that the Napo Formation consists of several transgressive-regressive packages related to Late Cretaceous eustatic sea-level fluctuations. The M2 Limestone is more fossiliferous, rich in glauconite, and contains oil-bearing sandstones (Rosero, 1997).

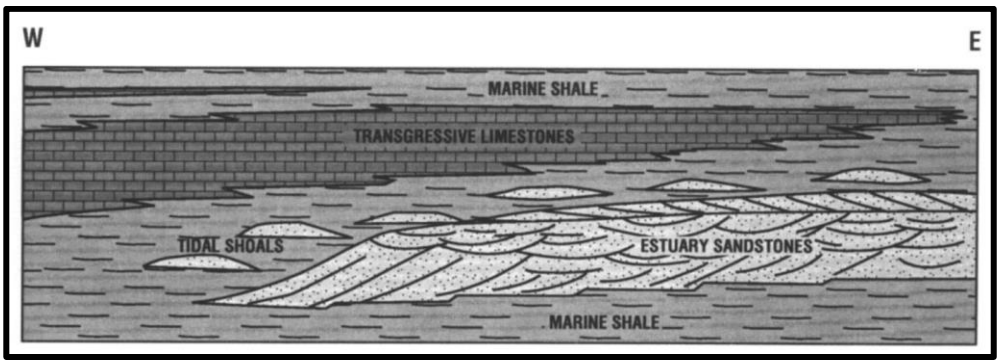

Figure 3.8. *Napo regressive-transgressive cycle of sedimentation showing rapid progradation followed by seal-level rise with marine onlap (from White et al., 1995).*

Paleontologic data was first incorporated into the analysis of different members by Vallejo et al. (2002), who reconstructed the sequence stratigraphy of the basin. The reconstruction was conducted through the compilation of palynofacies data, primary sedimentary structures, and faunal data previously described for the well Pungarayacu 30 (Jaillard, 1997). The following aspects were underscored in that study: 1) sequence

boundaries as karst surfaces, assumed to be formed during subaerial exposure, 2) presence of oysters, related with brackish-water conditions in inner neritic settings, 3) sparse bioturbation characteristic of brackish-water settings in a restricted basin, and 4) thinly laminated fine-grained facies interpreted as indicators of low-energy deposition.

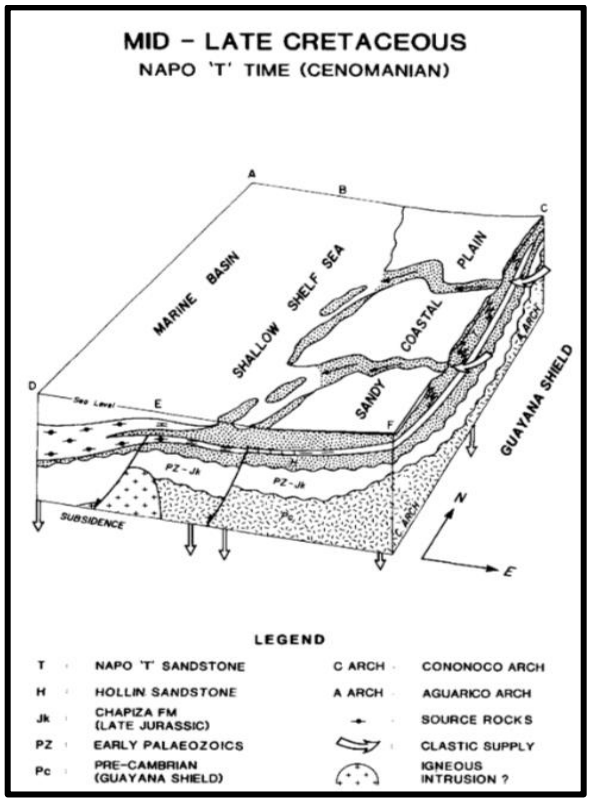

Figure 3.9. *Summary model for the oil gravity distribution in the Oriente Basin, Ecuador; during the Late Cretaceous (modified from Dashwood et al., 1990).*

The Eden Yuturi field, one of the fields covered in this project, was first described from a sedimentologic perspective by Vallejo et al. (2017). Sedimentation in this field was interpreted to have taken place in a series of westward progradding deltas, with an abrupt pinch-out of sandstone towards the southwest. However, the sharp-based, blocky middle sandstone (akin to the lower sandstone in the nearby Apaika field) is likely to be transgressive and estuarine in origin. It is very common that transgressive and regressive sands alternated during the construction of shelf platforms by repeated back-forth transits of the sediment delivery system (Steel et al., 2008).

CHAPTER 4

4. STUDY AREA LOCATION

The total thickness of the Cretaceous succession in the Oriente Basin exceeds 500 m (Hollin – Napo interval, 110-75 Ma). Accounting for compaction, the maximum original thickness of the succession is estimated in approximately 800 m, which represents a maximum sedimentation rate of ca. 22 m/Ma (Baby et al., 2004).

The study area covered in this project corresponds to the field 12, and is located in the eastern most part of the Ecuadorian Oriente Basin.

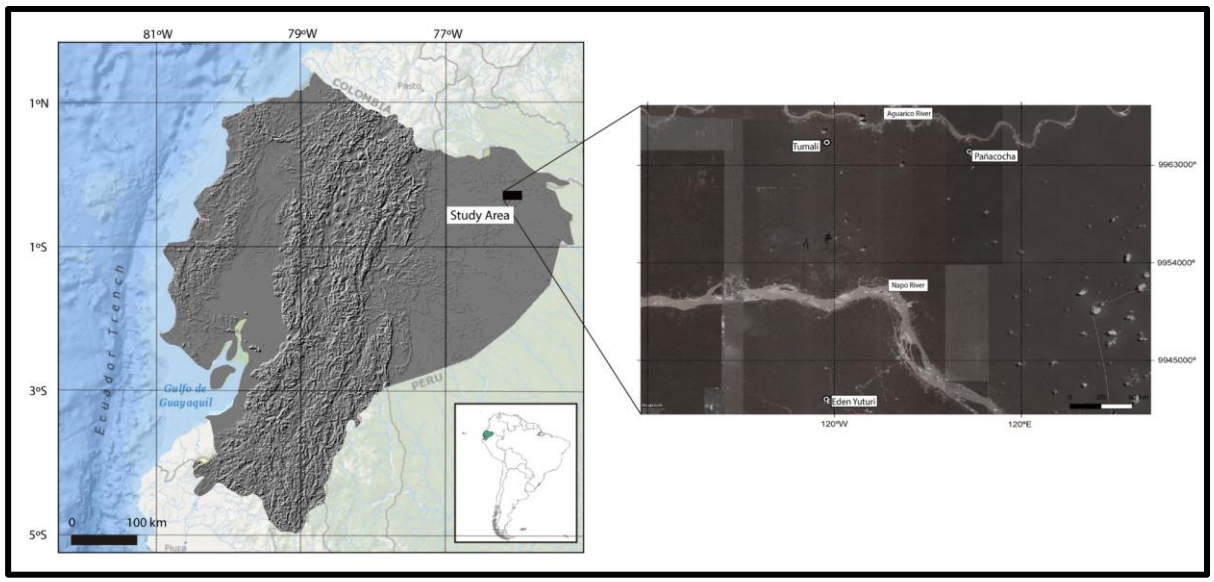

Figure 4.1. *Location map of the study area. Western Ecuadorian Basin. Satellite image from Google Earth ©.*

CHAPTER 5

5. METHODOLOGY

Stratigraphic sections were analyzed in a regional context to characterize the ichnology, sedimentology, and sequence stratigraphy of the U and M2 Sandstone members (Figure 8.6 and Figure 8.11, accordingly). Careful sedimentary facies descriptions were done based on the analysis of six cores, provided by Petroamazonas Ecuador E.P. Performed parallel to facies analysis, ichnologic analysis, comprising both ichnofacies and ichnofabrics characterization, was conducted in order to identify environmental controls on sedimentation.

5.1.Phase I: Literature Review

This phase consists of a compilation of geologic data of the study area in order to summarize the main geologic background of the Napo Formation. Relevant information was retrieved from literature and documents including published scientific articles, books, theses, and conference proceedings.

5.2.Phase II: Data Collection

Core images were provided by the public company E.P. Petroecuador, in total three wells penetrating the U Sandstone Member, and three wells penetrating the M2 Sandstone Member. The core description focuses on facies analysis and ichnology, taking into consideration lithology, color, grain size, grain distribution, mineralogy, sedimentary structures, body-fossil content and distribution, trace-fossil composition, and bioturbation index. Moreover, lithological interpretations are confirmed with well log data. Gamma Ray logs were used.

5.3.Phase III: Data Integration and Interpretation

This phase comprises the processing, integration and interpretation of the geologic data collected in phases I and II.

In this phase, an initial analysis of core images was performed for each well. For each one of them, trace fossils, sedimentary facies, and body-fossil content were characterized.

Analyses of each well core contribute to the definition of lithofacies, facies associations, ichnofacies and depositional paleoenvironments. Finally, the integration of these results with previous work allows proposing a novel depositional and sequence stratigraphic model for the U and M2 Sandstone members.

In this phase, a detailed database with the description of sedimentary facies and trace fossils in the U and M2 Sandstone members for the six different wells has been produced.

CHAPTER 6

6. LIMITATIONS

In this section, some limitations encountered while conducting this research are outlined:

- The cores owned by Petroamazonas Ecuador E.P. are stored in the "Litoteca de San Rafael" in Quito, Ecuador. Unfortunately, the cores were relocated on several occasions, resulting in the misidentification of various complete cores over time. Moreover, core access is hindered by lengthy company protocols.

- There are no confirmed outcrops of the M2 and U Sandstone members.

CHAPTER 7

7. LITHOFACIES, FACIES ASSOCIATIONS, AND TRACE-FOSSIL ANALYSIS

For this project, data from 25 wells was collected, but only 6 were used since the remaining wells did not reach the target interval (U and M2 Sandstone members) or the information lacked image quality. The information was provided by the public company Petroamazonas del Ecuador E.P.

A total of six cores have been analyzed and described, totaling ca. 150 m. Also, the log data information has helped to confirm petrographic analysis. The information gathered has allowed proposing sedimentary facies descriptions and interpretation.

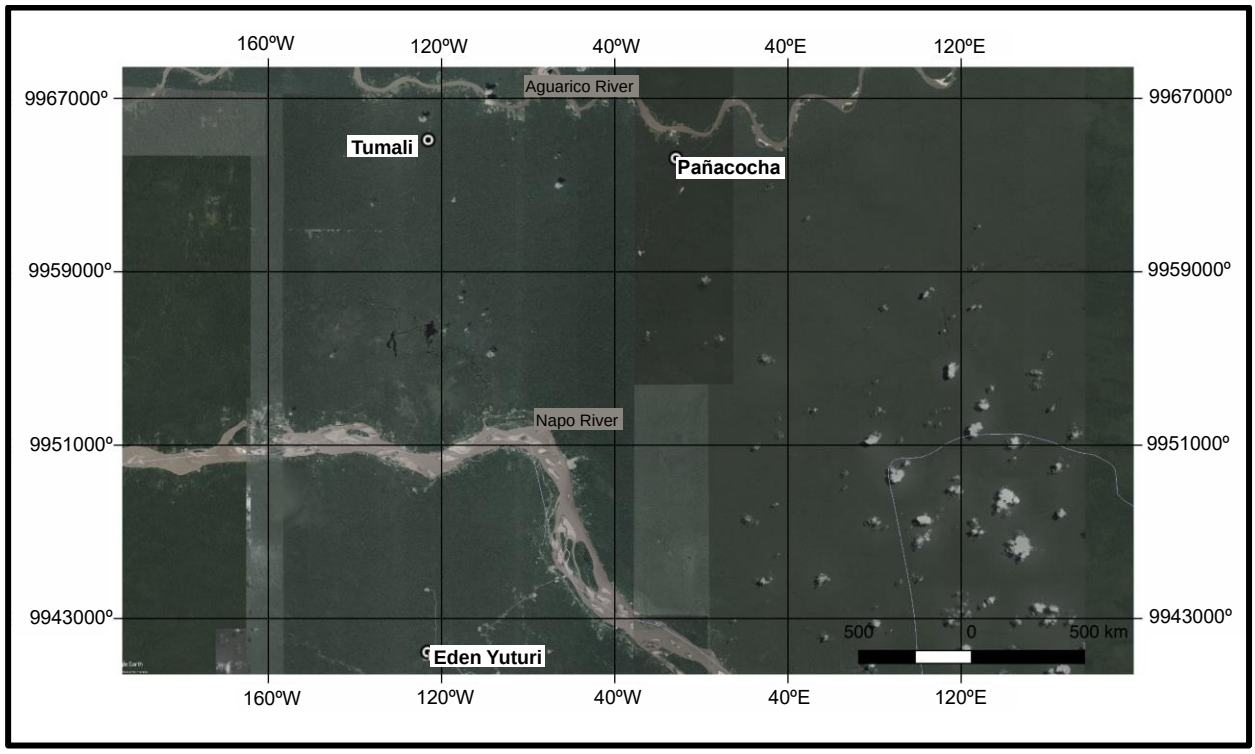

Figure 7.1. *Spatial distribution of oil fields studied for this project (modified from Google Earth©).*

7.1.Facies

Sedimentary facies were defined based on core analysis and preliminary labeled with numbers. Degree of bioturbation was assessed following Taylor & Goldring (1993; see also Reineck, 1967). In this scheme, a sedimentary unit characterized by no bioturbation (0%) corresponds to a bioturbation index (BI) of 0. Sediments that display sparse bioturbation with few discrete trace fossils equal BI 1 (1 to 4%). Low intensity of bioturbation in deposits that still have preserved sedimentary structures equals BI 2 (5 to 30%). BI 3 (31 to 60%) refers to sediment with discrete trace fossils, moderate levels of bioturbation, and still distinguishable bedding boundaries. A BI of 4 (61 to 90%) is characterized by intense bioturbation, high trace-fossil density, with common overlapping of trace fossils, and with primary sedimentary structures mostly erased. Deposits with completely disturbed bedding and showing intense bioturbation equals a BI of 5 (91 to 99%), and completely bioturbated and reworked sediment, owing to repeated overprinting of trace fossils, would be BI 6 (100%).

7.1.1. Facies 1. Trough cross-bedded, coarse-grained sandstone

Description: Facies 1 consists of brown to black colour, erosionally based, trough cross-stratified, coarse-grained sandstone (Figure 7.2). Some beds show massive appearance. Lithic fragments are present. Discrete beds are not readily apparent. The facies forms 0.6-4.7 m thick (average 1.5 m) intervals.

Bioturbation structures are locally present (BI= 0-3). *Palaeophycus* isp. is relatively common, and *Skolithos* isp. occurs in lower abundance and occasionally restricted to the top.

Distribution: Facies 1 was recognized in the U Sandstone Member in wells Pañacocha B003 (7243.1'-7251'; 7313.7'-7320.8'; 7323.5'-7330.7'; 7331.5'-7334'), Eden Yuturi 005 (7363'-7383.4'; 7421.5'-7444'), and Tumali 003 (8911'-8915.6').

Interpretation: Facies 1 is interpreted as fluvial channel-fills. Its coarse grain and erosional base are evidence for a high-energy, channelized environment. The trough cross-stratification indicates the migration of subaqueous 3D dunes, which is consistent with deposition in a fluvial environment. The presence of massive beds may suggest participation

of hyperpycnal flows (Zavala et al., 2011, 2018). The low abundance of trace fossils is consistent with high energy due to rapidly migrating bedforms (e.g. MacEachern et al., 2005; Dalrymple & Choi, 2007; Buatois et al., 2012). *Palaeophycus* is a facies-crossing ichnotaxon, which is present in both freshwater and brackish-water settings. However, monospecific occurrences are relatively common in the former (Buatois & Mángano, 2004). The restriction of *Skolithos* isp. to the top of a channel-fill below a flooding surface may suggest colonization by a highly tolerant brackish-water organism during transgression, although this ichnotaxon is not indicative of marine conditions *per se* (Buatois & Mángano, 2004). The fluvial channel-fill occurs either below Facies 2, regarded as floodplain deposits (i.e. Pañacocha B003, Figure 8.4) or below Facies 3, interpreted as estuarine channel and bars (i.e. Eden Yuturi 005, Figure 8.3). In the latter case, the upper boundary of Facies 1 is marked by a transgressive surface.

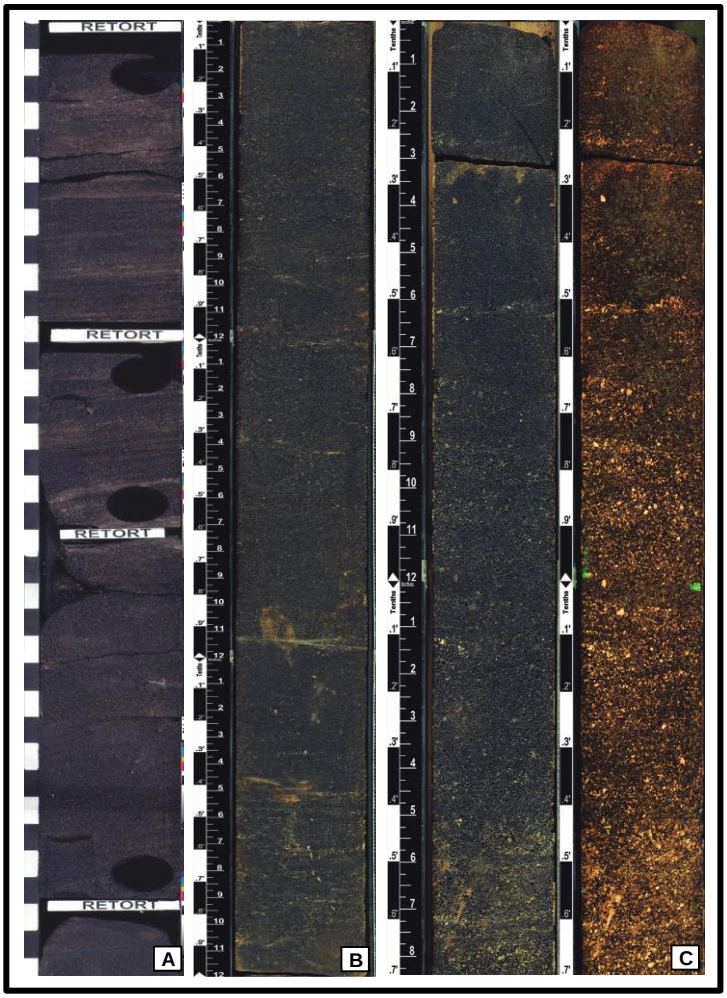

Figure 7.2. *Facies 1. Trough cross-bedded, coarse-grained sandstone (A) Trough cross stratification, and oily impregnated facies. Eden Yuturi 005 well, 7440'. (B) Coarse-grained sandstone. Pañacocha B003 well, 7332'. (C) Massive appearance. Pañacocha B003 well, 7329'.*

7.1.2. Facies 2. Lenticular-bedded mudstone, silty sandstone and structureless medium-grained sandstone

Description: Facies 2 consists of grey, massive mudstone (0.8–1.6 m thick), with sharp surfaces, and locally interbedded with a structureless medium-grained sandstone (0.15–0.3 m thick) (Figure 7.3). Very fine-grained silty sandstone interbedded within the mudstone intervals forming lenticular bedding. Some intervals may present soft-sediment deformation structures (e.g. convolute lamination). The facies forms 0.2-2.7 m thick (average 1.4 m thick) intervals.

Mudstone and structureless medium-grained sandstone intervals are commonly unbioturbated (BI=0). However, the silty sandstone layers display varying degrees of bioturbation (BI= 1-2). The bioturbation structures present are *Planolites* isp. and *Palaeophycus* isp.

Distribution: Facies 2 was described the U Sandstone Member in wells Pañacocha B003 (7312.1'-7313.7'; 7320.8'-7323.5'; 7330.7'-7331.5').

Interpretation: Facies 2 is interpreted as floodplain deposits. Dominant mudstone lithofacies represents low-energy suspension fallout as the dominant process during its deposition. The intercalated very fine-grained silty sandstone points to sand fraction movement representing occasional current action, most likely reflecting overbank flooding. The soft-sediment deformation structures represent sediment instability caused by density contrast between sand and mud and movement of pore fluids though the sediment as a result of rapid overbank deposition. The sparse bioturbation and low ichnodiversity suggest stressful conditions, but no ichnologic evidence of marine influence is apparent because both *Palaeophycus* and *Planolites* are facies-crossing ichnotaxa, which occur in both freshwater and marine environments (Buatois & Mángano, 2007). The trace-fossil association of Facies 2 does not have diagnostic ichnotaxa that allow to confidently assign it to an ichnofacies,

although it shows affinities with the depauperate *Mermia* Ichnofacies (Buatois & Mángano, 2004). This ichnofacies characterizes benthos colonization in low energy and permanently subaqueous freshwater zones. Deposition in a floodplain environment is further supported by stratigraphic relationships, as indicated by its presence on top of fluvial channel-fill deposits (Facies 1) (i.e. Pañacocha B003, Figure 8.4).

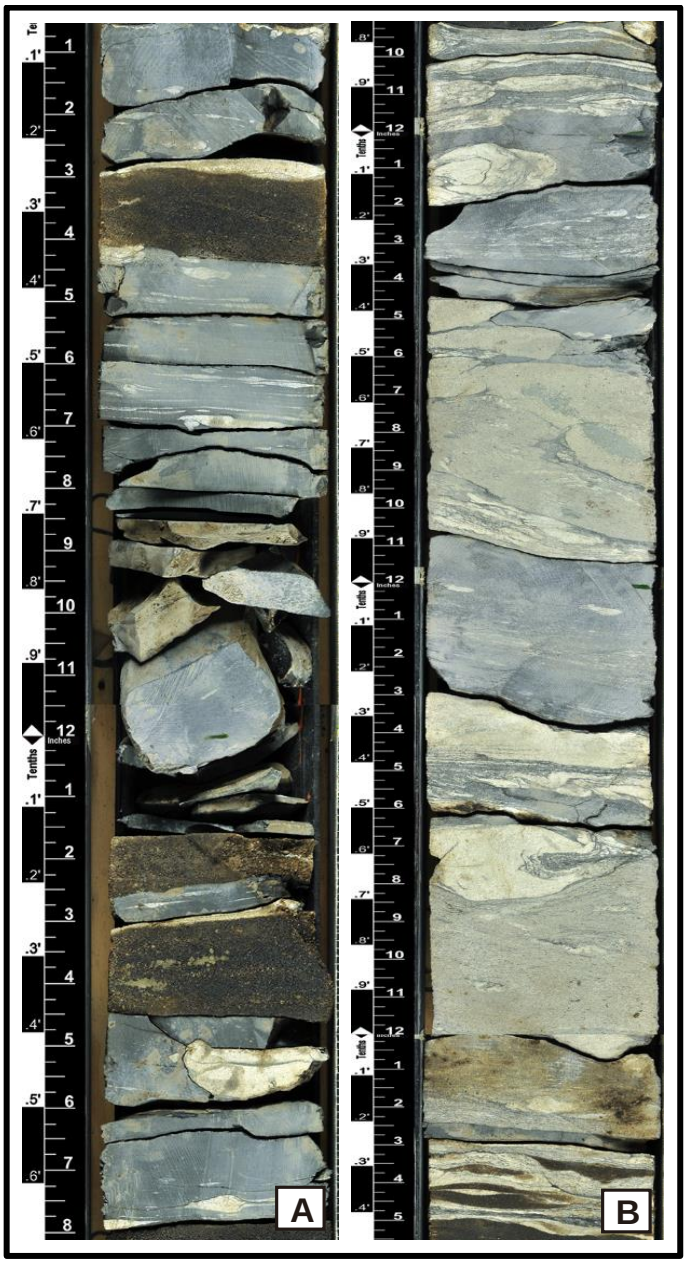

Figure 7.3. *Facies 2. Lenticular-bedded mudstone, silty sandstone and structureless medium-grained sandstone (A) Local lenticular bedding. Pañacocha B003 well, 7312'. (B) Bioturbated interval.* Palaeophycus *isp. and* Planolites *isp. Pañacocha B003 well, 7320'.*

7.1.3. Facies 3. Cross-stratified medium- to coarse-grained sandstone with mudstone drapes

Description: Facies 3 consists of yellow to dark brown, erosively based, trough to planar cross-bedded, medium- to coarse-grained sandstone, forming fining-upward successions (Figure 7.4). The base of facies intervals is commonly delineated by a scoured surface. Double- and single-mudstone drapes are typically present throughout the deposit. Massive unbioturbated mudstone is present locally. Oil impregnation is high in some intervals, locally affecting the visibility of sedimentary structures. Discrete beds are 0.1-0.3 m in thick. The facies forms 0.8-13.1 m thick (average 4.0 m thick) intervals.

Bioturbation structures are generally sparse (BI=2-3), and some mudstone intervals and coarse-grained sandstone layers are unbioturbated (BI=0). Where present, the ichnofauna consists of *Bergaueria* isp., *Palaeophycus* isp., *Planolites* isp., *Rhizocorallium commune*, *Skolithos* isp, *Teichichnus* isp, and *Thalassinoides* isp.

Distribution: Facies 3 was recognized in the U Sandstone Member in wells Eden Yuturi 005 (7334'-7363'; 7397.6'-7419.3'), Pañacocha B003 (7229.1'-7241.4'; 7242.1'-7242.7'; 7284.1'-7312.1'), and Tumali 003 (8901'-8910.5'; 8953.5'-8958.4'; 8960.4'-8969.5'; 8970.5'-8972'; 8973'-8988').

Interpretation: Facies 3 is interpreted as estuarine or deltaic tidal channel and bar deposits (e.g. Dalrymple et al., 1992; Dalrymple & Choi, 2007). The channelized environment is characterized by basal erosional contacts, and dune-scale current-generated sedimentary structures, such as planar and trough cross-stratification. The tide-influenced interpretation is supported by the presence of double- and single-mudstone drapes. Presence of multiple internal reactivation surfaces represent deposition in multi-storey channels. Moreover, the occasional presence of massive unbioturbated mudstone is interpreted as recording fluid muds, which represent slack-water periods where mud sediment concentration may become high preventing sediment consolidation, and settling of the suspended sediment (Ichaso & Dalrymple, 2009). Facies 3 may represent two different environments of deposition: estuarine and deltaic. Tidal channels and bars in these two environments are similar in terms of their sedimentary structures and lithology; however, differentiation between the two is based on stratigraphic relationships. Intervals of Facies 3

interpreted as estuarine tidal channel and bar deposits occur on top of fluvial channel fills (Facies 1), therefore representing transgressive deposition and a backstepping stacking pattern (e.g. Pañacocha B003 and Eden Yuturi 005, Figure 8.4 and Figure 8.3 respectively). On the other hand, intervals of Facies 3 interpreted as deltaic tidal channel and bar deposits occur in a progradational context, and are associated with facies interpreted as formed in various deltaic subenvironments (Facies 5, Facies 6, Facies 7, and Facies 8) (e.g. Pañacocha B003, Figure 8.4). Sparse bioturbation also supports the interpretation of a channelized environment because these are high stress settings that tend to preclude infaunal colonization. The trace-fossil assemblage in the deltaic tidal channel and bar deposits may represent an example of a depauperate *Cruziana* Ichnofacies (e.g. Moslow & Pemberton, 1988; Gingras et al., 2008).

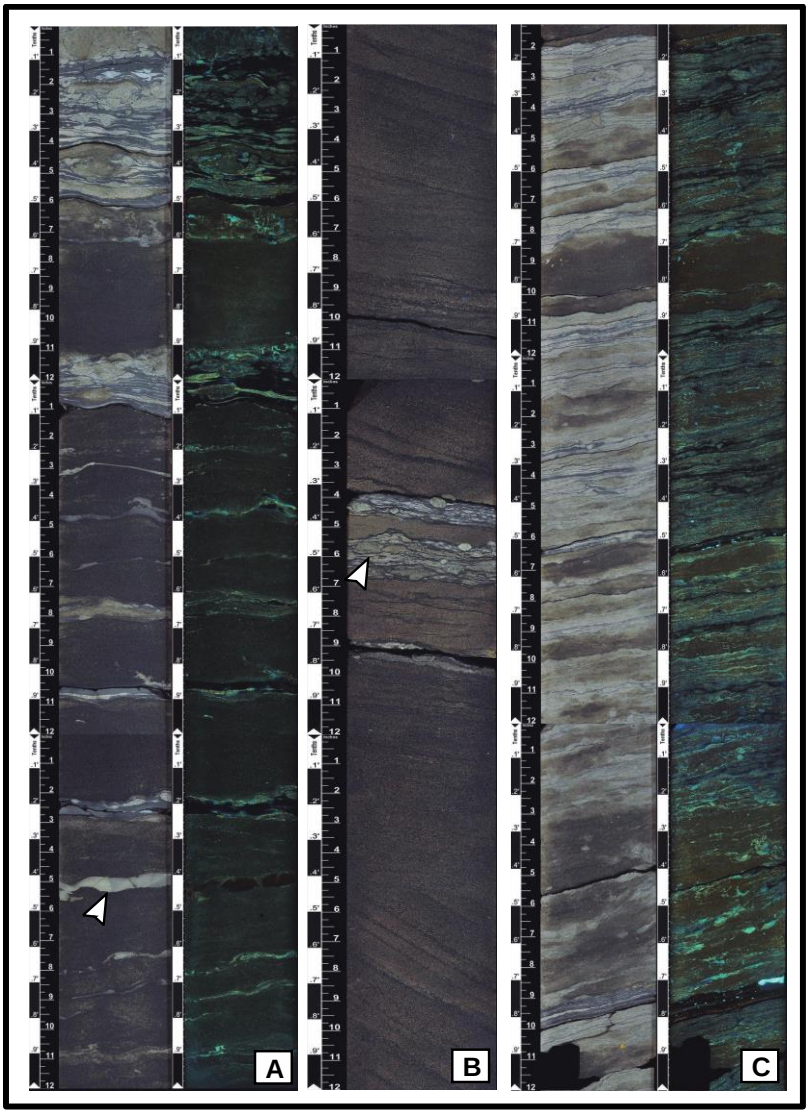

Figure 7.4. *Facies 3. Cross-stratified medium- to coarse-grained sandstone with mudstone drapes. (A) Fluid muds (arrowed). High-oil impregnation. Tumali 003 well, 8953'. (B) Double- and single-mudstone drapes and* Palaeophycus *isp (arrowed). Tumali 003 well, 8903'. (C) Medium-grained sandstone with double mudstone drapes and* Palaeophycus *isp. Local oil-impregnation. Tumali 003 well, 8963'.*

7.1.4. Facies 4. Flaser-, wavy- and lenticular-bedded mudstone and silty sandstone

Description: Facies 4 consists of grey, massive mudstone (0.6–1.0 m thick), locally interlayered with an erosionally based, very fine-grained silty sandstone (0.3-0.5 m thick), forming wavy-, flaser- and lenticular-bedded intervals (0.9-1.5 m thick) (Figure 7.5). Siderite bands and nodules may be present locally. The facies forms 0.4-3.5 m thick (average 1.6 m thick) intervals.

Mudstone intervals are commonly unbioturbated (BI=0). Silty sandstone layers display varying degrees of bioturbation (BI= 1-3). Heterolithic intervals are commonly sparsely bioturbated (BI=1-2). The bioturbation structures present are *Bergaueria* isp., *Palaeophycus* isp., *Planolites* isp., *Teichichnus* isp., and *Teichichnus rectus*.

Distribution: Facies 4 was described the U Sandstone Member in wells Eden Yuturi 005 (7396.3'-7397.6'; 7419.3'-7421.5'), Pañacocha B003 (7241.4'-7242.1'; 7242.7'-7243.1'), and Tumali 003 (8910.5'-8911'; 8915'-8916'; 8950.3'-8953.5'; 8958.4'-8960.4'; 8969.5'-8970.5'; 8972'-8973').

Interpretation: Facies 4 is interpreted as estuarine tidal flat deposits (e.g. Dyer, 1998, 2000). Dominant mudstone lithofacies suggests the predominance of low-energy suspension fallout. The interbedded, silty sandstone indicates the occasional influence of tractive currents. The heterolithic intervals with flaser, wavy, and lenticular bedding suggest alternating current-generated sandstone and suspension-fallout mudstone, the latter accumulated during slack-water periods, which supports the interpretation of tidal action during its deposition. Local siderite bands and nodules suggest brackish-water conditions (e.g. Postma, 1982; Solórzano et al., 2017). Moreover, the sparse bioturbation and low ichnodiversity indicate stressful conditions, most likely reflecting brackish water. This is further supported by the presence of the ichnogenus *Teichichnus*, which is only present in marine settings (e.g. Buatois et al., 2005; Knaust, 2018). The trace-fossil association of Facies

4 illustrates the depauperate *Cruziana* Ichnofacies (e.g. MacEachern & Pemberton, 1992). Deposition in an estuarine tidal flat environment is further supported by stratigraphic relationships, as indicated by its presence above estuarine tidal channel and bars deposits (Facies 3) (i.e. Tumali 003, Figure 8.2).

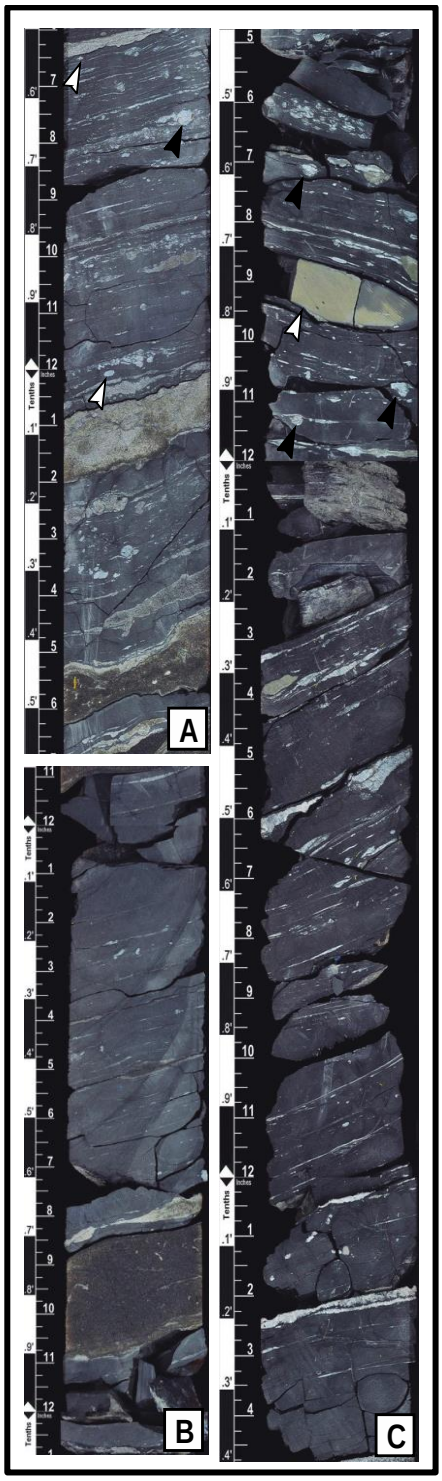

Figure 7.5. *Facies 4. Flaser-, wavy- and lenticular-bedded mudstone and silty sandstone (A) Lenticular and wavy bedding, locally showing sparse* Planolites *isp. (white arrow),* Teichichnus *isp. (black arrow). Tumali 003 well, 8969'. (B) Massive, lenticular-bedded mudstone. Tumali 003 well, 8972'. (C) Massive, lenticular-bedded mudstone locally with siderite nodules (white arrow) and* Teichichnus *isp. (black arrow). Tumali 003 well, 8958'.*

7.1.5. Facies 5. Intensively bioturbated, fine- to medium-grained sandstone with thin mudstone interbeds

Description: Facies 5 consists of greenish and brownish coloured, gradationally based, intensely bioturbated with a mottling texture, fine- to medium-grained sandstone. Mudstone drapes are locally present (Figure 7.6). Locally, erosively based, planar to locally trough cross-bedded, medium- to coarse-grained sandstone occurs. The green colour is due to >40% of glauconitic composition. Local sharp-based mudstone layers. Siderite bands and nodules. Thickness estimation of individual beds is typically hampered by the high bioturbation intensity; where possible to estimate, discrete sandstone beds are 0.5-3.5 m thick, whereas mudstone beds are 0.015-0.2 m thick. The facies forms 0.4-6.9 m thick (average 3.7 m thick) intervals.

Degree of bioturbation varies from sparse to intense (BI=0-3) in the sandstone. Bioturbation structures are abundant and diverse, including *Palaeophycus* isp., *Siphonichnus isp., Skolithos* isp., *Teichichnu*s isp., *Teichichnus rectus, Planolites* isp., *Thalassinoides* isp., and *Ophiomorpha nodosa*. Locally, burrow fills in the glauconitic intervals consist of glauconitic pellets. Bivalve fragments are present. However, mudstone intercalations are unbioturbated (BI=0).

Distribution: Facies 5 was recognized in the U and M2 Sandstone members in wells: Pañacocha B010 (7145.1'-7148.7'; 7149.3'-7153.3'; 7154,7'-7155,9'; 7158'-7165.7'; 7167.3'-7177.5'; 7177.9'-7178.8'; 7182.3'-7183.7'), Tumali 004 (8194.3'-8199'; 8217.5'-8220'; 8223'-8226'), Eden Yuturi 005 (7200.6'-7206.7'; 7207.5'-7209.6'; 7211.4'-7224.8'; 7225.2'-7229.2', 7233.4'-7237.7'; 7239.7'-7245.1'; 7245.9'-7252'; 7322'-7331.6'; 7383.4'-7386.5'), Tumali 003 (8916'-8919.1'), and Pañacocha B003 (7212'-7221.3'; 7223.2'-7224'; 7224.5'-7227.5'; 7251'-7255.1'; 7261.7'-7263.3'; 7266'-7268.1'; 7269'-7269.9'; 7271'-7272.9').

Interpretation: Facies 5 is interpreted as delta front deposits (Giosan & Bhattacharya, 2005). Fluid muds are represented by unbioturbated and homogeneous structureless mudstone layers deposited commonly in areas beneath the turbidity maximum (Ichaso & Dalrymple, 2009; Peng et al., 2018). Fluid muds are typically associated with hyperpycnal flows (Mulder et al., 2003; Bhattacharya & MacEachern, 2009), whereas the recurrence of local mudstone drapes are evidence for tidal influence (Davis & Dalrymple, 2012). The local presence of trough-cross stratification and planar cross-stratification indicates the migration of 3D and 2D dunes, respectively, in terminal distributary channels. Siderite nodules and bands are indicative of brackish-water conditions suggesting freshwater discharge (Bhattacharya & MacEachern, 2009). Glauconitic content indicates that the system experienced times of open marine conditions (Odin, 1988), arguing in favor of a deltaic context rather than more permanent brackish-water conditions, as in an estuary. The delta front origin is additionally supported by stratigraphic relationships, as indicated by the presence of Facies 5 above Facies 6, interpreted as proximal prodeltaic deposits (i.e. Pañacocha B010 well section Figure 8.8). Facies 5 shows suites recording low ichnodiversity compared with their fully marine counterparts, representing the *Skolithos* and *Cruziana* Ichnofacies in their depauperate versions. However, the sandstone intervals are intensively bioturbated which may be evidence of low stressors. Hence, the intense bioturbation may record a well-oxygenated seafloor, which could be related to tidal agitation (e.g. Gani et al., 2007), as well as significant pauses between sedimentary events.

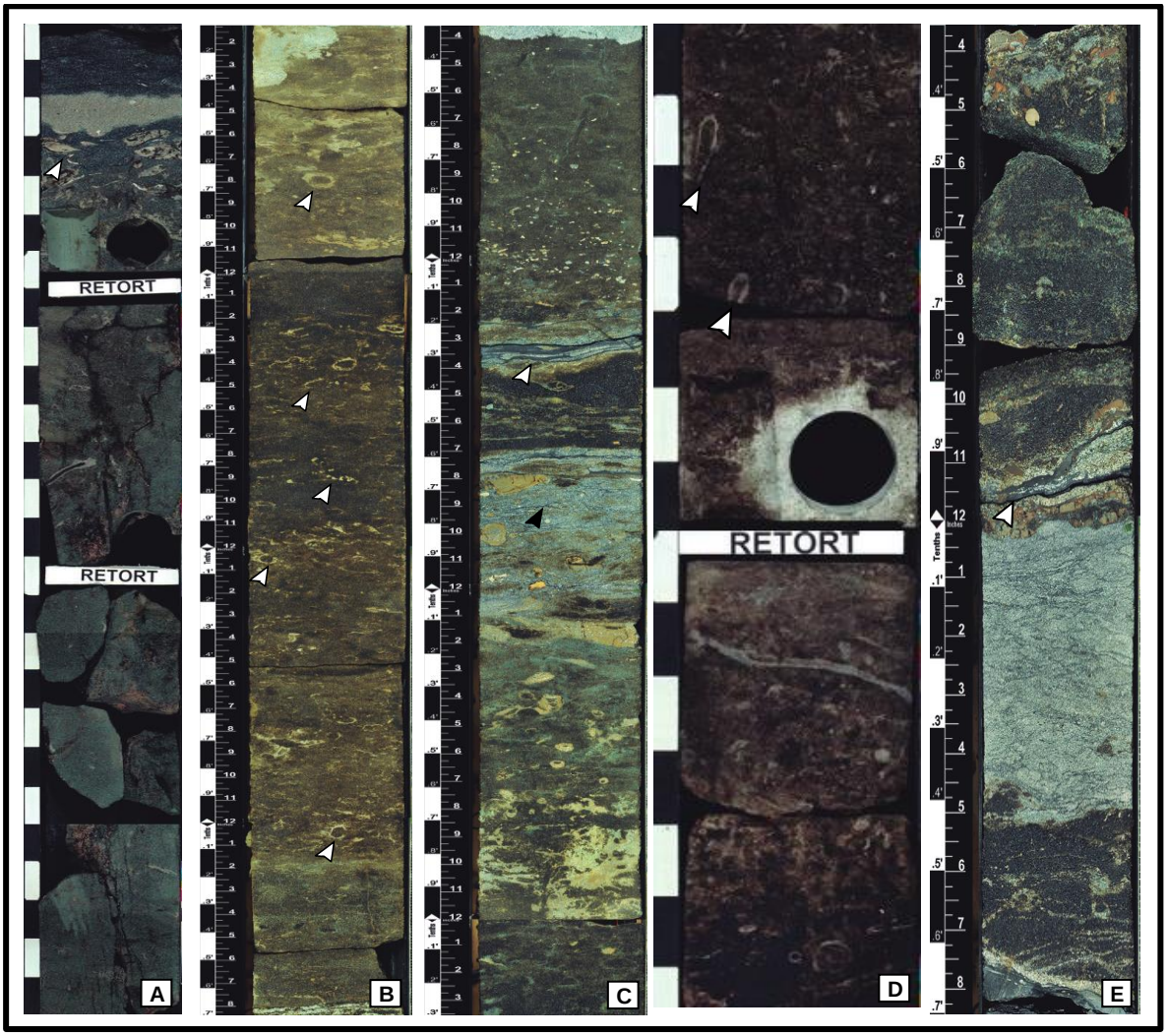

Figure 7.6. *Facies 5. Intensively bioturbated, fine- to medium-grained sandstone with thin mudstone interbeds. (A) Bivalve fragments in the uppermost part of the interval (arrowed). Eden Yuturi well, 7245'. (B)* Ophiomorpha nodosa (arrowed)*. Pañacocha B010 well, 7145'. (C) Fluid mud (white arrow) and mudstone drapes (black arrow). Pañacocha B010 well, 7167'. (D*) Ophiomorpha nodosa (arrowed)*. Eden Yuturi 005 well, 7203'. (E) Highly bioturbated sandstone and mudstone drapes (arrowed). Pañacocha B010 well, 7182'.*

7.1.6. Facies 6. Moderately bioturbated, very fine-grained silty sandstone and mudstone

Description: Facies 6 consists of dark grey massive mudstone irregularly interbedded with white-yellow coloured, gradationally or sharp based, very fine-grained silty sandstone (Figure 7.7). These heterolithic deposits are typically highly bioturbated; hence, sedimentary structures are hard to identify. However, some intervals show lenticular, flaser, and wavy

bedding. Silty sandstone/mudstone ratios are high (2:1). Estimation of thickness of discrete beds is locally difficult due to intense bioturbation. However, where estimation is possible, discrete silty sandstone beds are 0.15-0.6 m thick, whereas mudstone beds are 0.015-0.5 m thick. The facies forms 0.4-5.5 m thick (average 1.6 m thick) intervals.

Silty sandstone beds show varying degrees of bioturbation (BI=2-6), but mudstone intervals are commonly unbioturbated (BI=0). The ichnofauna consists of *Asterosoma* isp., *Bergaueria* isp., *Conichnus* isp., *Palaeophycus* isp., *Planolites* isp., *Rhizocorallium commune*, *Siphonichnus* isp., *Skolithos* isp., *Teichichnus* isp., *Teichichnus rectus*, *Thalassinoides* isp, and *Zoophycos* isp. Bivalve fragments are recognized in places.

Distribution: Facies 6 was recognized in the U and M2 Sandstone members in wells: Pañacocha B010 (7125'-7125.7'; 7131.2'-7131.7'; 7131.8'-7135.9'; 7136.3'-7140'; 7153,3'-7158'; 7177.5'-7177.9'; 7178.8'-7182.3'; 7183.7'-7185'), Eden Yuturi 005 (7224.8'-7225.2'; 7229.2'-7233.4'; 7237.7'-7239.7'; 7245.1'-7245.9'; 7331.6'-7334'; 7386.5'-7389'), Pañacocha B003 (7221.3'-7223.2'; 7224'-7224.5'; 7227.5'-7229.1'; 7255.1'-7257.6'; 7263.3'-7266'; 7272.9'-7274.2'), Tumali 004 (8187'-8192'; 8199'-8200'), and Tumali 003 (8896'-8901'; 8919.1'-8926.5'; 8932'-8940')

Interpretation: Facies 6 is interpreted as proximal prodeltaic deposits with occasional tide influence (e.g. Giosan & Bhattacharya, 2005). The presence of sedimentary structures in the silty sandstone beds, such as lenticular, flaser, and wavy bedding, are evidence of alternation of tractive sand sedimentation (i.e. current action) and suspension fallout (Reineck & Wunderlich, 1968). However, the silty sandstone is interpreted as the result of sediment-gravity flows that accumulated from highly concentrated bedload layers formed beneath these flows to posteriorly being driven by turbulent overlying flows (Mulder et al., 2003). Sharp-based very fine-grained silty sandstone to mudstone record migration of fluid mud as result of hyperpycnal flow discharge (Mulder et al., 2003). Silty sandstone may locally be scoured by the mudstone layers (fluid muds), consistent with hyperpycnal emplacement (Bhattacharya & MacEachern, 2009). Therefore, these deposits are interpreted as the result of turbulent flows of fluctuating energy that reached the more distal areas, in this case the prodelta, where high suspended-sediment concentration was the dominant process (e.g. Zavala et al., 2006; Soyinka & Slatt, 2008). The presence of *Thalassinoides* in these

deposits may represent opportunistic colonization of these hyperpycnal deposits (Buatois et al., 2011). The glauconitic content for some silty sandstone intervals supports the interpretation of open marine conditions. Unbioturbated mudstone (BI=0) successions grade into bioturbated (BI=2-6) silty sandstone of the tide-influenced prodelta. The unbioturbated thin mudstone intervals reinforce the fluid-mud interpretation. However, the highly bioturbated silty sandstone intervals indicate suitable conditions for colonization by the infauna. The intense and more uniform bioturbation, and the higher ichnodiversity in the sandstone-dominated intervals suggest a lesser impact of stress factors, pointing to relatively prolonged times of open marine conditions between times of river-induced discharge. In general, uniform bioturbation is regarded as reflecting homogeneous distribution of food, marine salinity, and available oxygen in the seawater due to a longer colonization window reflecting slow deposition rates and low energy. The trace-fossil suites in these deposits show affinities with the *Cruziana* Ichnofacies. In contrast, silty sandstone intervals in between the fluid muds may present moderate bioturbation (BI 2-4) and ichnodiversity (e.g. *Palaeophycus* isp., *Planolites* isp.) representing the depauperate *Cruziana* Ichnofacies. Deposition in a tide-influenced prodelta is further supported by stratigraphic relationships, as indicated by its presence below Facies 5, interpreted as delta front deposits (i.e. Eden Yuturi 005 well section, Figure 8.3).

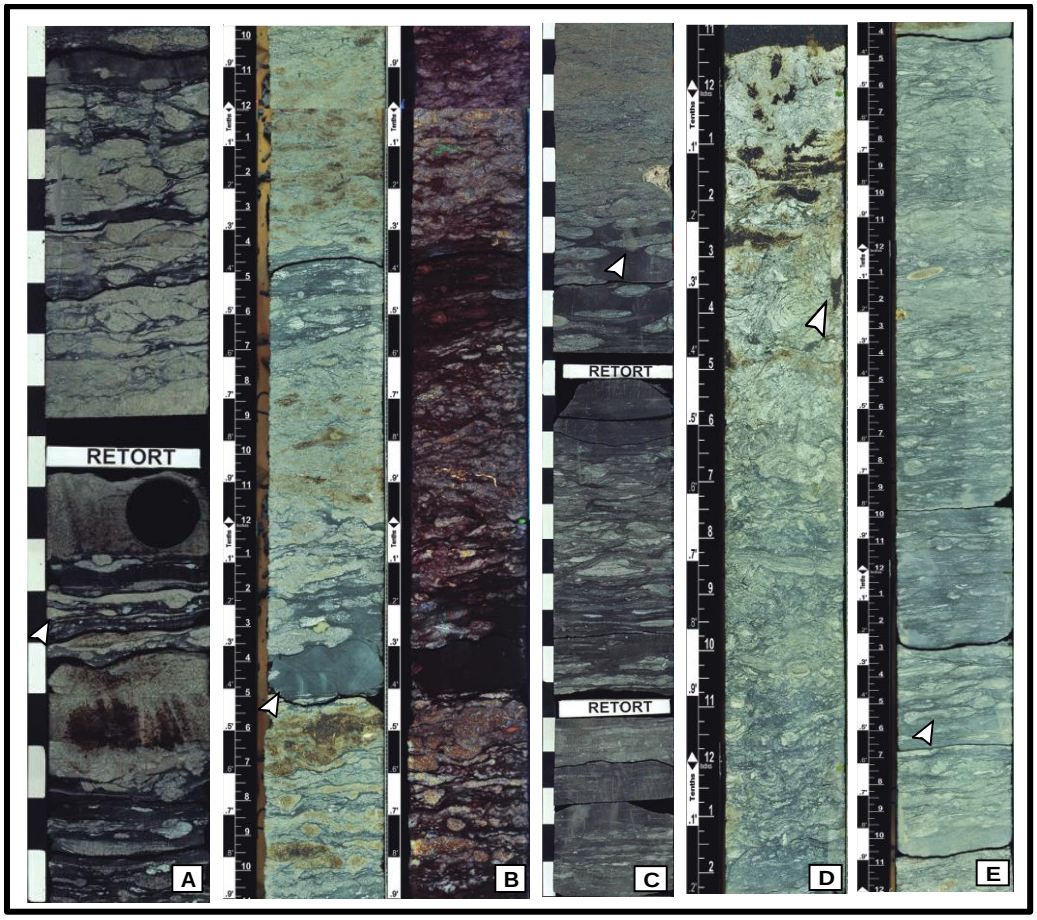

Figure 7.7. *Facies 6. Moderately bioturbated, very fine-grained silty sandstone and mudstone. (A) Wavy and lenticular bedding (arrowed). Eden Yuturi 005 well, 7231'. (B) Fluid-muds (arrowed). Pañacocha B010 well, 7133'. (C)* Thalassinoides *isp. (arrowed), Eden Yuturi 005 well, 7386'. (D) Highly bioturbated section.* Conichnus *isp. (arrowed). Pañacocha B003 well, 7272'. (E) Highly bioturbated facies*. Rhizocorallium commune *(arrowed). Pañacocha B003 well, 7263'*

7.1.7. Facies 7. Mudstone

Description: Facies 7 consists of dark grey colored, gradationally based mudstone. Most of this facies has a structureless appearance (Figure 7.8). Siderite nodules and bands are present locally in the lowermost part of the intervals. Silty sandstone with local lenticular and flaser bedding may be present. Discrete beds are not readily apparent. This facies forms 0.1-7.4 m thick (average 2.0 m thick) intervals.

Commonly mudstone intervals are unbioturbated (BI=0); however, bioturbation is recognized in some silty sandstone intervals (BI=0-5). The trace fossils suites are typically

relatively diverse, including *Palaeophycus* isp., *Planolites* isp., *Teichichnus rectus*, *Thalassinoides* isp., and *Zoophycos* isp.

Distribution: Facies 7 was recognized in the U and M2 Sandstone members in wells: Pañacocha B010 (7125.7'-7131.2'; 7131.7'-7131.8'; 7135.9'-7136.3'; 7140'-7141.5'), Tumali 004 (8192'-8294.5'; 8200'-8202'; 8204'-8205'), Eden Yuturi 005 (7257.6'-7258.3'; 7274.2'-7279.4'; 7389'-7393.1'), Pañacocha B003 (7257.6'-7258.3'; 7274.2'-7279.4'), and Tumali 003 (8940'-8947.4').

Interpretation: Facies 7 is interpreted as distal prodeltaic deposits. The prodelta interpretation is further supported by stratigraphic relationships, as indicated by its presence below Facies 6, regarded as proximal prodeltaic deposits (i.e. Pañacocha B010 well section, Figure 8.8). The ichnogenus *Zoophycos* is commonly associated with silt and clay that accumulate continuously and slowly due to suspension fallout, allowing for intense bioturbation (MacEachern et al., 2007). The trace-fossil association of this facies illustrates the *Cruziana* Ichnofacies. The siderite nodule and bands suggest brackish-water conditions (e.g. Postma, 1982; Solórzano et al., 2017).

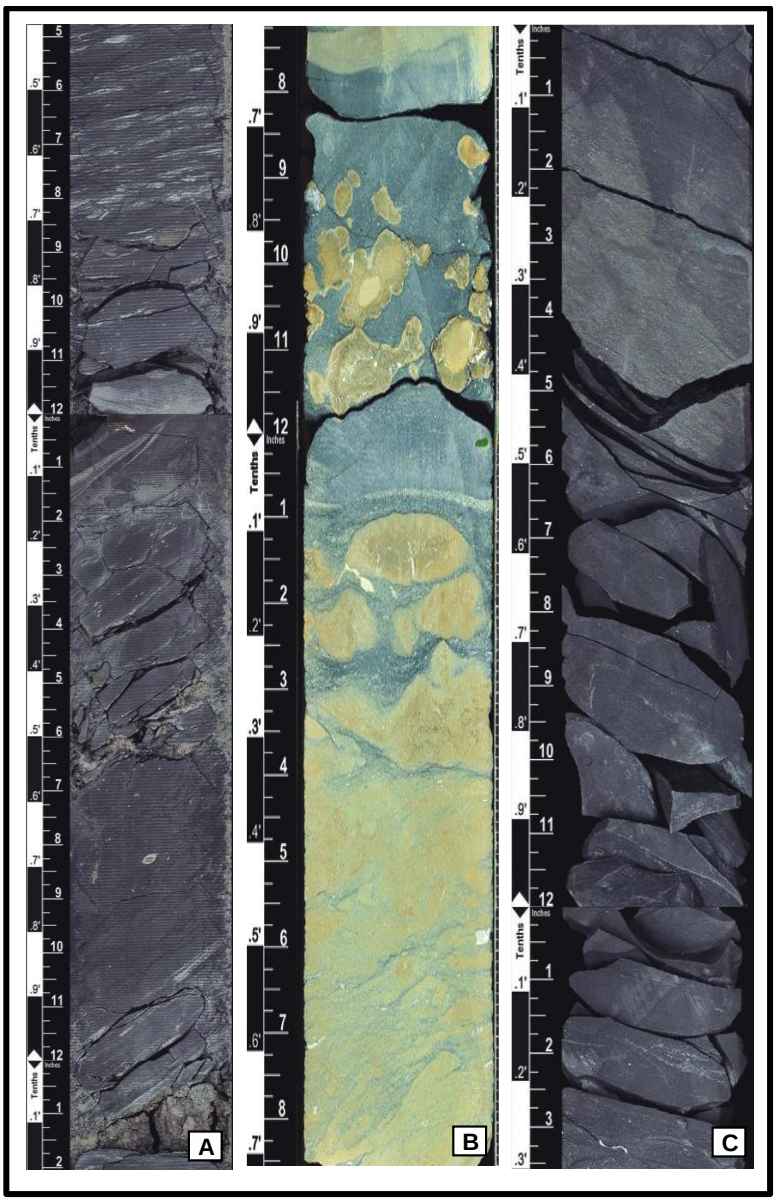

Figure 7.8. *Facies 7. Mudstone. (A) Local presence of lenticular lamination. Tumali 004 well, 8192'. (B) Phosphatic nodules. Pañacocha B003 well, 7257'. (C) Unbioturbated black mudstone. Tumali 003 well, 8946'.*

7.1.8. Facies 8. Bioclastic wackestone

Description: Facies 8 consists of a white-green colored, erosionally based, locally bioturbated, bioclastic wackestone (Figure 7.9). No primary sedimentary structures are observed. Local fractures may occur in some intervals. Discrete beds are 0.33-0.6 m thick. This facies forms 0.6-11.0 m thick (average 3.0 m thick) intervals.

Locally bioturbation is intense (BI= 4-6). Bioturbation structures are abundant, but poorly diverse, including *Palaeophycus* isp., *Planolites* isp., and *Teichichnus* isp. Bivalve fragments are abundant.

Distribution: Facies 8 was recognized in the U and M2 Sandstone members in wells: Pañacocha B010 (7141.5'-7145.1'; 7148.7'-7149.3'; 7165.7'-7167.3'), Tumali 004 (8202'-8204'; 8205'-8217.5'; 8220'-8223'), Pañacocha B003 (7258.3'-7261.7'; 7268.1'-7269'; 7269.9'-7271'; 7279.4'-7284.1'), Tumali 003 (8926.5'-8932'; 8947.4'-8950.3'), and Eden Yuturi 005 (7393.1'-7396.3').

Interpretation: Facies 8 is interpreted as transgressive deposits (e.g. Cattaneo & Steel, 2003; Steel et al., 2008; Buatois et al., 2012). This facies may represent mixed sediments generated by prolonged transgressions with rapid accumulation. The bioclasts mixed along the margins of contrasting facies trough the *in-situ* accumulation of calcareous organisms, as evidenced by the presence of entire body fossils. The paucity of gradational contacts represents shoreline retreat or abandonment of the deltaic deposition. Moreover, the vertical recurrence of this facies may represent punctuated shoreline migration. In this case, the shoreline trajectory may have recorded short-term regressions during an overall transgression due to changes in accommodation space or sediment supply. Punctuated transgressions may record a change in sediment supply rate due to climate change, a relative sea-level rise, or that the land surface did not slope linearly towards the sea (Cattaneo & Steel, 2003). Vertical facies transitions (i.e. Facies 8 occurring above Facies 5 interpreted as delta front deposits and below Facies 7, regarded as distal prodelta deposits) support the interpretation of Facies 8 (i.e. Pañacocha B003 well section, Figure 8.4). In this scenario, Facies 8 records high-energy ravinement surfaces (Cattaneo & Steel, 2003) and transition to deeper-water deposits, during deltaic abandonment. Moreover, the intense bioturbation is also indicative of stable conditions for organism colonization, representing the *Cruziana* Ichnofacies (e.g. Pemberton et al., 1982; Pemberton & Winghtman, 1992; MacEachern & Pemberton, 1994; Buatois et al., 2002; Mángano & Buatois, 2004; MacEachern & Gingras, 2007).

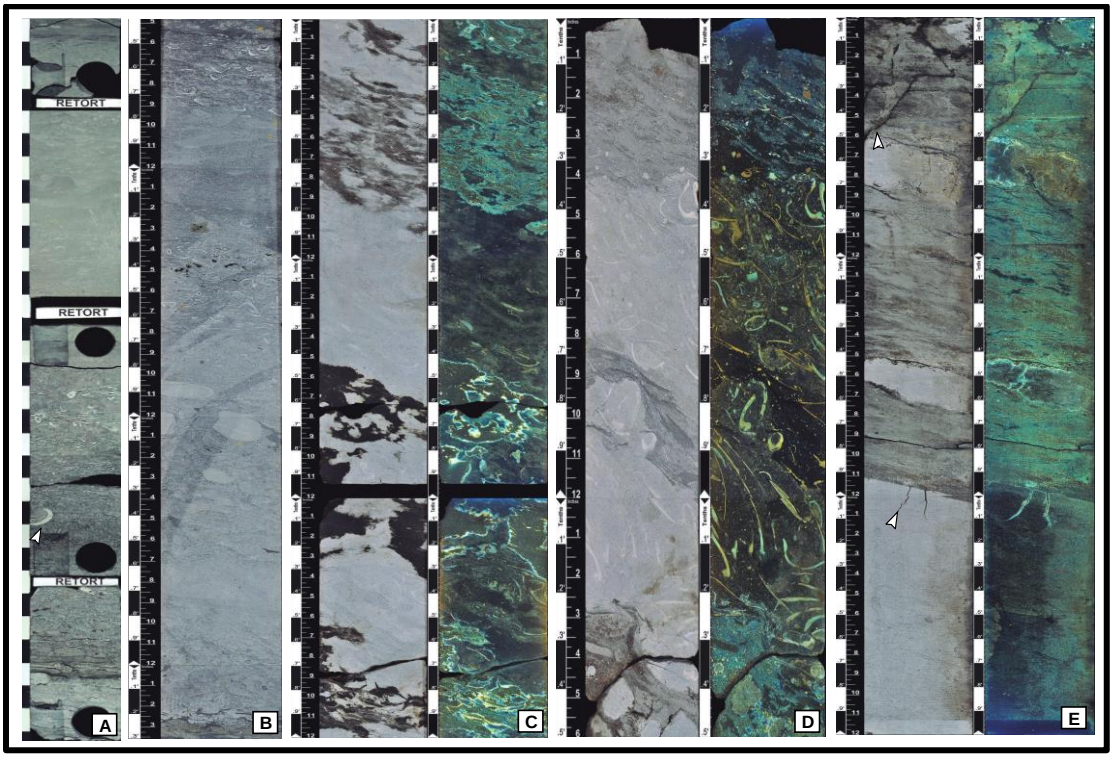

Figure 7.9. *Facies 8. Bioclastic wackestone (A) Bivalve fragments (arrowed). Eden Yuturi 005 well, 7393'. (B) Massive wackestone. Tumali 003 well, 8948'. (C) Isolated bioturbation structure in the upper part of the interval. Tumali 004 well, 8212'. (D) Abundant content of bivalve fragments. Lower section highly bioturbated. Tumali 004 well, 8205'. (E) Wackestone and medium-grained oil impregnated sandstone with local fractures (arrowed). Tumali 004 well, 8221'.*

7.1.9. Facies 9. Calcareous sandstone

Description: Facies 9 consists of a white colour, erosionally based, medium-grained sandstone with an overall massive appearance and calcareous cement (Figure 7.10). Discrete beds are not readily apparent. The facies forms 0.8-3.6 m thick (average 2.0 m) intervals.

Degree of bioturbation is moderate (BI=3-4). This facies presents bioturbation structures, such as *Thalassinoides* isp., *Asterosoma* isp.?, and indeterminate burrow mottling. Bivalve fragments are common.

Distribution: Facies 9 was recognized in the M2 Sandstone Member in Eden Yuturi 005 (7206.7'-7207.5'; 7209.6'-7211.4'),

Interpretation: Facies 9 is interpreted as transgressive deposits recording high-energy wave ravinement and the vertical transition to deeper water deposits during delta lobe-abandonment (Cattaneo & Steel, 2003). The calcareous component of this facies is interpreted as resulting from partial dissolution of shells. Its erosional base makes this facies clearly visible due to the difference in its lithology (Zonneveld et al., 2003). The transgressive interpretation of Facies 9 is further supported by stratigraphic relationships, as indicated by its presence above Facies 5, interpreted as delta front deposits (i.e. Eden Yuturi 005 well section, Figure 8.9). *Thalassinoides* isp. and *Asterosoma* isp.?, represents suites attributable to the *Cruziana* Ichnofacies, recording transition to deeper-water deposits (e.g. Pemberton et al., 2001; Buatois & Mángano, 2011).

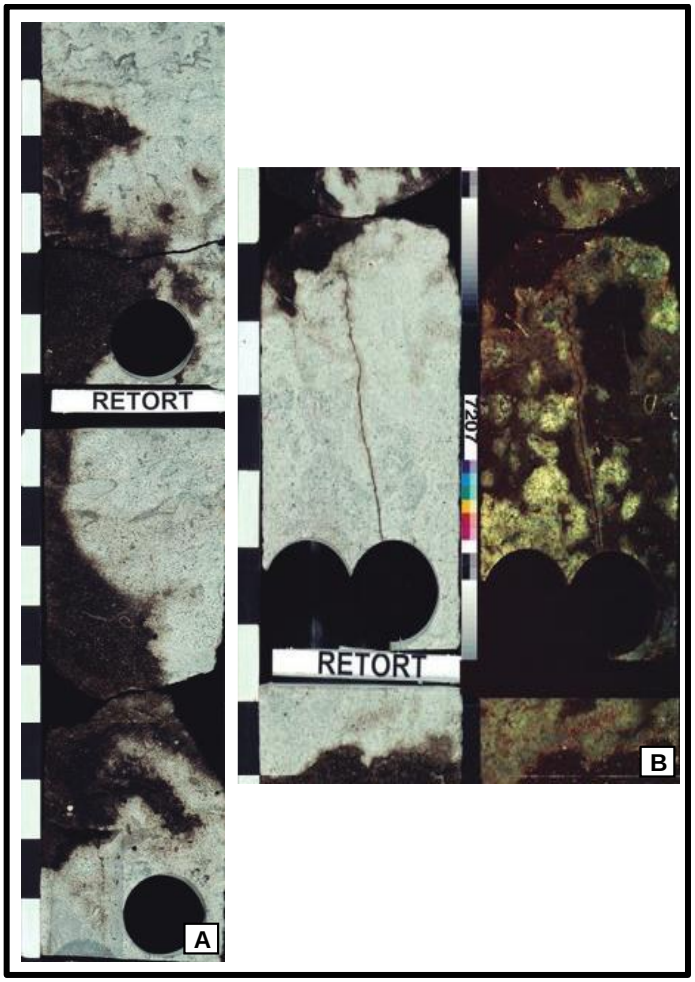

Figure 7.10. *Facies 9. Calcareous sandstone (A) white colour sandstone partially oil impregned. Eden Yuturi 005 well, 7209'. (B) Burrows in the right section with UV filter. Eden Yuturi 005 well, 7206'.*

7.2.Trace Fossils

This section provides a brief description of trace fossils identified in the wells analyzed for the U and M2 sandstone members. Twelve ichnotaxa have been recognized.

7.2.1. Asterosoma isp.

Description: Asterosoma isp. consists of concentrically filled burrows, radiating outwards from a central axis and tapering towards the end extremities (Figure 7.11A-B). Its typical appearance in core consists of clusters of "bulbs", where sandstone acts as the core and mudstone laminae surround this sand lumen. Burrows are 4-6 mm wide in cross section.

Remarks: Concentric infill and the lack of spreite help to distinguish *Asterosoma* from *Teichichnus* (e.g. Gerard & Bromley, 2008). Only fractions of the entire burrow system are visible in core (Pemberton, 1992; Knaust, 2017). The studied specimens are not classified at ichnospecific level due to the limited field of view in core. The producers of *Asterosoma* tend to show a preference for sandy substrates (e.g. Knaust, 2017), which is in agreement with the associated lithofacies. This ichnotaxon is common in fully marine environments (Pemberton, 1992). *Asterosoma* is particularly abundant in the lower shoreface to offshore, although it may occur in slightly deeper-water settings, such as the shelf (e.g. Farrow, 1966; Howard, 1972; Gowland, 1996; MacEachern & Bann, 2008; Joseph et al., 2012; Pemberton et al., 2012). However, *Asterosoma* isp. producers may tolerate high stress conditions, such as reduced and fluctuating salinities, which are typical of estuaries, deltas and other paralic settings (e.g. Greb & Chesnut, 1994; MacEachern & Gingras, 2012; Pearson et al., 2013), as well as tidal flats (e.g. Miller & Knox, 1985; Knaust et al., 2012). In particular, *Asterosoma* is common in deltaic successions, particularly in the prodelta and delta front (e.g. Mcllroy, 2004; MacEachern et al., 2005; Gani et al., 2007; Carmona et al., 2008; Dafoe et al., 2010; Tonkin, 2012). *Asterosoma* typically needs well-oxygenated environments, although exceptions may exist (e.g. Neto de Carvalho & Rodrigues, 2003). With respect to reservoir quality and fluid migration, *Asterosoma* isp. is a burrow with an active (mud-dominated) fill, which may be detrimental for porosity and permeability (Knaust, 2017).

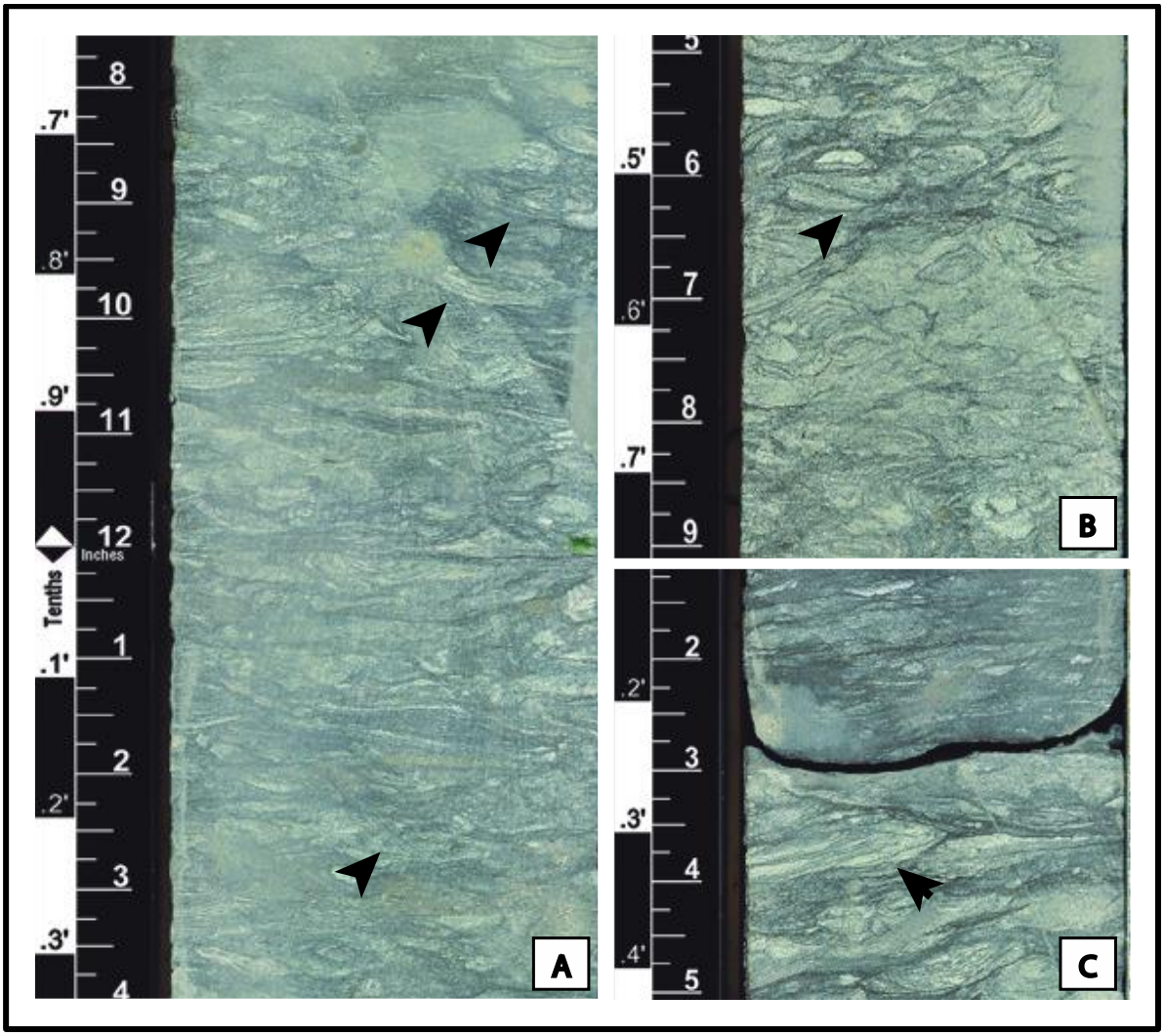

Figure 7.11. Asterosoma *isp. (A) Dense fabric with numerous burrows (arrowed). (B) Side view of* Asterosoma *isp. (arrowed) in a fine- to medium-grained sandstone layer. (C) Large* Asterosoma *isp. (arrowed) preserved in a sandstone layer. All from Pañacocha B003.*

7.2.2. Bergaueria isp.

Description: Single-entrance, hemispherical to shallow cylindrical burrows with rounded base (Figure 7.12). Diameter is generally greater than or equal to length. *Bergaueria* isp. is 5-10 mm deep and 6-10 mm wide. Burrow fill is generally structureless and most commonly attached to the overlying bed.

Remarks: Bergaueria is commonly present in high-energy nearshore environments, such as beaches and sandy tidal flats, although it may extend into deeper-water settings, from the

offshore to the basin plain (e.g. Prantl, 1945; Pemberton & Jones, 1988; Pemberton & Ranger, 1992; Pemberton & Wightman, 1992). Presence of radial ridges or central depressions could not be determined in core view. It is not possible to make an ichnospecific determination due to its poor preservation and low abundance in the cores. Because of its passive fill, the occurrence of *Bergaueria* generally has a positive effect on reservoir quality (Knaust, 2017).

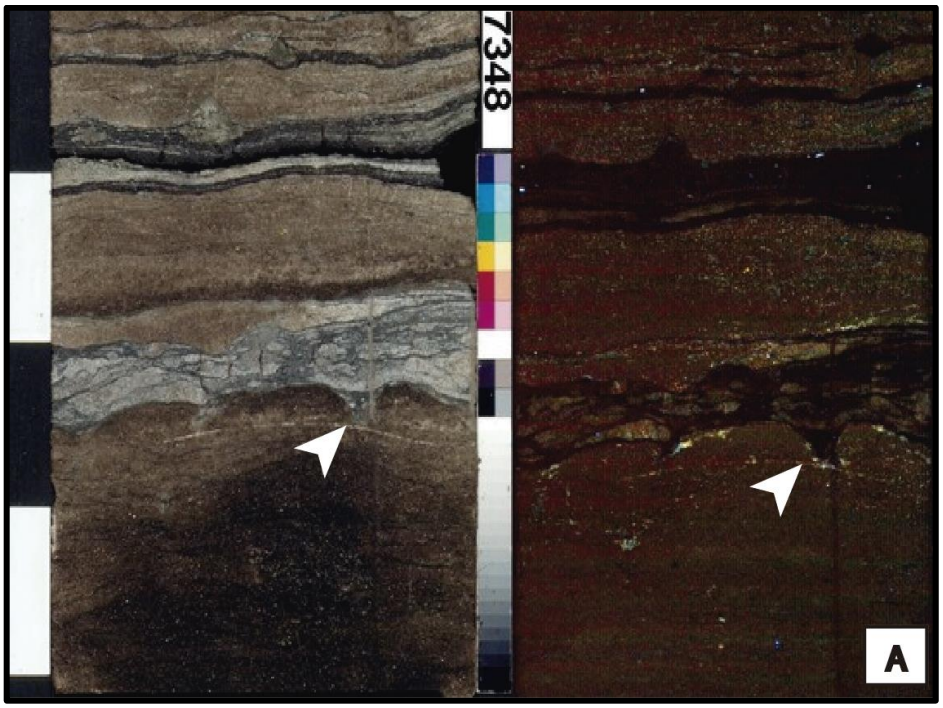

Figure 7.12. Bergaueria isp. *(A) Plug-shaped vertical burrow (arrowed) in sandstone-dominated facies. Eden Yuturi 005.*

7.2.3. *Conichnus* isp.

Description: Vertical, unornamented, conical-shaped, passively filled burrow (Figure 7.13). Diameter is about two times the height. Only one specimen, 9.1 mm wide and 29.46 mm high, has been observed. It may not be possible to identify complete specimens of *Conichnus* in cores due to its large size.

Remarks: Conichnus is common in wave-dominated shallow-marine environments with high hydrodynamic energy and frequent shifting substrates, such as coastal to shallow marine environments (e.g. Abad et al., 2006). It is also present in tide-dominated settings,

including both intertidal and shallow subtidal environments (e.g. tidal flats, estuaries; Curran & Frey, 1977). *Conichnus* isp. is associated with the response to sediment aggradation. Central depressions and radial ridges cannot be determined in core. *Conichnus* in this case cannot be classified in an ichnospecific level due to its scarcity. Because of its passive fill, *Conichnus* is considered to increase net-reservoir distribution and vertical connectivity (Knaust, 2017).

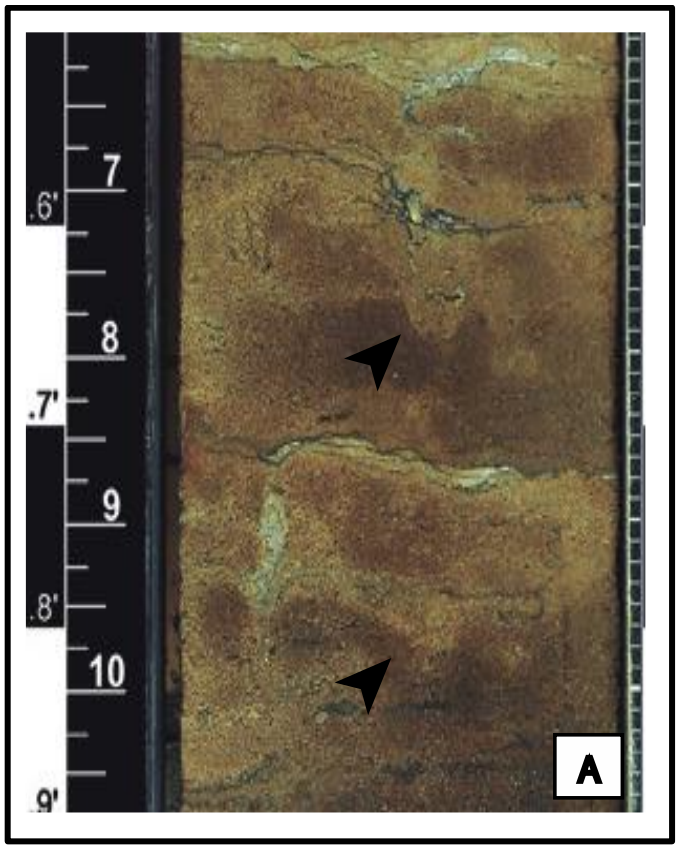

Figure 7.13. Conichnus *isp. (A, B) Vertical, conical- shaped burrow (arrowed). Pañacocha B003.*

7.2.4. Ophiomorpha nodosa

Description: This ichnotaxon consists of 9-27 mm wide, passively filled, horizontal burrows, seen as circular to elliptical in cross-section (Figure 7.14). The wall is made of sand pellets with their typical knobby exterior.

Remarks: Ophiomorpha nodosa is typically associated with clean sandstones. It is also one of the most common trace fossils in post-Paleozoic strata and occurs in a wide range of marine environments (e.g. Kennedy & Sellwood, 1970; Frey et al., 1978; Tchoumatchenco & Uchman, 2001). Identification of *Ophiomorpha* in core is facilitated by its diagnostic pelleted wall (Pollard et al., 1993) (Figure 7.14). However, its characteristic horizontal maze morphology is not appreciable in core. Regarding reservoir quality, the presence of *Ophiomorpha* may improve or diminish reservoir quality (Knaust, 2017).

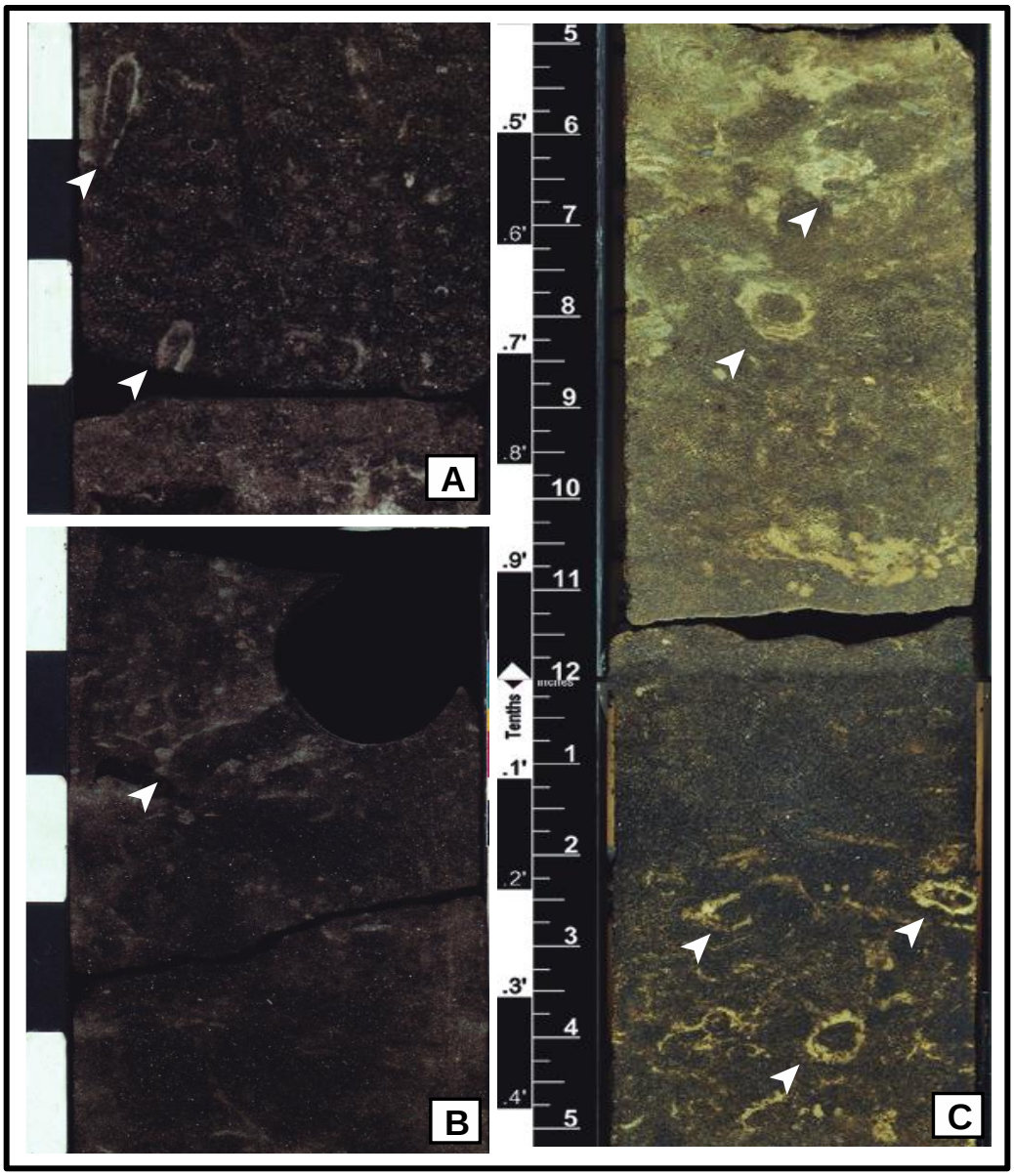

Figure 7.14. Ophiomorpha nodosa. *(A, B)* Ophiomorpha nodosa *pelleted wall (arrowed). Eden Yuturi 005. (C) High abundance of* Ophiomorpha nodosa *(arrowed). Pañacocha B010.*

7.2.5. *Palaeophycus* isp.

Description: This ichnotaxon consists of essentially cylindrical, thinly lined, unbranched, predominantly horizontal, 5-15 mm wide burrows (Figure 7.15). Burrow fill is passive and identical to the host layer (usually medium- to coarse-grained sand) and structureless.

Remarks: According to Pemberton & Frey (1982), *Palaeophycus* occurs in a wide range of environments in marine and continental settings. Low-diversity assemblages with diminutive burrows occur in marginal-marine environments under brackish-water conditions (e.g. estuarine). *Palaeophycus* is also common in shoreface and offshore deposits, where it is in assemblages with much higher ichnodiversities (e.g. Hubbard et al., 2012; Uchman & Wetzel, 2012). Regarding reservoir quality, the presence of *Palaeophycus* in high densities may improve porosity and permeability due to its passive sand-fill (Knaust, 2017).

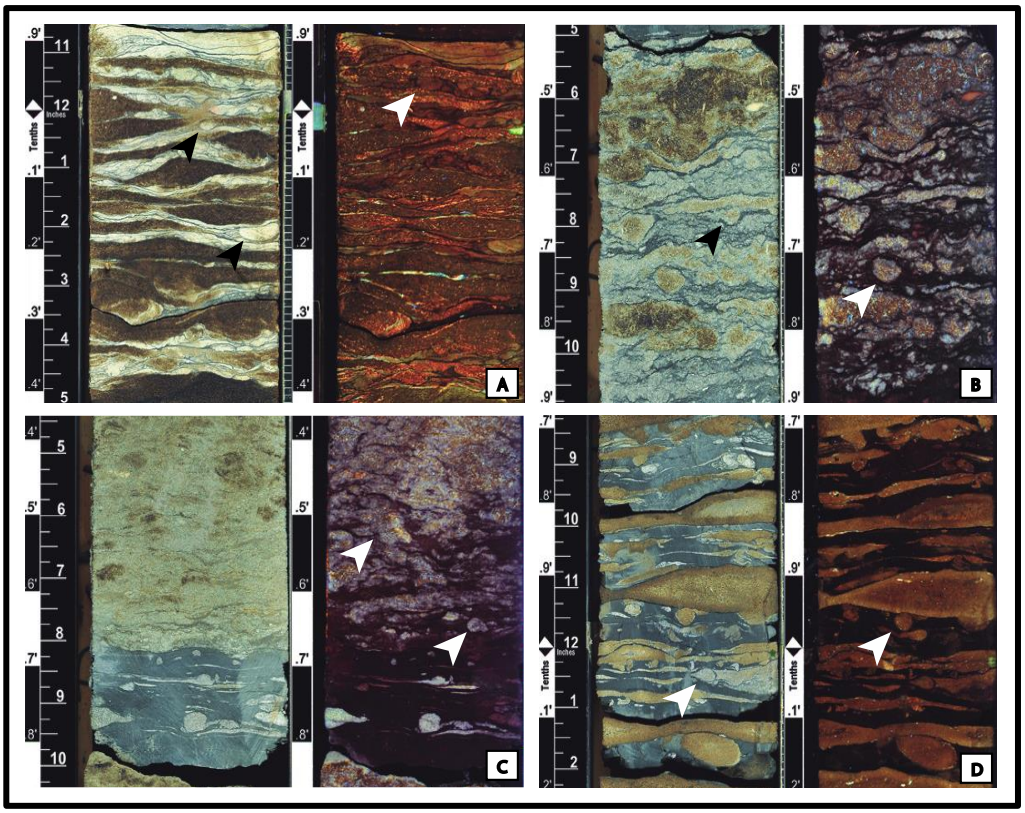

Figure 7.15. Palaeophycus *isp. (A) Interbedded medium-to coarse-grained sandstone, siltstone and mudstone containing* Palaeophycus *isp. (arrowed). Pañacocha B003. (B) Thinly lined small* Palaeophycus *isp. (arrowed)in a medium-grained sandstone. Pañacocha B010. (C) Highly bioturbated sandstone layer with abundant* Palaeophycus *isp. (arrowed). Pañacocha B010. (D) Intercalation of medium-grained sandstone and mudstone containing small* Palaeophycus *isp. (arrowed) in the sandstone layers. Pañacocha B003.*

7.2.6. Planolites isp.

Description: Unbranched, small, 2-8 mm wide, unlined horizontal burrows, circular to elliptical in cross section (Figure 7.16). Burrow fill is structureless and contrasting with the host rock.

Remarks: Planolites has been described from all aquatic depositional environments in marine as well as non-marine environments. Restriction to cross-section views prevents ichnospecific assignment. *Planolites* may be confused with other ichnogenera in core. However, its structureless and contrasting fill is the main ichnotaxobase to differentiate *Planolites* from *Palaeophycus* (e.g. Pemberton & Frey, 1982). Besides the similarities between *Planolites* and *Palaeophycus*, *Macaronichnus* also shares share the same overall geometry. Notwithstanding, *Macaronichnus* surrounding mantle differs from the smooth margin of *Planolites* (e.g. Pemberton & Frey, 1982). With respect to reservoir quality, little is known about the impact of this trace fossil. However, Dawson (1981) described the presence of *Planolites* as less favorable factor for reservoir quality. This may be attributed to the fact that its active fill leads to increased heterogeneity of the sediment.

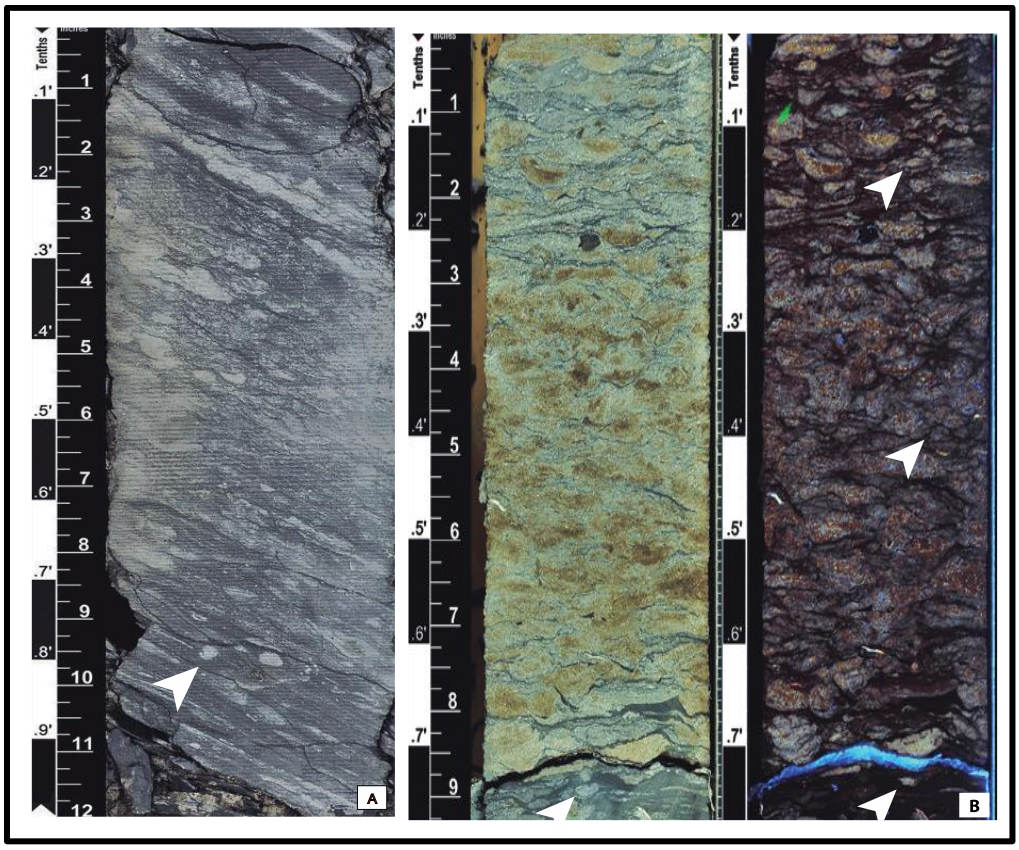

Figure 7.16. Planolites *isp. (A)* Planolites *isp. (arrowed)in a mudstone-dominated interval. Tumali 004. (B) Sand-filled* Planolites *isp. (arrowed) in a highly bioturbated interval,* Teichichnus *fabric. Pañacocha B010.*

7.2.7. Rhizocorallium commune

Description: U-shaped horizontal to sub-horizontal burrows with spreite (Figure 7.17). Burrow width is 15-20 mm; length cannot be determined in core. The two marginal tubes with circular to elliptical cross section, connected with a spreite (denoting former positions of the burrow), are visible in cross-section.

Remarks: Rhizocorallium commune producers tolerate a wide range of salinity conditions, from hypersaline to mesohaline (e.g. Wignall, 1991; Kotlarczyk & Uchman, 2012). Additionally, they tolerate various ranges of oxygen conditions (Fursich, 1974; Basan & Scott, 1979; Wignall, 1991; Schlirf, 2011). *Rhizocorallium commune* has been described in shelf and nearshore environments (Farrow, 1966), as well as intertidal and shallow subtidal environments (Knaust, 2013). *Rhizocorallium commune* is expected to reduce the reservoir quality due to its spreite and the local muddy fecal pellets. However, the latter are not present in the studied specimens and in fact are rare elsewhere (Knaust, 2017).

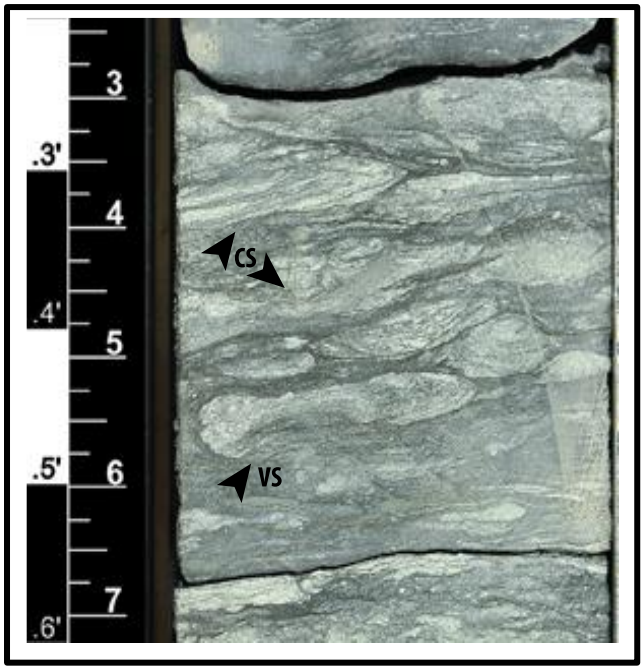

Figure 7.17. Rhizocorallium commune (arrowed). *Pañacocha B003.*

7.2.8. Siphonichnus isp.

Description: This ichnotaxon consists of vertical cylindrical burrows with a bow-shaped morphology (Figure 7.18). It is characterized by its meniscate backfill laminae mantle (active fill) and distinctive core. Length is 0.7-5.6 cm.

Remarks: Siphonichnus isp. has been reported from both sandstone and mudstone. The studied specimens predominantly occur in sandstone-dominated facies. In core, *Siphonichnus* may appear as elongate, elliptical or circular sections (Knaust, 2017). The *Siphonichnus* isp. structures may represent upward movement as a response to rapid sedimentation or as downward movement as a response to rapid erosion (Reineck, 1958; Stanistreet et al., 1980).

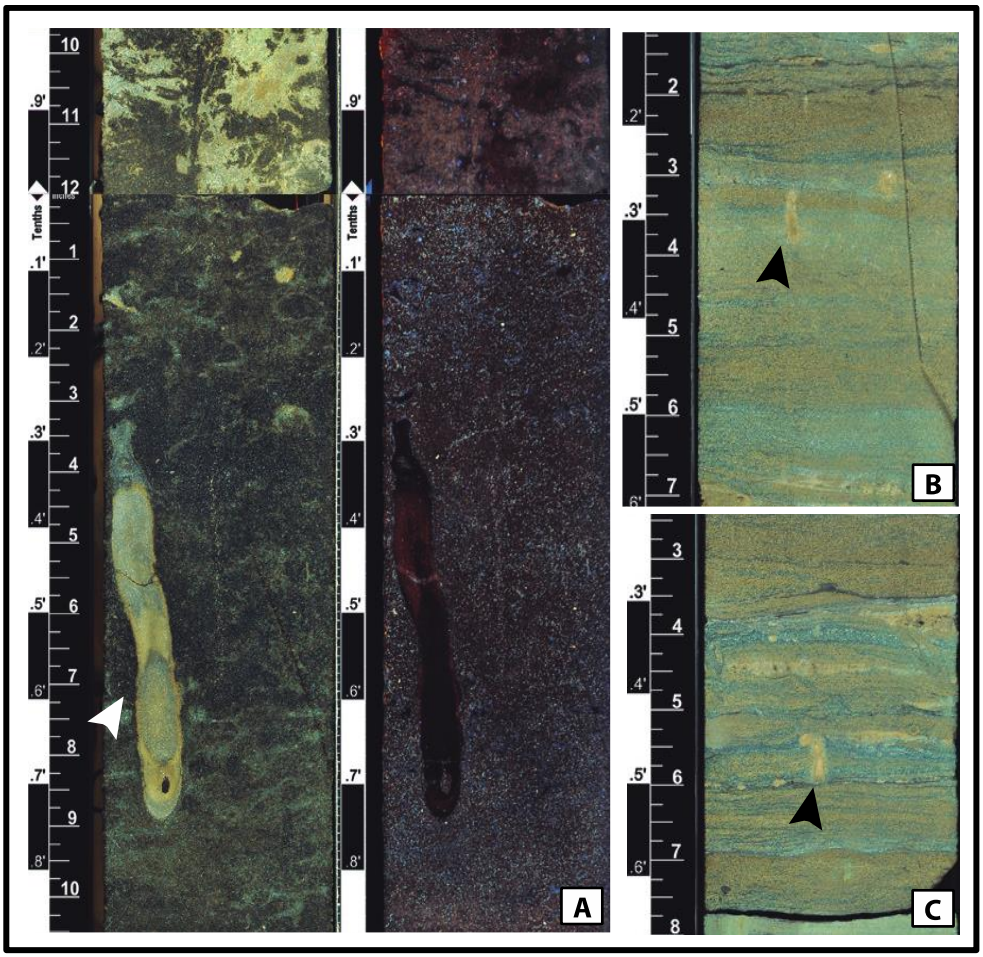

Figure 7.18. Siphonichnus *isp. (A) Low abundance of large* Siphonichnus *isp. (arrowed). Pañacocha B010. (B) Short and small* Siphonichnus *isp. (arrowed). Pañacocha B003.*

7.2.9. Skolithos isp.

Description: The specimens studied consist of narrow, unbranched, vertical to slightly inclined simple burrows, filled with the same material as the host layer (Figure 7.19). Burrow diameter is 2-12 mm. Burrow length is 13-55 mm. *Skolithos* is mainly present in sandstone layers (Figure 7.19 A, D). The burrows appear isolated.

Remarks: According to Schlirf & Uchman (2005), *Skolithos* is easy to recognize in core, appearing as more or less straight burrows with distinctive lining and fill commonly contrasting with the surrounding rock. However, burrows may have been affected by erosion at reactivation surfaces shortening its original length. *Skolithos* is interpreted as vertical dwelling burrows of suspension feeders in moderate to high energy environments (Alpert, 1974; Buatois & Mángano, 2011; Knaust et al., 2018). *Skolithos* has been described as a common indicator of relatively high energy, shallow-water, nearshore to marginal-marine environments. However, *Skolithos* has been reported in shelfal and deep-environments and it is a common constituent of fluvial and other continental deposits as well (e.g. Hasiotis, 2002; Melchor et al., 2012). Regarding reservoir quality, its passive fill and the fact that crowded occurrences are common make *Skolithos* horizons good candidates to increase reservoir quality and vertical connectivity, in cases helping to connect reservoir layers (Knaust, 2017). However, this is not the case for this area.

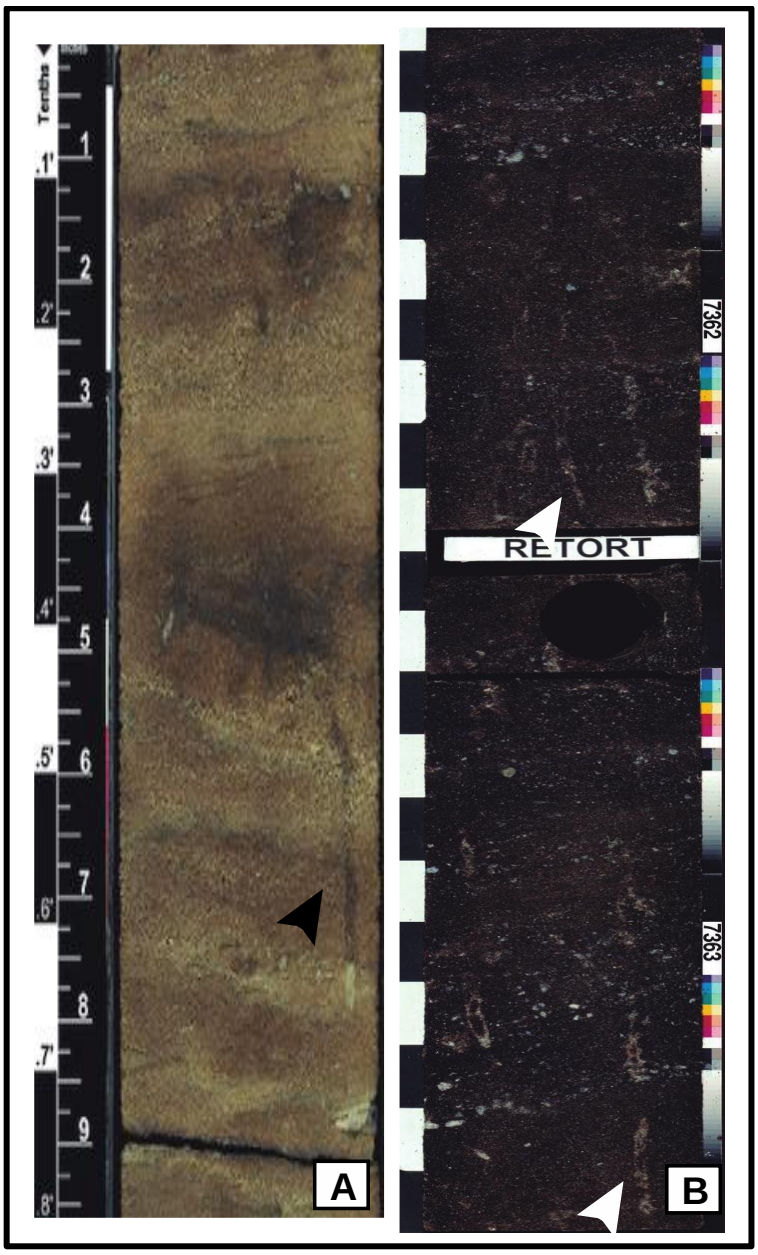

Figure 7.19. Skolithos isp. *(A) Small* Skolithos *(arrowed) in the medium-grained sandstone. Pañacocha B003. (B) Several* Skolithos *isp. (arrowed), which can be appreciated at different levels. Eden Yuturi 005.*

7.2.10. *Teichichnus* isp.

Description: Vertical burrows with retrusive spreite (Figure 7.20). Burrow are filled with fine- to medium-grained silty sand. Width is 5-19 mm and length is 4-16 mm.

Remarks: By virtue of its characteristic spreite development, *Teichichnus* is easy to recognize in cores; however; in this case its visualization is not clear enough in order to assign *Teichichnus* an ichnospecific level. Consistently, in vertical sections in cores, *Teichichnus* appears as many stacked burrows on top of each other, with a readjustment representing different sedimentation and colonization events (Figure 7.20D). Commonly, *Teichichnus* dominates in heterolithic facies with high mud content, locally defining layers with high bioturbation indices. Regarding reservoir quality, the active fill spreite that characterized *Teichichnus* results in permeability reduction; hence, poor reservoir quality (Knaust, 2017).

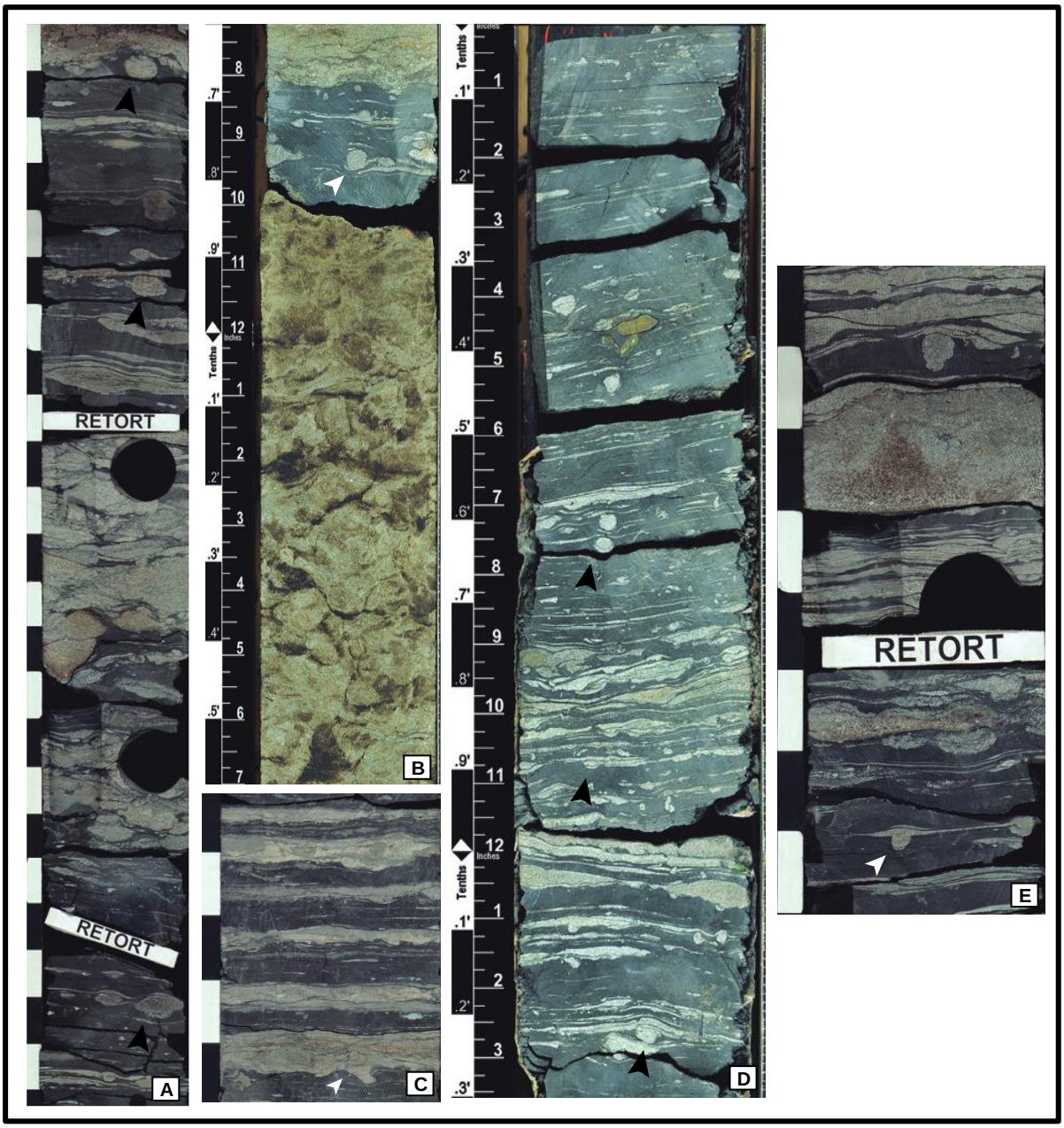

Figure 7.20. Teichichnus *isp: (A) Eden Yuturi 005. (B) Pañacocha B010. (C)* Teichichnus *isp. (arrowed) in a heterolithic facies. Eden Yuturi 005. (D) small* Teichichnus *isp. (arrowed). Pañacocha B010. (E) Eden Yuturi 005.*

7.2.11. Teichichnus rectus

Description: Vertical burrows with retrusive and straight spreite (Figure 7.21). Burrows are filled with fine- to medium-grained sand. Width is 7-20 mm and length is 4-14 mm.

Remarks: Teichichnus rectus is diagnosed as long, straight full-relief unlined burrows, vertically aligned lamellae, displaying U-shaped with elongate horizontal retrusive sections and commonly poorly preserved vertical tubes (Seilacher, 1955). The specimen should be assigned to an existing ichnospecies based on its spreite feature, in this case *Teichichnus rectus* presents straight wall (Knaust, 2018). *Teichichnus rectus* has been interpreted as the result of deposit-feeding crustaceans (Stanton & Dodd, 1984). *Teichichnus rectus* trace fossils is the most common ichnospecies in marginal-marine to deep-marine settings, involved too other ichnospecies (Knaust, 2018). It is also commonly related with low-energy depositional systems such as lower shoreface to offshore transition (e.g. Fürsich, 1974; Pemberton et al., 2001) occurring scattered as one element of a highly diverse ichnofauna. Likewise, several studies have demonstrated mass occurrences of monoichnospecific *Teichichnus rectus* in marginal-marine environments with stressed conditions, for example in estuaries and deltas (e.g. Pemberton & Winghtman, 1992; Buatois, 2005; Buatois & Mángano, 2011). Regarding reservoir quality, its active fill spreite leads to a reduction in the permeability of the rock; hence poor reservoir quality (Knaust, 2017).

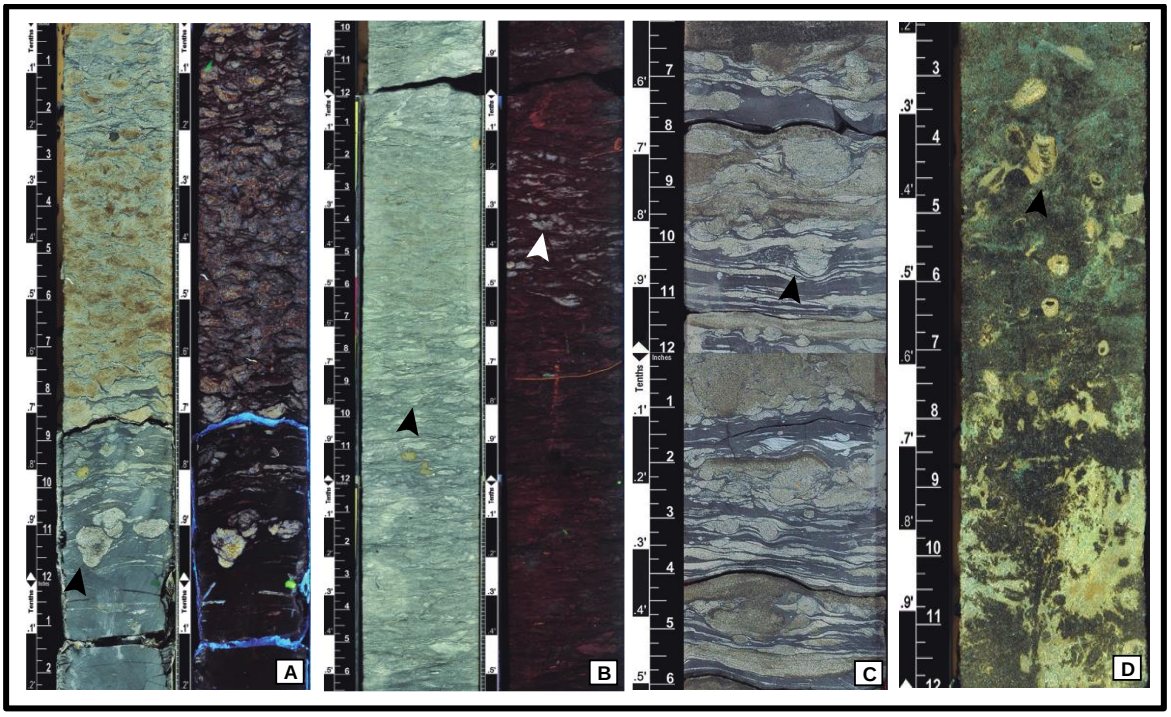

Figure 7.21. Teichichnus rectus. *(A) Dense fabric of* Teichichnus *isp. (arrowed). Pañacocha B010. (B) Highly bioturbated facies. Cross-sections of mud-rich spreiten burrows (arrowed) with* Teichichnus *isp. Common specimen overlapping. Pañacocha B010. (C)* Teichichnus rectus *(arrowed) and other traces in rhythmically interbedded facies. Tumali 004 (D)* Teichichnus rectus *(arrowed) in sandstone-dominated facies. Pañacocha B010.*

7.2.12. *Thalassinoides* isp.

Description: Horizontal, unlined, passively filled burrows, expressed as circular to elliptical cross sections in core view (Figure 7.22). Burrows are 7-28 mm wide.

Remarks: Thalassinoides is most common in shallow-marine environments, such as the shoreface (e.g. Nickel & Atkinson, 1995). However, *Thalassinoides* also occurs in a wide range of environments from marginal to deep-marine environments (e.g. Monaco et al., 2007). *Thalassinoides* producers may tolerate changes in salinity and, as a result, this trace fossil is common in brackish-water environments, such as estuaries (e.g. Swinbanks & Luternauer, 1987). Typical Y- and T-shaped branching is not possible to detect in core. The complete burrow system might penetrate vertically several meters into the substrate. With respect to reservoir quality, *Thalassinoides* may increase the reservoir quality due to its distribution, length, and fill (Knaust, 2017).

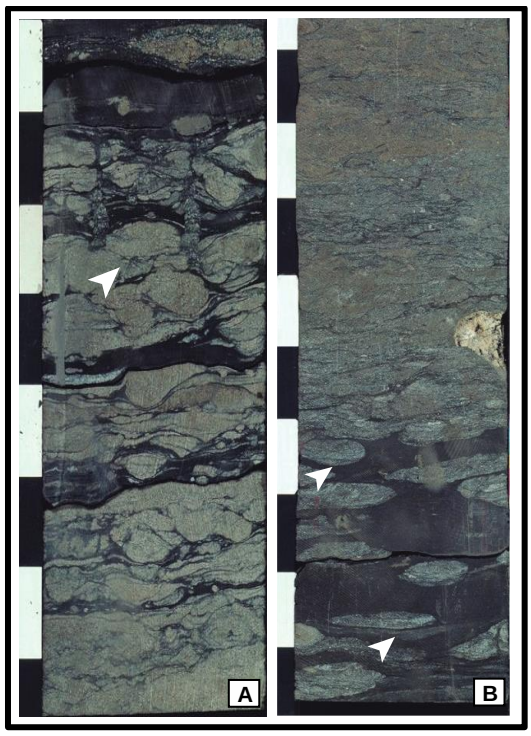

Figure 7.22. Thalassinoides *isp. (A) Passively filled burrows (arrowed). Note the occurrence of spreite due to retrusive burrow. Eden Yuturi 005. (B) Notable elliptical-shaped burrow (arrowed). Eden Yuturi 005.*

7.2.13. Zoophycos isp.

Description: Zoophycos is a horizontal, actively filled, spreite burrow (Figure 7.23). The internal lamellae are composed of alternating fine-grained sand and mud. It presents arched grooves. Width is 11.43 mm and length is 58.4 mm.

Remarks: Zoophycos commonly presents a marginal tube filled with pellets (Bromley, 1996); however, in core the causative tube is not easy to recognize; moreover, this ichnotaxon was recognized in a moderately bioturbated facies where trace fossils are overlapping each other. Its preference for fine-grained sediments makes *Zoophycos* suitable for low-energy distal environments, which is consistent with its presence in prodeltaic deposits (Wetzel, 1984). However, *Zoophycos* producers tolerate a considerable range of water depths, substrates types, food resource, energy levels, and oxygen content (Buatois & Mángano, 2011). Therefore, *Zoophycos* can be found in a wide range of marine environments

(e.g. shallower and deeper water). With respect to reservoir quality, due to its active fill and common grainy burrow fill, *Zoophycos* typically increases permeability (Knaust, 2017).

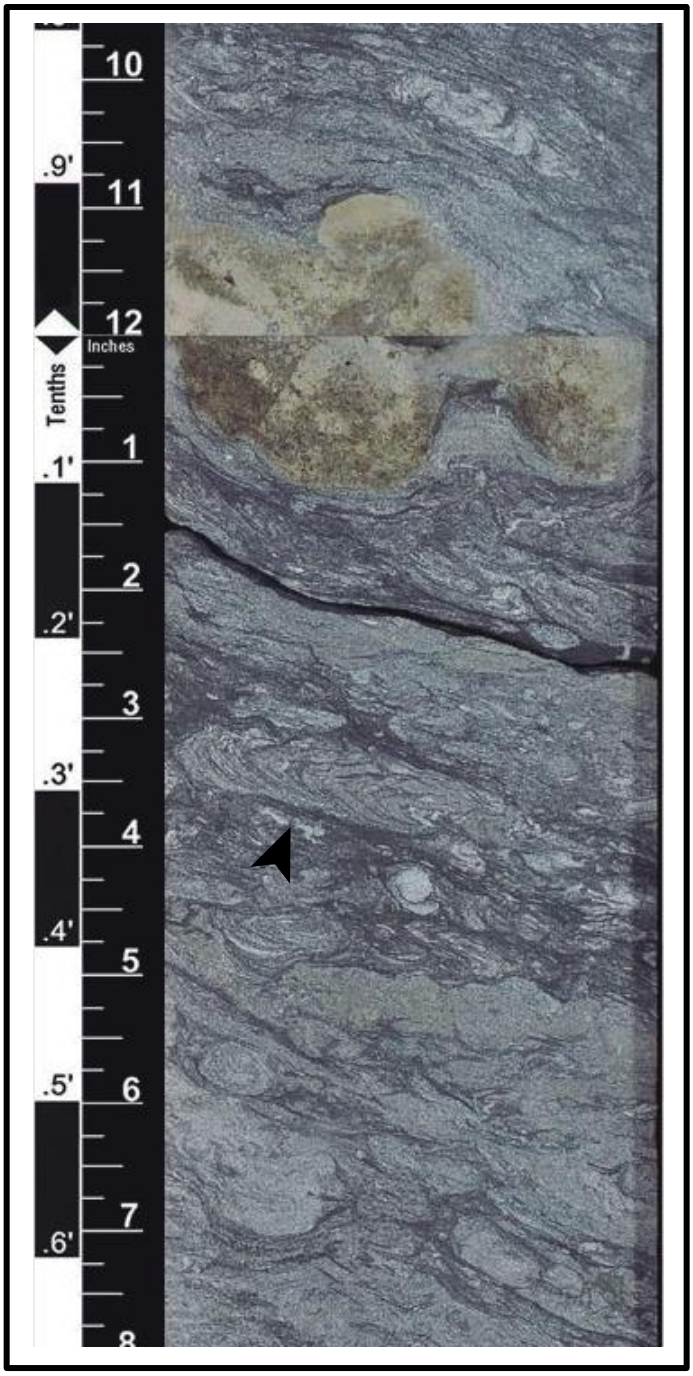

Figure 7.23. Zoophycos *isp. in highly bioturbated facies, showing its characteristic internal lamellae (arrowed). Tumali 003.*

CHAPTER 8

8. DEPOSITIONAL EVOLUTION: INTEGRATION OF SEDIMENTOLOGIC, SEQUENCE-STRATIGRAPHIC, AND ICHNOLOGIC DATASETS

Integration of sedimentologic, sequence-stratigraphic, and ichnologic datasets is a powerful tool to propose more robust models of depositional evolution. The sedimentary facies previously characterized are articulated in this section in order to provide depositional models for both U and M2 Sandstone members. Information derived from process sedimentology is enhanced by ichnologic data. Trace fossils provide useful paleoenvironmental information due to their restricted facies range (e.g. Pemberton & Ranger, 1992). Moreover, trace fossils are *in situ* evidence of soft-bodied infaunal communities (Bromley, 1996). The U and M2 Sandstone members provide a good opportunity to discuss how organisms reacted in estuaries and in a tide- and river-influenced deltaic environment characterized by a variable combination of stressors. From an ichnologic perspective, three main situations can be typified in the deposition of the U and M2 sandstone members: (a) freshwater, (b) brackish water, and (c) open marine conditions. Finally, in order to assess depositional evolution, paleoenvironmental reconstructions are framed from a sequence-stratigraphic perspective through delineation of allostratographic surfaces and stratal stacking patterns.

The sequence-stratigraphic analysis of the U and M2 Sandstone members follows the Depositional Sequence Model II (Posamentier & Vail, 1988; Catuneanu, 2006), because identification of a Falling Stage Systems Tract (FSST) was not possible in this instance. In the case of the U Sandstone Member, the first regional transgression in the studied area (expressed as bioclastic wackestone deposits, Facies 8) was used as a datum. Two depositional sequences (DSU1-DSU2) were recognized in the study area for the U Sandstone Member. In the case of the M2 Sandstone Member, the same conceptual approach as with

U Sandstone Member was used, and the first regional transgression was used as datum. The different thickening- and coarsening-upward successions that form the M2 Sandstone Member are identified as either parasequences or deltaic avulsion cycles. In the first scenario, the parasequences are interpreted as stacked forming progradational parasequence sets. Two depositional sequences, DSM1 and DSM2, were recognized in the study area. The underlying A Limestone Member is included as part of DSM1.

8.1. U Sandstone Member

In the studied area, the U Sandstone Member represents deposition in three main broad environments: fluvial, estuarine, and deltaic. In the three different cores described for the U Sandstone Member, trace fossils are commonly present in the sandstone-dominated facies. However, although mudstone-dominated facies are commonly unbioturbated, they may locally present trace fossils.

Fluvial deposition within incised valleys is recorded in the lower to middle intervals of the U Sandstone Member, comprising channels (Facies 1, section 7.1.1) separated by overbank (Facies 2, section 7.1.2) areas. No evidence of lateral accretion is apparent in the channel-fill facies, suggesting that fluvial sinuosity was not high. The presence of associated overbank fine-grained deposits, however, is consistent with moderate sinuosity rather than with low sinuosity river systems. Thick beds of fluvial sandstone-dominated facies indicate that the shoreline was extended northeast-southwest within the study area during the late Cenomanian-early Turonian. Fluvial systems transitioned vertically and towards the east-southeast into estuarine systems (i.e. Tumali003, Figure 8.2.). Likewise, a predominant sediment source came from cratonic areas (the Guyana Shield). The core intervals studied for the U Sandstone Member were sampled in the eastern most part of the Oriente Basin, which tend to be dominated by more proximal deposits. The incised valley interpretation is based on local observations in the study area, and needs to be tested at a regional scale.

The base of the U Sandstone Member is represented by a subaerial unconformity (sequence boundary or SB) formed as a result of valley incision during a relative fall of sea level. This surface (SBU1) marks the base of depositional sequence 1 (DSU1), which comprises the lower and middle intervals of the U Sandstone Member and the lower part of the upper interval. DSU1 consists of ca. 19 m thick fluvial, estuarine, and deltaic deposits in

the proximal areas, whereas in the distal area it is ca. 22 m thick. Reduced thickness in the proximal zone reflects strong erosion of the upper interval of the U Sandstone Member due to truncation of the overlying SB (SBU2). During relative sea-level fall, the area experienced non-deposition and by-pass. Subsequently, a relative rise of sea level resulted in the creation of accommodation space, and fluvial deposition was restricted to the incised valley representing the lowstand systems tract (LST). In distal areas, no fluvial LST deposits are present, and DSU1 is expressed as a co-planar surface of lowstand erosion and transgressive erosion (amalgamated flooding surface/sequence boundary or FS/SB).

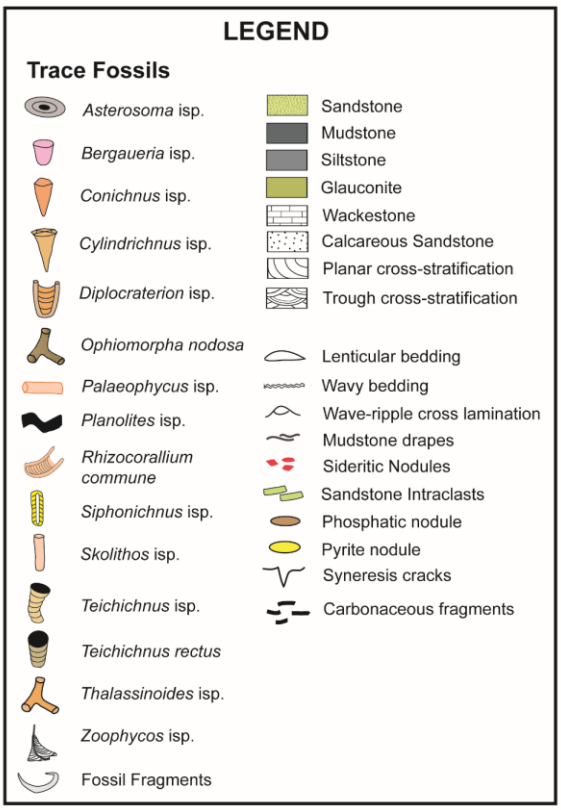

Figure 8.1. *Trace fossils, facies and sedimentary structure legend for Figs 8.2 to 8.13.*

No evidence of biogenic activity is recorded in the fluvial channels, most likely reflecting a combination of high hydrodynamic energy and freshwater. However, the facies-crossing ichnogenera *Palaeophycus* and *Planolites* are locally present in the overbank facies forming low-diversity suites in sparsely bioturbated deposits (BI 0-3). Ichnologic information suggests low-energy conditions, submerged soft substrates, and long pauses

between flooding events. This occurrence indicates colonization of floodplain ponds, most likely by insect larvae (e.g. Buatois & Mángano, 1995, 2002; Mikuláš, 2003), potentially representing an example of the depauperate *Mermia* Ichnofacies.

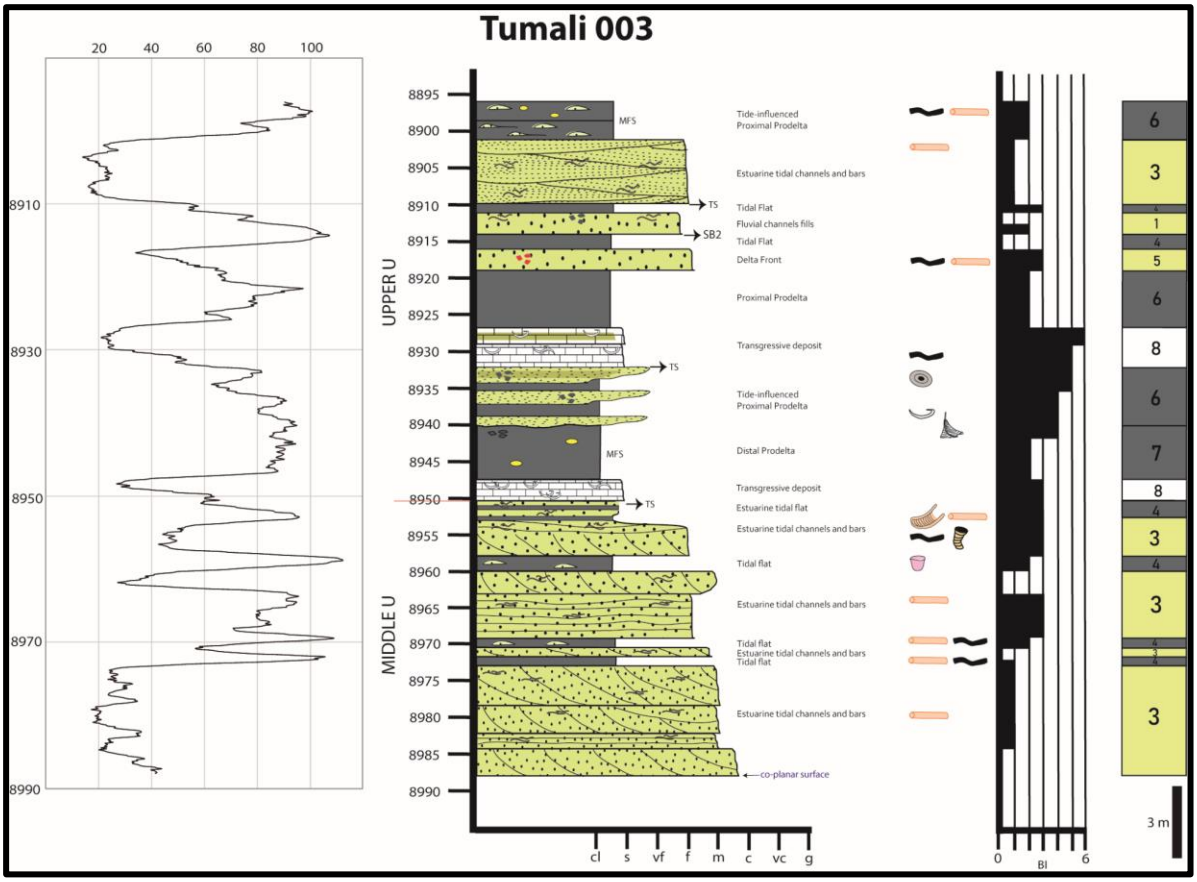

Figure 8.2. Gamma ray, sedimentologic, and ichnologic log for well Tumali 003.

Fluvial deposition was replaced by estuarine sedimentation as evidenced in the lower to middle intervals of the U Sandstone Member. Estuarine systems are represented by tidal channels and bars (Facies 3, section 7.1.3) flanked by tidal flats (Facies 4, section 7.1.4). Tidal action is indicated by the presence of mudstone drapes on bedforms, double mudstone layers, and thick and thin alternations of siltstone and claystone layers. Regional information suggests that the estuary was trending northwest-southeast. Accordingly, the most proximal facies of the estuarine system are present in Eden Yuturi 005 (e.g. Figure 8.3), whereas more distal expressions are seen in Tumali 003 (e.g. Figure 8.2) and Pañacocha B003 (e.g. Figure 8.4). No basal fluvial deposits are recorded in Tumali 003. Fine-grained, central estuarine

basin deposits are absent. Accordingly, the classic tripartite sand-fine-sand division that characterizes most estuaries (e.g. Dalrymple et al., 1992) is not seen. Overall facies architecture suggests a tide-dominated estuary. However, no clear evidence of outer estuarine subtidal sandbodies is present in the study area.

The base of the estuarine package is delineated by a transgressive surface (TS), typically showing the vertical passage from fluvial channel-fills to estuarine channel and bar (e.g. Pañacocha B003) or tidal flat deposits (e.g. Eden Yuturi 005). In Tumali 003, this surface is amalgamated with the basal subaerial unconformity, representing a co-planar surface. Estuarine deposits represent the initial transgressive systems tract (TST), which records deposition still restricted to the incised valley. In this correlation scheme, the contact between the lower and middle intervals of the U Sandstone Member corresponds to this initial transgressive surface. Accordingly, the lower interval of the U Sandstone Member is not present in Tumali 0003.

The regional trend is further supported by the trace-fossil content. Biogenic activity became more common in the more marine end of the estuarine system (e.g. Tumali 003, Figure 8.2). The estuarine bar and tidal flat deposits in this western most part of the studied area record more evidence of bioturbation, as reflected by more intense biogenic mixing (BI 0-3) and the appearance of more typical marine ichnotaxa, such as *Bergaueria* isp. and *Rhizocorallium commune*. In any case, brackish-water conditions were predominant all through the estuarine system, as indicated by ichnologic characteristics (e.g. low ichnodiversity, low abundance, dominance of simple trace fossils), therefore representing the depauperate *Cruziana* Ichnofacies. The most important controlling factors on the benthos in the estuarine system were freshwater discharge which produces salinity dilution considered as a major stressor in these settings (Pemberton et al., 1982; MacEachern & Pemberton, 1994; Buatois et al., 1997), and the associated increase in water turbidity provoking fine-grained material to clog the filter-feeding devices of suspension feeders, therefore resulting in suppression of suspension-feeding strategies (Perkins, 1975). In addition, high energy affected channelized areas, particularly in more proximal zones where hyperpycnal flows reached maximum energy, as reflected by the absence of bioturbation in these deposits. The hyperpycnal flow energy dissipated through the channel (C. Zavala et al., 2011).

Above a regional TS mantled by thick bioclastic wackestone beds (Facies 8, section 7.1.8), fully marine transgressive deposits accumulated, representing shoreline retrogradation. These transgressive deposits commonly contain marine bivalve fragments, providing further evidence of transition into environments of normal-marine salinity, in hand with the association of the *Cruziana* Ichnofacies characteristic of these deposits. This TS marks the contact between the middle and upper intervals of the U Sandstone Member. This TS is of regional extension, and is regarded as a wave ravinement surface (WRS) (Zaitlin et al., 1994). These transgressive deposits mantle the whole studied area, representing the late stage of the TST. The transgressive deposits pass upwards into prodeltaic deposits, which are commonly highly bioturbated (BI 2-6). The maximum flooding surface (MFS) is thought to be present within this regionally extensive prodelta interval, although its precise position is hard to locate.

Deltaic deposits are present in the upper interval of the U Sandstone Member. Tidal influence is revealed by the presence of mudstone drapes, double mudstone layers, and thick and thin alternations of siltstone and claystone layers. Wave influence is considered negligible, as there is an absence of sedimentary structures produced by oscillatory flows. River influence is indicated by the presence of prodeltaic deposits interpreted as produced by sediment gravity flows. Also, the presence of fluid mud deposition, represented by thin, unbioturbated mudstone, is considered as evidence of fluvial processes. Fluid mud is formed by fluidization of sediment and has the capacity to horizontally move in response to overriding shear flow (fluvial flow) (McAnally et al., 2007). Regional information suggests that the delta prograded from southeast to northwest.

Deltaic deposits are stacked forming coarsening- and thickening-upward successions, typically ranging from delta front (Facies 5, section 7.1.5), proximal prodelta (Facies 6, section 7.1.6), and distal prodelta (Facies 7, section 7.1.7) deposits. These packages may represent parasequences resulting from deltaic progradation, illustrating a highstand systems tract (HST). These progradational deposits are stacked forming a single parasequence set. Parasequences are bounded by erosively based bioclastic wackestone (Facies 8, section 7.1.8), representing minor transgressive events. On the other hand, the deltaic successions may also represent deltaic avulsion cycles, therefore the coarsening- and thickening-upward

successions resulted from autogenic mechanisms. Although both autogenic and allogenic factors may have played a role in governing the formation of coarsening- and thickening-upward successions during deltaic progradation, their relative dominance cannot be resolved in this study. The distinction between autogenic and allogenic factors needs to be analyzed with outcrop, additional cores and/or seismic data. The differentiation relies on observations that are expected to vary on coverage, quality, and resolution as a function of data types and dimensionality; these analyses may help to unravel the significance of stratal trends and surfaces (Walker & James, 1992). Moreover, interpretations of the possible autogenic (lobe switching) origin of deltaic parasequences need to consider that the resulting abandonment of parts of a delta could be controlled by sea-level changes (allogenic processes).

Biological activity is recorded through the whole delta system, albeit affected by different controlling factors. Controlling factors were expressed differently in the various deltaic subenvironments, namely delta front and prodelta (e.g. Gani et al., 2009). The trace-fossil assemblage in the delta front (Facies 5, section 7.1.5) (BI 1-3) was influenced by a combination of stress factors, such as substrate type and consistency, rapid rates of sedimentation, high energy, water turbidity, and changes in salinity. The delta front deposits present moderate diversity, including *Palaeophycus* isp., *Skolithos* isp., *Teichichnus* isp., *Teichichnus rectus, Planolites* isp., *Thalassinoides* isp., and *Ophiomorpha nodosa*, representing the *Skolithos* and *Cruziana* Ichnofacies in their depauperate versions.

Microfossil studies have evidenced that high water turbidity limits the productivity specifically in the more proximal delta positions, affecting the food supply for organisms, including both suspension feeding and deposit feeding infauna (e.g. Nix-Morris, 1996; Leithold & Dean, 1998). Likewise, an increased sedimentation rate is directly linked to the proximity of the distributary channel to the delta front. The increased sedimentation rates impeded permanent domiciles to be constructed, and reduced the concentration of food, rapidly burying sediments (e.g. Nittrouer et al., 1986; Alexander et al., 1991). Rapid sedimentation was associated to the lack of uniformity in bioturbation (Gugliotta et al., 2016), as evidenced in the delta front and proximal prodeltaic deposits. In addition, freshwater discharge during the generation of the hyperpycnal flows resulted in ambient salinity dilution, generating brackish-water conditions (Pemberton et al., 1982; Mángano & Buatois, 2004a;

Buatois, 2005). Both subenvironments, prodelta and delta front, were affected by hyperpycnal flows which are characterized by high energy and unstable conditions for organism colonization. However, hydrodynamic energy played a major role in the more energetic events that characterize the more proximal areas, the delta front. Hydrodynamic energy and sedimentation rate may have controlled the timing and duration of the colonization window in the delta front. Additionally, delta front and proximal prodeltaic deposits are characterized by the presence of fluid mud intervals with absence of trace fossil due to unfavorable substrate condition. Organisms need specific substrate conditions in order to be able to excavate and stabilize their burrow walls, finding fluid muds an unfavorable substrate to colonize (Ichaso & Dalrymple, 2009). Likewise, with the presence of fluid mud deposition, all processes result in the overall depauperate nature of the ichnological assemblage.

Moderately to intensely bioturbated (BI 4-6) proximal prodeltaic deposits are affected by stress factors, such as water turbidity, substrate type and consistency, high energy, and rapid rates of sedimentation in different intensity compared with the delta front. The proximal prodeltaic deposits (Facies 6, section 7.1.6) commonly present relatively higher diversity than the delta front and distal prodeltaic deposits (Facies 7, section 7.1.7), including *Asterosoma* isp., *Bergaueria* isp., *Conichnus* isp., *Palaeophycus* isp., *Planolites* isp., *Ophiomorpha nodosa*, *Siphonichnus* isp., *Skolithos* isp., *Teichichnus* isp., *Teichichnus rectus.*, *Thalassinoides* isp., *Ophiomorpha* isp., and *Zoophycos* isp., representing the *Cruziana* Ichnofacies. In the case of the prodeltaic deposits, the increased amount of fine-grained sediment, such as claystone or siltstone, in fluid mud, as well as in water turbidity, results in clogging the filter-feeding apparatus of the organism (MacEachern et al., 2005; Dasgupta, Buatois, & Mángano, 2016) affecting the colonization window of the deposits. In addition, prodeltaic deposits accumulated from sediment-gravity flows (hyperpycnal flows) which are themselves characterized by high turbulence and water turbidity, among other control factors are high stress factor that inhibit infauna colonization.

Delta front to proximal prodeltaic deposits reflect the return, at times, to more normal marine conditions permitting colonization of the substrate by a less tolerant marine infauna. Although the stress factors that characterize the delta front and proximal prodelta may be

seen as negatively impacting on organism colonization, the occasional uniform bioturbation reflects times of homogeneous distribution of food, normal salinity, and available oxygen in-between floods, compared with the more stressful brackish-water conditions in estuarine environments where stress conditions are more permanent in nature. In contrast, distal prodeltaic deposits on the other hand, are commonly unbioturbated displaying reduced oxygen levels which are detrimental for organism colonization, controlling the diversity and abundance of burrowing organisms (e.g. Pearson & Rosenberg, 1978; Savrda, 1995).

Deltaic progradation was interrupted by renewed, pronounced fluvial deposition within an incised valley in the more proximal areas. This subaerial unconformity (SBU2) marks the base of depositional sequence 2 (DSU2), which comprises the upper part of the upper interval of the U Sandstone Member. DSU2 consists of ca. 18 m thick fluvial, estuarine, and deltaic deposits in the proximal areas, whereas in the distal area consists of ca. 6 m thick deposits. Lateral thickness changes are essentially controlled by fluvial incision. Incision was deeper in proximal sections allowing for accumulation of thicker successions (e.g. Eden Yuturi 0005), whereas distal areas are characterized by very thin successions (e.g. Tumali 003). As a result of incision, a significant part of the underlying HST, as well as some of the transgressive wackestone marker beds, have been removed in proximal areas, as is particularly evident in Eden Yuturi 0005. Fluvial deposition is characterized by stacked, amalgamated channel-fills (Facies 1, section 7.1.1), representing the lowstand systems tract (LST). No evidence of lateral accretion is shown in the fluvial channel-fill facies, suggesting low-sinuosity braided channels. This is also supported by the absence of overbank deposits. Participation of hyperpycnal flows is suggested by the presence of massive sandstone. River flow evolution at different basin locations may provide information on hyperpycnal flow sedimentation. Flow velocity and acceleration reach their maximum at the axial zone and diminishes progressively towards the distal areas (Zavala et al., 2006). It is proposed that the studied deposits represent the infill of a single incised valley. The valley is trending NW-SE and, based on the distance between Eden Yuturi and Pañacocha wells, a valley of at least 25 km wide is suggested. Compilations based on the ancient record indicates that incised valleys may be 0.1-105 km wide (Gibling, 2006) and, therefore, the studied system is well within this range. A similar situation is envisaged for the incised valley present in the lower and middle intervals of the U Sandstone Member. The succession present in Tumali represents

the transition from the fluvial incision to more marine areas, presenting thinner intervals of estuarine tidal channel and bar deposits. No evidence of biogenic activity is recorded in the fluvial channels reflecting high energy and freshwater conditions.

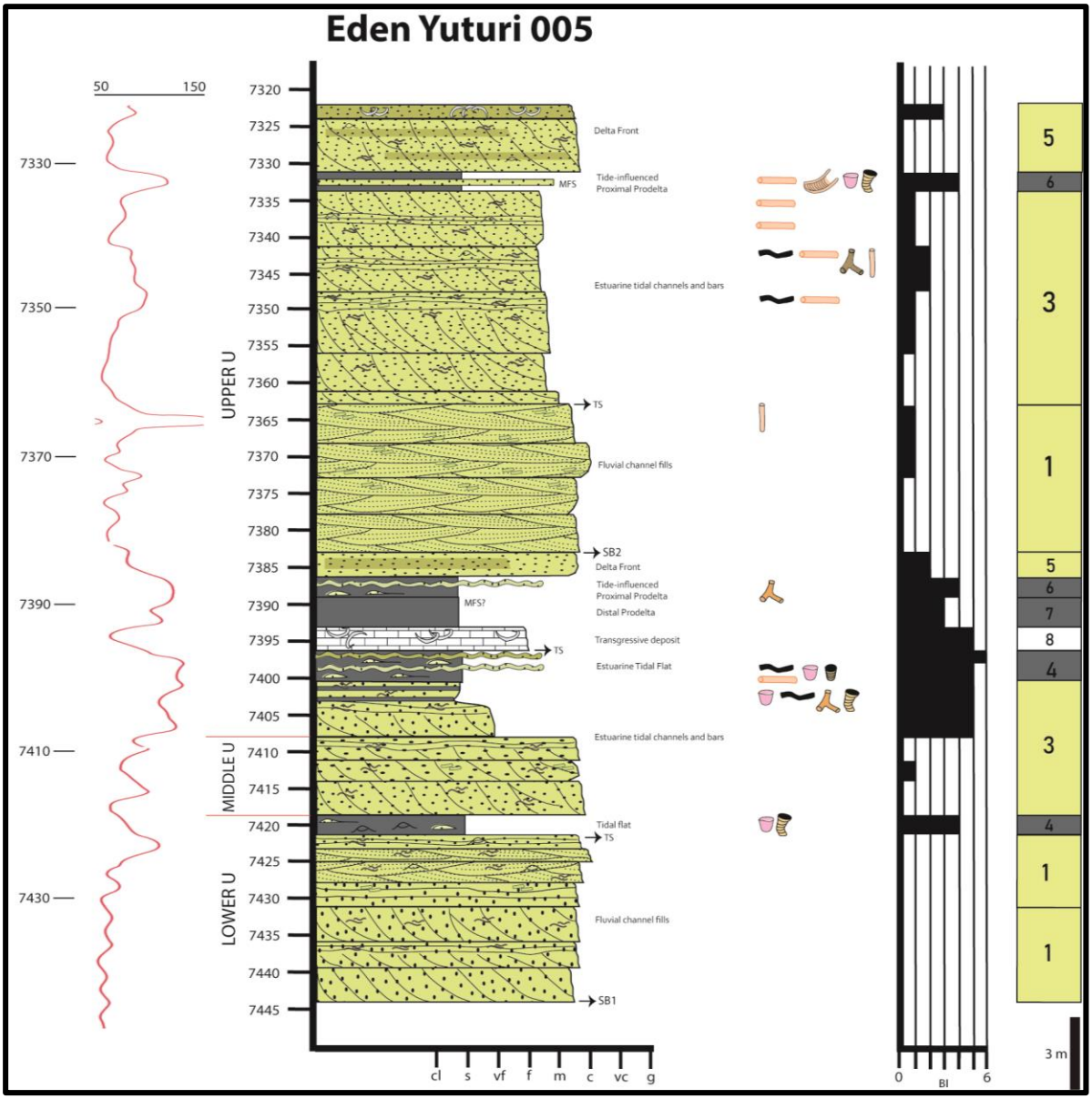

Figure 8.3 *Gamma ray, sedimentologic, and ichnologic log for well Eden Yuturi 005.*

Fluvial deposition was replaced by estuarine deposition as evidenced towards the uppermost interval of the U Sandstone Member. The estuarine system is represented by tidal-influenced channels and bars (Facies 3, section 7.1.3). Tidal action is supported by the

presence of mudstone draped bedforms and double mudstone layers. Tidal flat deposits (Facies 4, section 7.1.4) are very scarce, suggesting significant erosion due to lateral migration of the channels.

The base of the estuarine package is delineated by a transgressive surface (TS), typically showing vertical passage from fluvial channel-fills to estuarine channel and bar (Eden Yuturi 005, Figure 8.3) or tidal flat (Pañacocha B003 and Tumali 003, Figure 8.4 and Figure 8.2 respectively) deposits. Estuarine deposits represent the initial transgressive systems tract (TST), which records deposition restricted to the incised valley.

The ichnofauna in the estuarine system is characterized by low diversity and abundance. Estuarine channels and bars deposits are sparsely bioturbated to unburrowed (BI 0-2), comprising *Palaeophycus* isp., *Planolites* isp., *Ophiomorpha nodosa?*, and *Skolithos* isp., representing the depauperate *Skolithos* Ichnofacies, therefore a dominance of vertical dwelling structures of suspension feeders. The tidal flat deposits are slightly more bioturbated (BI 1-3), and include *Asterosoma* isp., *Bergaueria* isp., *Teichichnus* isp., *Palaeophycus* isp., and *Planolites* isp, representing the depauperate *Cruziana* Ichnofacies. Ichnologic information suggests dominance of brackish-water conditions. This is in sharp contrast with the underlying unbioturbated fluvial deposits, further reinforcing the interpretation of estuarine deposition during transgression. The most important controlling factors on the benthos in the channel and tidal flat deposits were changes in salinity, substrate type, and energy levels. In estuarine channels and bars, the salinity gradient may have controlled the general distribution of ichnofossils along the incised valley, from freshwater condition in the fluvial and tide-fluvial transition environments to brackish water along the estuary and near-normal-marine salinity conditions at the seaward end of the estuary valley (Pemberton & Wightman, 1992). Substrate type may have also played an important role in benthos colonization. For example, tidal flat deposits consist of fine-grained suspended sediments, promoting clay flocculation and rarely preserving biogenic structures (Potter et al., 2005; Buatois & Mángano, 2011). In contrast, vertical burrows are dominant in estuarine channel and bar sandstone. High-energy levels in the channels are supported by the presence of the *Skolithos* Ichnofacies, which is an indicator of strong currents that keep organic particles in suspension. On the other hand, tidal flats may be composed of heterolithic deposits, allowing

trace fossils of the depauperate *Cruziana* Ichnofacies to be preserved (e.g. Mángano & Buatois, 2004).

Estuarine deposition was replaced by deltaic progradation as evidenced in the uppermost part of the upper interval of the U Sandstone Member. Deposition is represented by a regressive succession resulting from deltaic progradation, forming the HST. These deposits are stacked forming coarsening-and thickening-upward successions, typically ranging from proximal prodelta (Facies 6, section 7.1.6) to delta front deposits (Facies 5, section 7.1.5). Deltaic deposits are dominated by tide-generated structures, such as mudstone drapes, double mudstone layers, flaser and lenticular bedding, and intercalation of siltstone and claystone, suggesting a tide-influenced deltaic environment.

Biogenic activity records a restricted infaunal colonization in the delta front deposits (BI 0-3). The ichnotaxa present are *Bergaueria* isp., *Palaeophycus* isp., *Planolites* isp., *Siphonichnus* isp., and *Skolithos* isp, in hand with bivalve fragments in the upper part of the delta front deposits. The ichnofacies attributed for these deposits is the depauperate *Cruziana* Ichnofacies characterized by a reduced variety of ethologic categories and low ichnodiversity levels (Pemberton et al., 2001). On the other hand, proximal prodeltaic deposits present evidence of moderate levels of infaunal colonization (BI 2-4). The ichnotaxa present are *Asterosoma* isp., *Bergaueria* isp., *Palaeophycus* isp., *Planolites* isp., *Skolithos* isp, *Rhizocorallium commune*, and *Teichichnus* isp., representing the depauperate *Cruziana* Ichnofacies. In comparison with the earlier cycle of deltaic sedimentation, these deposits are less bioturbated and display lower levels of ichnodiversity. This suggests a higher stress level on the benthos and that the tracemakers were most likely euryhaline organisms that were able to adapt to a wide range of salinity. Therefore, salinity is inferred as the most important stressor during deposition in both delta front and prodelta subenvironments. In addition, the lower degrees of bioturbation in delta-front deposits may suggest that high sedimentation rates and energy levels in the proximity of the distributary channels may have been a controlling factor as well.

Following the model by Zaitlin et al. (1994), the U Sandstone Member represents the outer segment (i.e. segment 1) of an incised valley. This segment is represented by a sequence boundary recording lowering of base level. The lowstand fluvial interval is thin as the fluvial

deposits were eroded or the area have acted as transport conduit (a bypass zone) at that time; for this reason, the fluvial deposits are absent in the more distal areas (e.g. Tumali 003, Figure 8.2). As sea level began to rise, the incised valley started to be filled and transgressed, becoming an estuarine system. As the transgression proceeded, estuarine conditions which were established at the seaward end of the valley migrated landward. The transgression is overlain by a prograding deltaic succession associated with the succeeding highstand deltaic system.

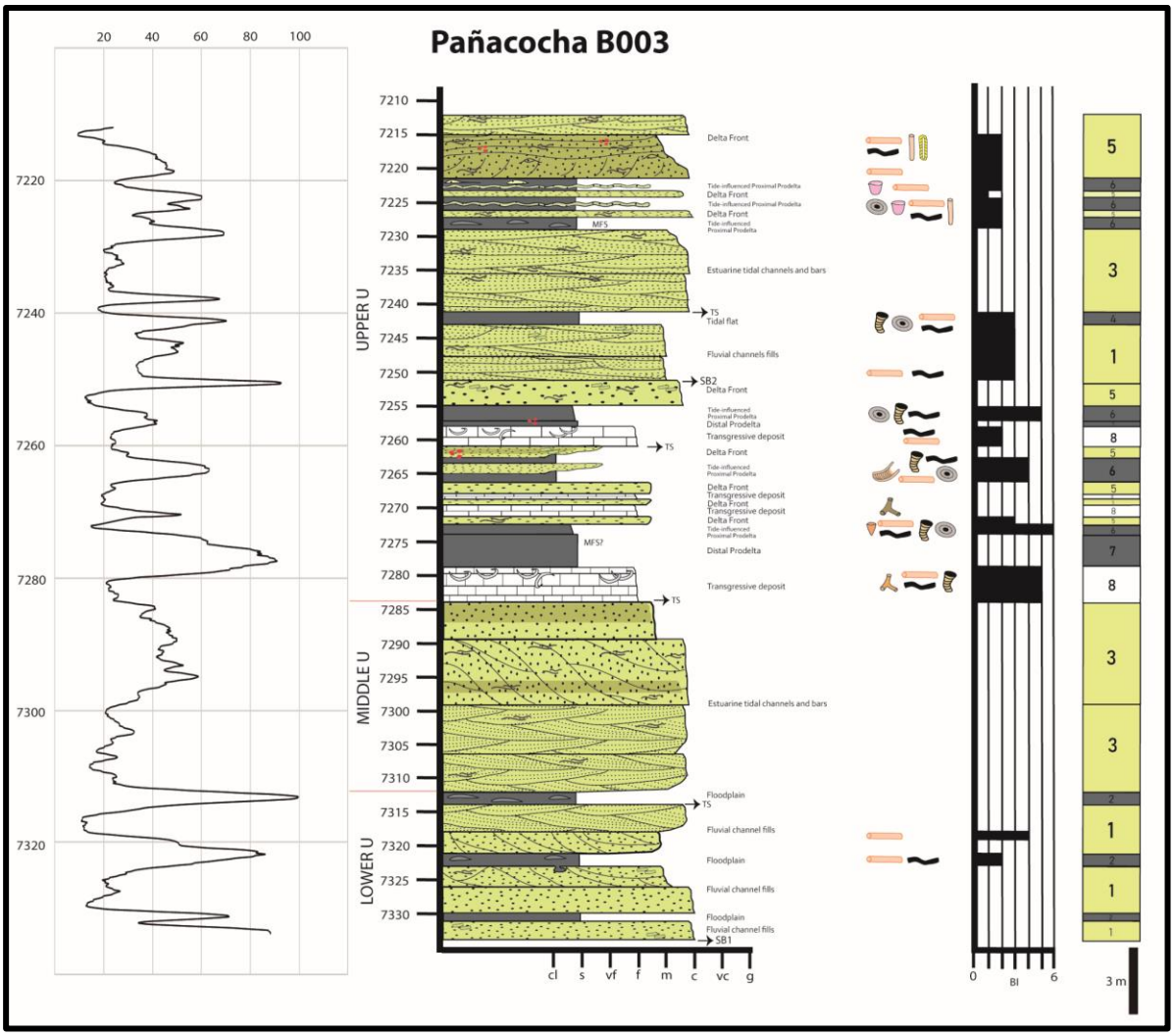

Figure 8.4 *Gamma ray, sedimentologic, and ichnologic log for well Pañacocha B003.*

A modern analogue that displays similar facies to those of the incised fluvio-estuarine valleys recorded in the U Sandstone Member is the Betsiboka estuary in the homologous bay,

Madagascar (Raharimahefa & Kusky, 2010). The oncoming freshwater from the Betsiboka river has high sediment concentrations, flowing to the Mozambique Channel, followed by deposition in an estuarine-channel environment. Figure 8.5 show clearly the multiple streams that converge to form the Betsiboka River, the small islands in the Betsiboka estuary, and the Bombetoka Bay. As is the case of the U Sandstone Member, tides influence sedimentation, as evidenced by the presence of bars oriented perpendicular to the shoreline.

Figure 8.5 *General view of the Betsiboka estuary (source: Google Earth©).*

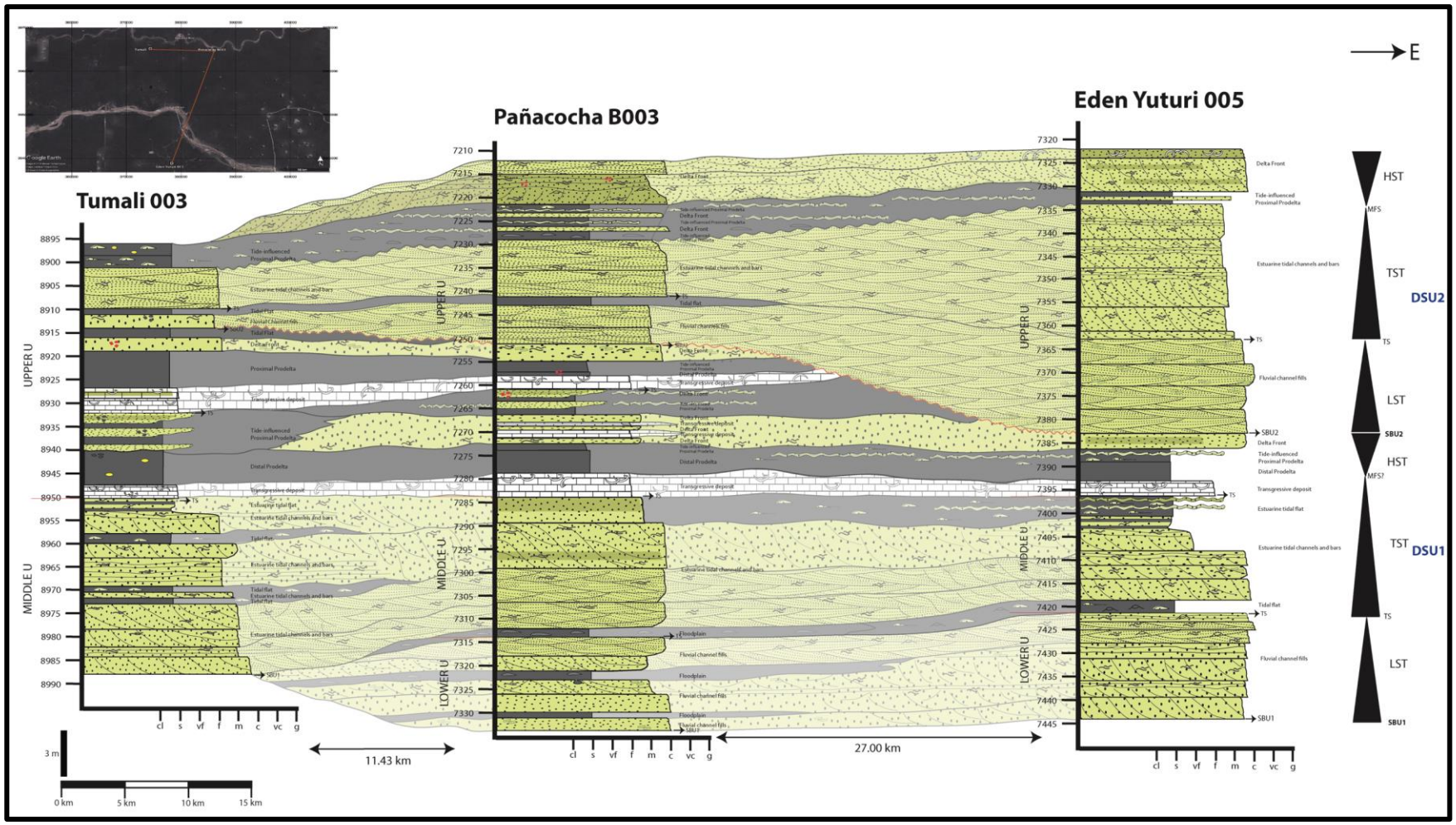

Figure 8.6 *Correlations and sequence-stratigraphic architecture of the U Sandstone Member. Sections constructed based on well cores descriptions, left upper section location in the Oriente Basin, Ecuador.*

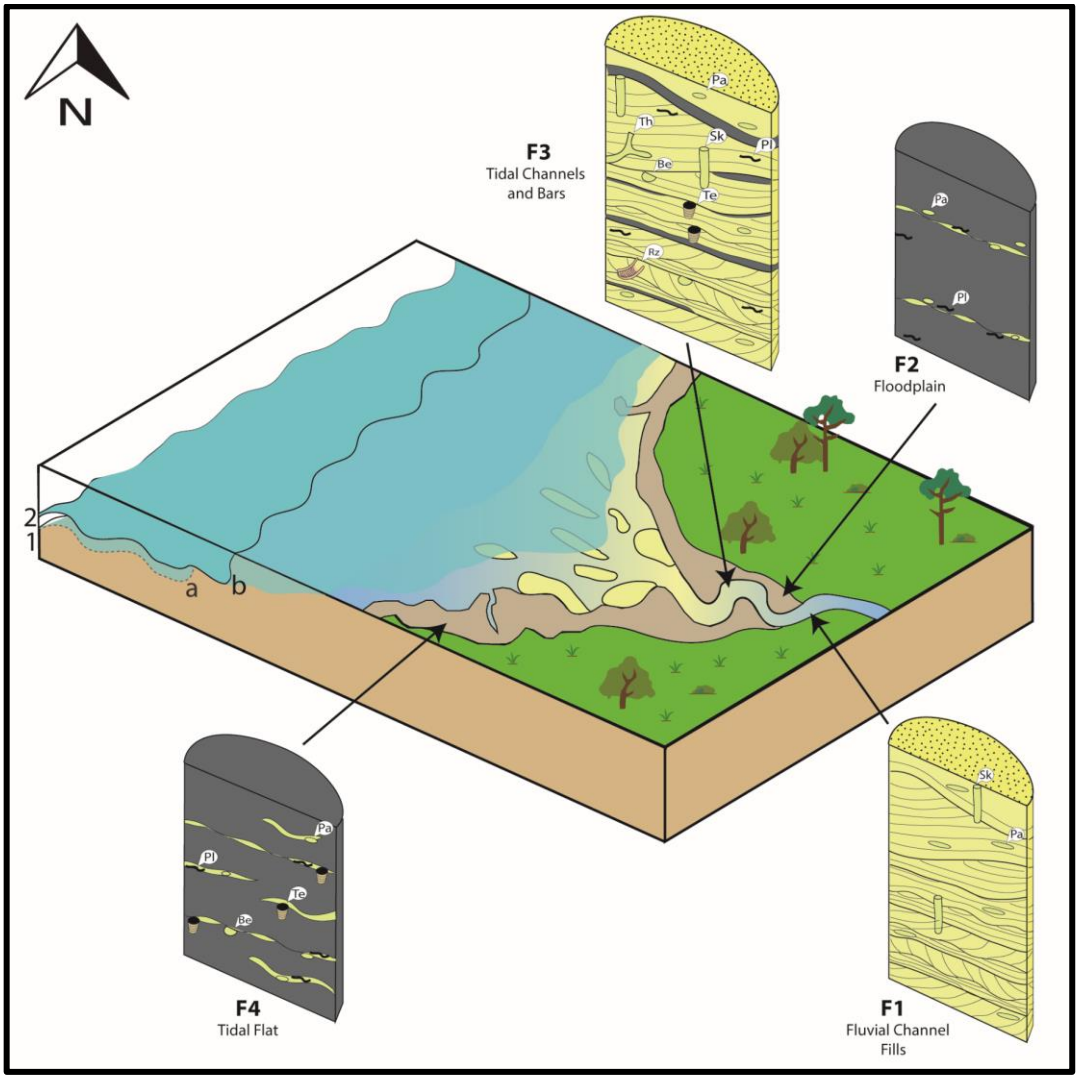

Figure 8.7. *Schematic reconstruction of trace-fossil distribution in the various subenvironments of the fluvio-estuarine system during the deposition of the U Sandstone Member, Napo Formation, Oriente basin of Ecuador. The ichnotaxa shown are as follows:* Bergaueria *isp. (Be),* Palaeophycus *isp. (Pa),* Planolites *isp. (Pl),* Rhizocorallium commune *(Rz),* Skolithos *isp. (Sk),* Teichichnus *isp, and* Teichichnus rectus *(Te), and* Thalassinoides *isp. (Th).*

8.2.M2 Sandstone Member

The onset of the Andean compression during the Turonian (90 Ma) affected sedimentation rates and accommodation space, impacting on the uppermost depositional cycles, represented by the M2 Sandstone Member, which thins towards the west in the Subandean zone (Baby et al., 2004). Therefore, depositional architecture of the M2

Sandstone Member differs from that the U Sandstone Member, even though both represent sedimentation, at least in part, in deltaic environments. The M2 Sandstone Member encompasses delta front and prodelta subenvironments, as well as transgressive deposits. Stratigraphic architecture suggests repeated creation and filling of accommodation space, but no fluvial incision as it was locally the case of the U Sandstone Member. The M2 Sandstone Member may have been controlled by the interplay of eustatic changes, tectonism, and active volcanism.

The M2 Sandstone Member records deposition in a mixed tide- and river-influenced delta environment. This member consists of discrete thickening- and coarsening-upward packages that may represent either parasequences or intervals recording delta lobe switching. As discussed for the U Sandstone Member, distinguishing between both cannot be done on the basis of available data. The expression of depositional sequences varies following a proximal to distal trend, reflecting clinoform geometry as a result of deltaic progradations. Depositional sequence (DSM1) and depositional sequence (DSM2) were recognized in the study area in the M2 Sandstone Member.

The base of DSM1 is not seen in core, and is included at the base of the A Limestone Member, which occurs between the U and M2 Sandstone members. This limestone thins and pinches out towards the east, but well log information suggests that it is present in the study area. In this scheme, the base of DSM1 is considered a co-planar surface and the A Limestone Member is regarded as the TST of DSM1. Only the HST of this depositional sequence is present in the M2 Sandstone Member. HST deposits of DSM1 consist of ca. 12 m of delta front (Facies 5, section 7.1.5) and prodeltaic deposits (Facies 6 and 7, section 7.1.6 and 7.1.7 respectively) in proximal areas, whereas in distal areas reaching just ca. 2 m of delta front and transgressive deposits (Facies 8, section 7.1.8). The parasequences are associated with overall progradational coastlines that represent higher-frequency sea-level cycles of coastal regression within the overall trend of shoreline shift. The upper and lower bounding surface of the depositional sequences are co-planar surfaces. The parasequences have clinoformal geometry, and exhibit both vertical and lateral facies changes from delta front to proximal and distal prodelta. In general, the parasequences are tide-influenced, indicated by the presence of mudstone drapes on bedforms, double mudstone layers, flaser, wavy, and

lenticular bedding, and thick-and- thin alternations of siltstone and claystone layers. On the other hand, fluvial influence is supported by silty sandstone scoured by mudstone layers (fluid muds) consistent with a hyperpycnal emplacement interpretation (Bhattacharya & MacEachern, 2009). Wave-generated sedimentary structures have not been recognized, indicating that oscillatory flows were not significant processes. Likewise, in the Eden Yuturi area, medium- to coarse-grained sandstone-dominated deposits comprising trough-cross stratification reveal migration of subaqueous 3D dunes, which is consistent with proximity to the fluvial discharge.

The base of DSM2 is represented by a co-planar surface that separates the underlying HST deltaic strata of DSM1 from the overlying TST deposits of DSM2. Absence of LST deposits are explained by erosion and by-pass at times of sea-level fall and initial rise. TST deposits of DSM2 consist of ca. 3 m of delta front and transgressive deposits in proximal areas, whereas in distal areas reaches ca. 9 m of delta front, transgressive, and prodeltaic deposits. Carbonate facies overlying the co-planar surface display short-term retrogradational stacking patterns, and are represented by bioclastic wackestone (Facies 8, section 7.1.8), indicating a thin TST within an overall progradational trend. The MFS occurs at the top of the TST within carbonate deposits (Facies 8, section 7.1.8). HST deposits of DSM2 consist of coarsening and thickening upward packages, ranging from the prodelta to the delta front. Overlying abrupt appearance of carbonate facies indicates the base of the M2 Limestone Member.

Parasequences from the Eden Yuturi-Pañacocha cross-section represent the strike cross section of a series of laterally shifting delta lobes and therefore the landward pinchouts of their near-marine sandstone facies exhibit no stratigraphic rise relative to the final paleo shoreline of the underlying parasequence, as it is with the Pañacocha-Tumali cross-section. Several (approx. 0.3-4.0 m thick) discrete packages are distinguished in each section. Each package from the Pañacocha-Tumali area represents a set of westerly dipping clinoforms. In the easternmost area, the clinothems comprise trough- cross stratified medium- to coarse-grained sandstone, revealing proximity to the fluvial discharge. Towards the west, on the other hand, the individual clinoforms are relatively gently dipping with a higher proportion of interbedded mudstone. The clinoforms were fed by a river outlet that came from the north-

east of the studied area, and in general the deltaic system is mixed tide- and river-influenced (e.g. Michels et al., 1998; Patruno et al., 2015).

The M2 Sandstone Member shows interfingering of gently dipping delta-front sandstone with prodelta mudstone, following the so-called deltaic shazam lines pattern instead of sharp surfaces (Giosan & Bhattacharya, 2005). The shallower-water portion of the deltaic parasequence is generally sandstone bounded (delta front deposit) or separated from overlying and underlying strata by easily recognizable marine-flooding surfaces or erosional unconformities (e.g. co-planar surfaces).

High sedimentation rates lead to rapid shoreline progradation which forced rivers to rapidly readjust their equilibrium profiles. This rapid adjustment of the stream equilibrium profile is followed by upstream vertical aggradation and frequent local avulsion (Patruno & Helland-Hansen, 2018). High avulsion frequency would have the effect of preventing a delta lobe from prograding for long distances before avulsion, abandonment, and subsequent re-establishment of deltaic deposition in another adjacent location (Giosan & Bhattacharya, 2005). High avulsion in this case prevents the delta lobe to reach the more distal areas as is the case of Tumali 004 where, for example, the lower parasequence set is remarkably thinner than in the other two wells.

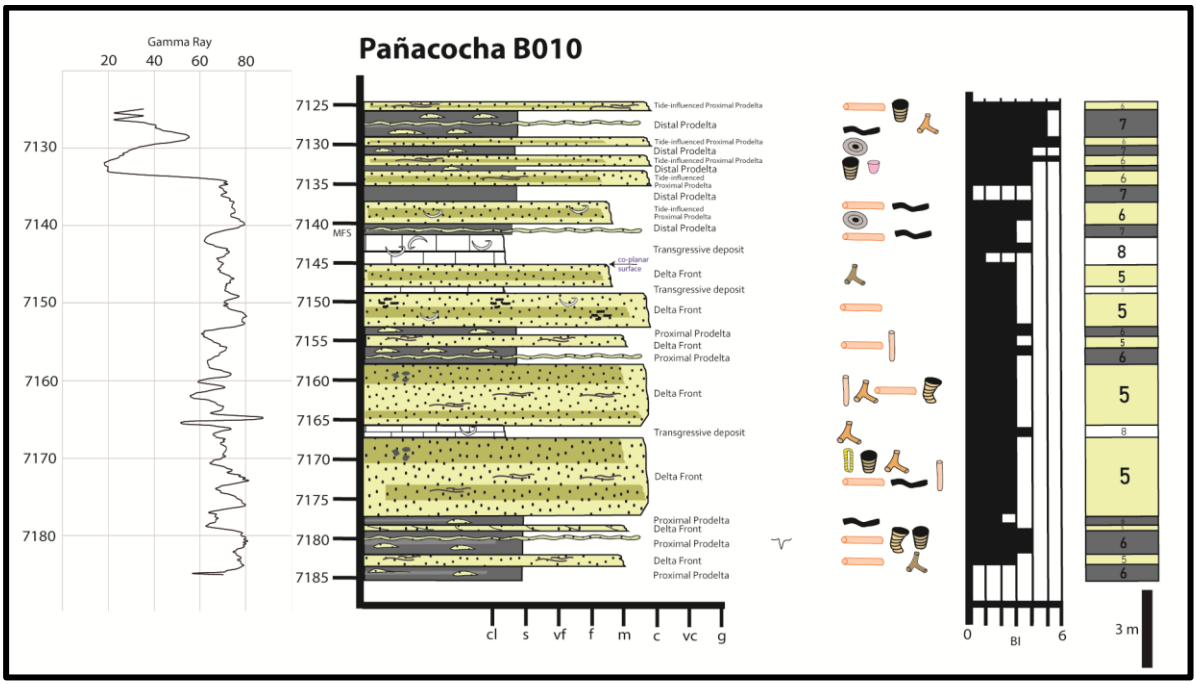

Figure 8.8. *Gamma ray log, sedimentologic, and ichnologic log for well Pañacocha B010.*

The M2 Sandstone Member trace fossils are commonly present in the sandstone-dominated facies. Mudstone-dominated facies may present bioturbation, although some intervals are unburrowed. In general, intense biogenic activity is recorded through the whole deltaic system. Delta front deposits (Facies 5, section 7.1.5) show variable degrees of bioturbation (BI 1-3), and contain a relatively diverse trace-fossil assemblage, including *Conichnus* isp., *Ophiomorpha nodosa*, *Palaeophycus* isp., *Planolites* isp., *Siphonichnus* isp., *Skolithos* isp., *Teichichnus* isp., *Teichichnus rectus*, and *Thalassinoides* isp. Proximal and distal prodeltaic (Facies 6 and Facies 7, section 7.1.6 and 7.1.7, respectively) deposits also shows variable degrees of bioturbation (BI 0-5) and a relatively diverse trace-fossil assemblage, including *Asterosoma* isp., *Bergaueria* isp., *Palaeophycus* isp., *Planolites* isp., *Skolithos* isp., *Teichichnus* isp., *Teichichnus rectus*, and *Thalassinoides* isp. Therefore, the trace-fossil assemblages in both the delta front and prodeltaic deposits represent the *Cruziana* Ichnofacies.

In general, overall high intensities of bioturbation are associated with long-term colonization windows (e.g. Bromley, 1996), with high oxygen availability and normal salinities, aided by tide agitation if compared with the U Sandstone Member. The most important controlling factors on infaunal colonization during deposition of the sandstone-dominated facies were sedimentation rate, hydrodynamic energy, and substrate type, although controlling factors may have affected each subenvironment differently. The delta front is close to the source of hyperpycnal discharge; therefore, sedimentation rate is higher if compared with the other subenvironments, negatively affecting infaunal colonization in the more proximal zones. Likewise related with the hyperpycnal flow discharge, high hydrodynamic energy is a controlling factor in the proximity of the fluvial source (Mulder et al., 2003, Buatois et al., 2011) and it dissipates throughout the delta front and the prodelta. Substrate type was the dominant controlling factor in the prodelta where fluid mud content negatively impacted on infaunal colonization because organisms need specific substrate conditions in order to excavate and stabilize their burrow walls (Ichaso & Dalrymple, 2009). Regardless, the increase in degree of bioturbation, if compared with the U Sandstone

Member, may indicate lower levels of hydrodynamic energy and sedimentation rate, as well as more persistent times of normal marine salinities.

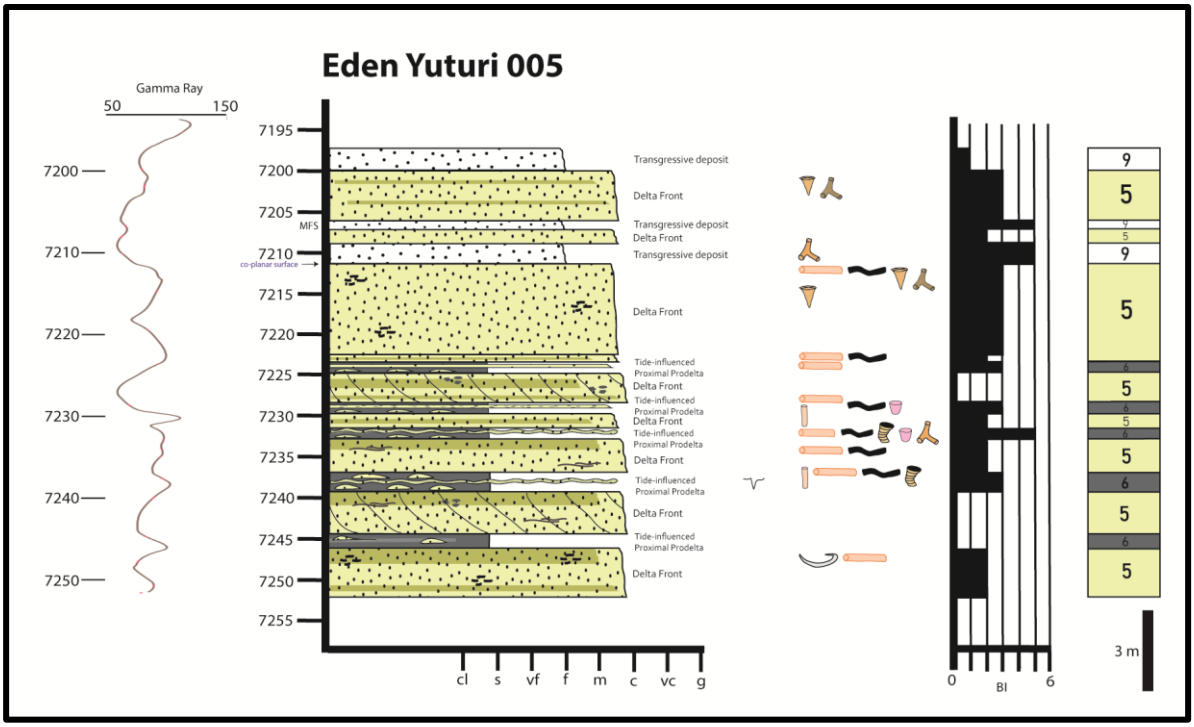

Figure 8.9. *Gamma ray log, sedimentologic, and ichnologic log for well Eden Yuturi 005.*

The presence of numerous flooding surfaces without a regional extension may have been generated due to deltaic lobe switching. At this time, these areas of the delta may develop into an estuary, and the fill is commonly transgressive. However, no clear evidence of estuarine deposition has been detected in the M2 Sandstone Member. Instead, laterally extensive transgressive deposits were formed, represented by Facies 8 (section 7.1.8) in the more proximal areas and Facies 9 (section 7.1.9) in the more distal areas (well Pañacocha B010 and Tumali 004), the latter showing and increase in the carbonate content.

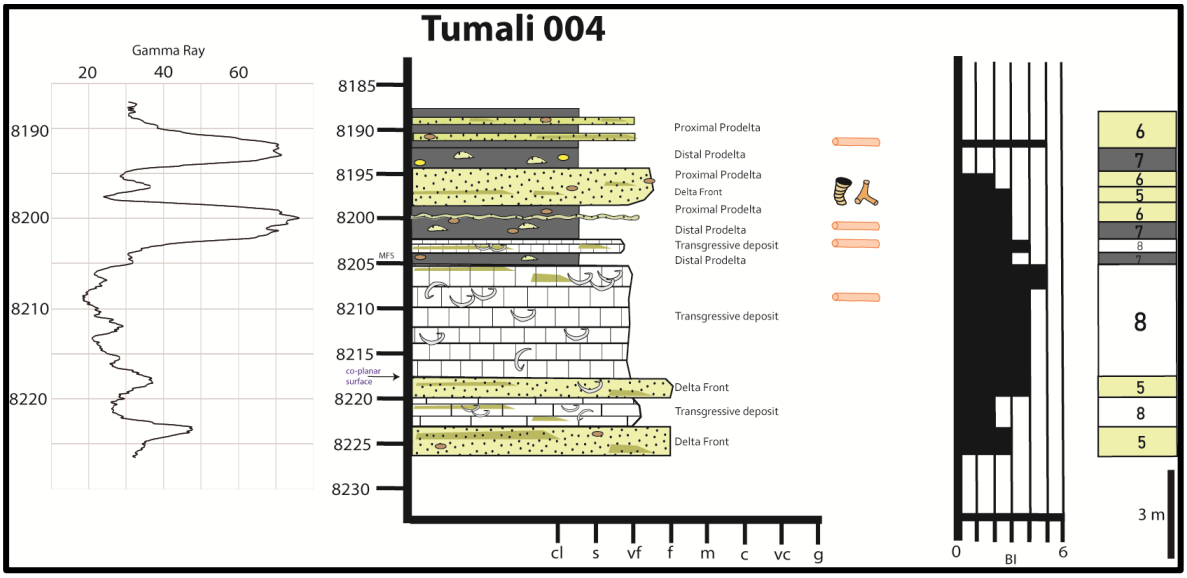

Figure 8.10. *Gamma ray, sedimentologic, and ichnologic log for well Tumali 004.*

Biogenic activity in the transgressive deposits records restricted infaunal colonization (BI 1-5), and varies according to the area. For example, the ichnotaxa present in Facies 9, present just in the more proximal areas, are mainly *Thalassinoides* isp., and very sparse *Asterosoma* isp.?, as well as indeterminate burrow mottling. On the other hand, the ichnotaxa present in Facies 8, present in the more marine areas, are *Palaeophycus* isp., *Planolites* isp., and *Teichichnus* isp. The trace-fossil assemblage in Facies 8 tends to show slightly higher diversity than that of Facies 9. In Facies 9, most occurrences are represented by a monospecific suite of *Thalassinoides* isp. Both assemblages show affinities with the *Cruziana* Ichnofacies. The most significant controlling factor seems to have been high hydrodynamic energy, which may have restricted benthic colonization in the transgressive deposits.

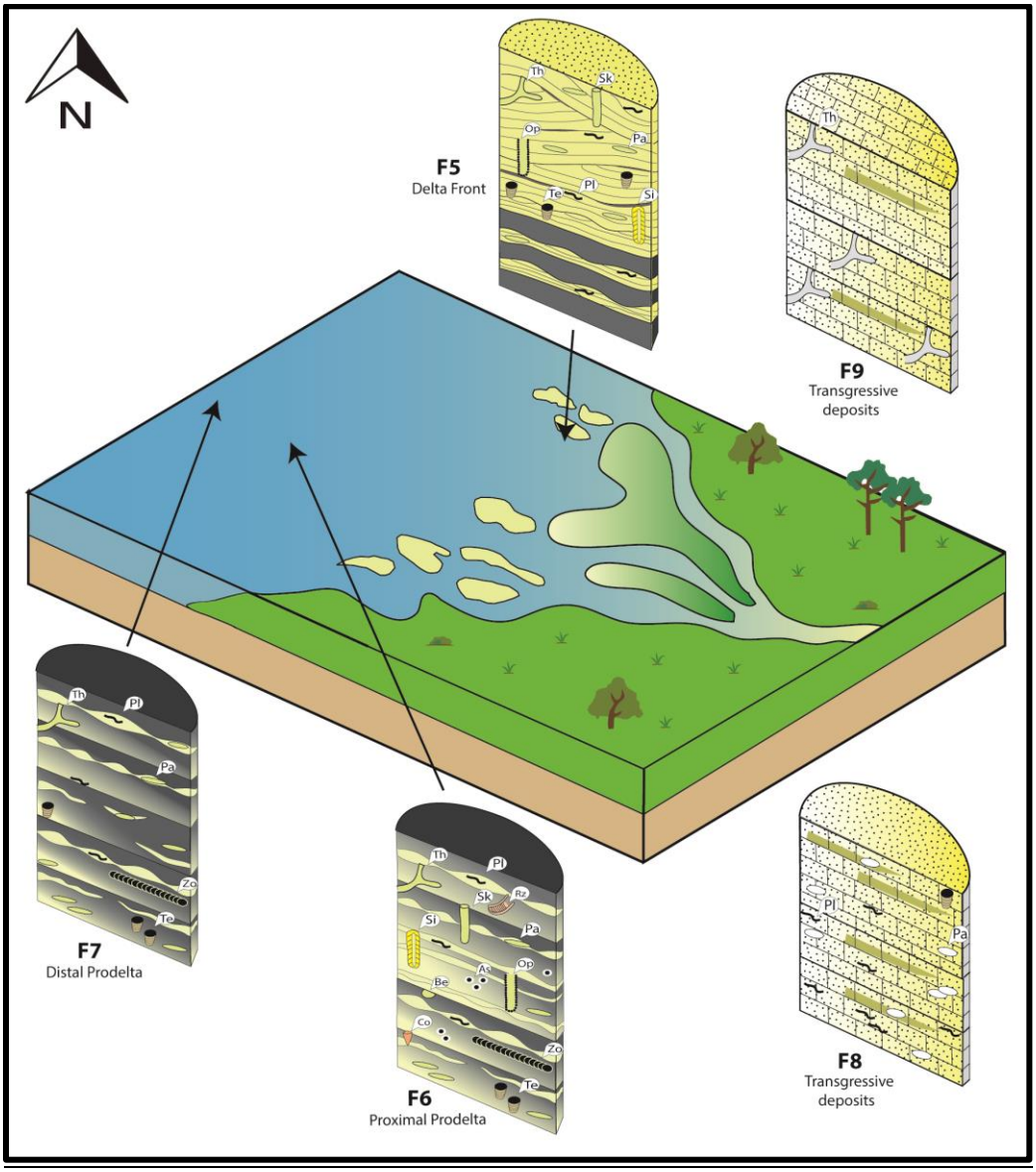

Figure 8.11. *Schematic reconstruction of trace-fossil distribution in the various subenvironments of the deltaic system during the deposition of the U and M2 Sandstone members, Napo Formation, Oriente basin of Ecuador. The ichnogenera shown are as follows:* Asterosoma *isp. (As),* Bergaueria *isp. (Be),* Conichnus *isp. (Co),* Ophiomorpha nodosa *(Op),* Palaeophycus *isp. (Pa),* Planolites *isp. (Pl),* Rhizocorallium commune *(Rz),* Siphonichnus *isp. (Si),* Skolithos *isp. (Sk),* Teichichnus *isp, and* Teichichnus rectus *(Te),* Thalassinoides *isp. (Th),* and Zoophycos *isp. (Zo).*

A modern analogue that displays similar facies stacking pattern to the M2 Sandstone Member and to the deltaic deposits in the U Sandstone Member is the tide-dominated Mahakam Delta located on the southeastern coast of Kalimantan, Indonesia. Up to 8000 m

of sediment have been deposited from the late Miocene to the Pliocene/Pleistocene, comprising several stages of fluvio-estuarine and deltaic sedimentation (Allen et al., 1979; Carbonel & Moyes, 1987). The Mahakam Delta is a mixed system composed of a network of straight distributary channels and sinuous tidal channels, where tides are certainly the most important sedimentary processes, fluvial processes play a subordinate role, and waves have a minor influence (Nummedal et al., 2003). Its deposition is strongly influenced by the north-south currents of the Makassar Strait and, therefore, sand is concentrated in the central and southern portions of the delta. The muddy sediment is spread over a large area, and is transported far to the south (Lambert, 2003).

Studies revealed that within 10 to 50 km from the delta apex, the tides alter the river discharge division by about 10% in all bifurcations (e.g. Sassi et al., 2011). The tidal impact increases seaward, with a maximum value of the order of 30%. Tidal range varies from less than 0.5 m during neap tides to 2.5 m during spring tides (Sassi et al., 2011). Tides affect essentially the whole delta plain with an enough tidal range to inundate the delta plain up to 20 km inland from the coastline. Tidal processes generate cross-bedded medium sands with mud drapes and plant debris (Salahuddin & Lambiase, 2013). A few vertical burrows (i.e. incipient *Skolithos*) have been recorded. Bioturbation intensity increases upwards into the overlying bioturbated, muddy fine sand (Salahuddin & Lambiase, 2013). On the other hand, wave energy is low due to limited fetch in the Makassar Strait. The wave energy is mostly attenuated on the broad subaqueous delta plain. The waves concentrate detrital organic debris along muddy shorelines forming peat beaches and ridges (Salahuddin & Lambiase, 2013). Moreover, the delta rarely experiences storms because of its equatorial location (Roberts & Sydow, 2003).

The Mahakam Delta comprises several subenvironments, namely the delta plain, which is subdivided in two areas, fluviatile and tidal, the delta front, and the outermost part represented by the prodelta. The tidal delta plain is composed of muddy distributary channels and associated organic-rich muddy interdistributary areas. The sand-dominated delta front width ranges between 8 and 10 km, is mainly composed of incised terminal distributary channels that extend seaward terminating in a mouth bar; the inner portion is mainly composed of tidal flats (Lambert, 2003; Sassi et al., 2011). The prodelta is 30 km wide and

dominated by clay deposited off the southern distributary system. The sediment transport patterns and facies distribution suggest that the Mahakam Delta is presently subsiding and that it is, in essence, a drowned delta that is being transgressed and modified by marine processes. Moreover, evidence suggest that the Mahakam Delta was retrogradationally backfilled and sediment transport patterns suggest that distributaries are the principal areas of sedimentation (Salahuddin & Lambiase, 2013).

These subenvironments resemble those recorded in the M2 Sandstone Member, essentially reflecting similar role of the tides and riverine processes, with limited to negligible influence of wave processes. In addition, the backfilling pattern see in the Mahakam Delta is roughly similar to DSM2 in which progressively finer-grained and more marine influenced deposits occur upwards in the stratigraphic succession. The Mahakam Delta reflects increase in tidal impact in a seaward direction with a maximum value of the order of 30% (Sassi et al., 2011).

During the deposition of the Mahakam Delta, transgressions and regressions alternated in response to major global glacio-eustatic cycles, as well as to local tectonics (Carbonel & Moyes, 1987; Lambiase et al., 2017). The Mahakam delta shows several meter-thick successions deposited during transgressive phases, some of them resulting from regionally extensive major transgressions. However, some transgressions were short-lived within dominantly progradational phases (Salahuddin & Lambiase, 2013; Lambiase et al., 2017), such as those recorded during deposition of the M2 Sandstone Member.

Figure 8.12 *Mahakam River Delta, Indonesia (source: Google Earth©)*

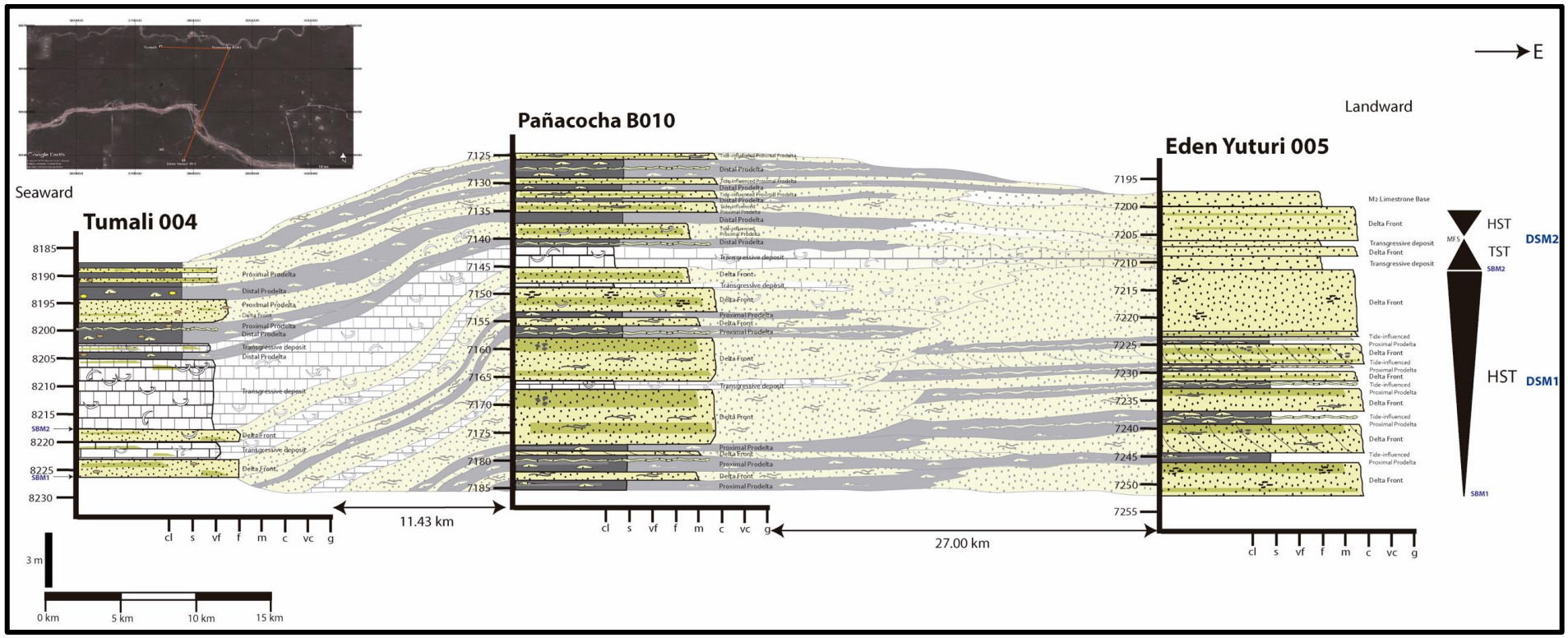

Figure 8.13. *Correlations and sequence-stratigraphic architecture of the M2 Sandstone Member. Sections constructed based on well cores descriptions, left upper section in the Oriente Basin, Ecuador.*

CHAPTER 9

9. CONCLUSIONS

(1) Nine sedimentary facies (F1-F9) have been identified in the U and M2 Sandstone members in the Oriente Basin of Ecuador.

(2) In the study area, the U Sandstone Member represents deposition in three different environments: fluvial, estuarine, and deltaic, comprising two depositional sequences (DSU1 and DSU2).

(3) The base of depositional sequence 1 (DSU1) represents a subaerial unconformity formed as a result of valley incision during relative fall of sea level. DSU1 comprises the lower and middle intervals of the U Sandstone Member and the lower part of its upper interval. Fluvial channel-fill deposits (F1) locally separated by overbank deposits (F2) make up the LST, which is replaced upwards by retrogradational estuarine tidal channel and bar (F3), tidal flat (F4) and transgressive (F8) deposits of the TST. HST is represented by distal prodelta (F7), proximal prodelta (F6), and delta front (F5) deposits forming a progradational succession, punctuated by transgressive deposits (F8).

(4) The base of DSU2 is a subaerial unconformity due to renewed valley incision. DSU2 comprises the upper part of the upper interval of the U Sandstone Member. In the more proximal section, this incision has truncated a significant part of the underlying highstand deltaic deposits of DSU1. Fluvial deposition is characterized by amalgamated channel fills (F1) of the LST, followed by estuarine deposition represented by tidal-influenced channels and bars (F3) and tidal flat deposits (F4) of the TST. Estuarine deposits are replaced by HST deltaic progradation, represented by

coarsening- and thickening-upward successions typically ranging from proximal prodelta (F6) to delta front (F5).

(5) The M2 Sandstone Member represents deposition in a deltaic environment, encompassing delta front, prodeltaic, and transgressive deposits, and comprising two depositional sequences (DSM1 and DSM2).

(6) The base of DSM1 has not been cored, but well log information suggests that the underlying A Limestone Member represents its TST. The base of DSM2 is a co-planar surface. Both sequences consist of thick HST coarsening- and thickening-upward deltaic successions, encompassing from distal prodelta (F7), proximal prodelta (F6) to delta front (F5) deposits, separated by thin TST carbonate (F8) and siliciclastic (F9) deposits. Deltaic strata exhibit progradational-stacking (seaward) patterns, and have clinoformal geometry.

(7) Mudstone drapes, double mudstone drapes, and heterolithic intervals suggest tidal influence during deposition of both the U and M2 Sandstone members. River influence is indicated by the presence of hyperpycnal deposits. No wave-generated structures have been documented. Accordingly, the estuarine systems are regarded as tide-dominated, and the deltas as mixed tide- and river-influenced.

(8) Thirteen ichnospecies have been identified in the studied deposits. A few trace fossils, suggestive of the freshwater depauperate *Mermia* Ichnofacies, are recorded in the fluvial deposits. The bulk of trace fossils occurs in the estuarine and deltaic deposits, recording brackish-water conditions. These trace-fossil assemblages essentially illustrate the depauperate *Cruziana* and *Skolithos* Ichnofacies. However, times of reduced fluvial discharge are associated with the archetypal *Cruziana* Ichnofacies, characterized by increased ichnodiversity.

(9) Ichnofacies variability in both units reflects the role of different controlling factors in each subenvironment, most notably salinity, hydrodynamic energy, substrate, sedimentation rate, and oxygen.

CHAPTER 10

10.RECOMMENDATIONS

Addition of high-resolution seismic data in sequence stratigraphic interpretations will allow extensive mapping of key surfaces (e.g. transgressive surfaces, sequence boundaries). Characterizing these surfaces is difficult with just scattered cores.

Additional well log data will be instrumental in the interpolations between the studied wells, allowing to improve interpretations within a more precise architectural framework.

A more refined understanding of lateral facies changes is needed in order to be able to predict the geometry of sandstone bodies and their internal heterogeneities at reservoir scale.

CHAPTER 11

11.REFERENCES

Abad, M., Ruiz, F., & Pendón, J. G. (2006). Escape and equilibrium trace fossils in association with *Conichnus conicus* as indicators of variable sedimentation rates in Tortonian littoral environments of SW Spain. *Geobios*, 39, 1–11.

Alava-Toro, J., & Jaillard, E. (2005). Provenance of the Upper Cretaceous to upper Eocene clastic sediments of the Western Cordillera of Ecuador: Geodynamic implications. *Tectonophysics*, 399, 279–292.

Alexander, C. R., DeMaster, D. J., & Nittrouer, C. A. (1991). Sediment accumulation in a modern epicontinental-shelf setting: The Yellow Sea. *Marine Geology*, 98, 51–72.

Allen, G. P., Laurier, D., & Thouvenin, J. (1979). Etude sédimentologique du delta de la Mahakam. *TOTAL Compagnie Française Des Pétroles, Notes et Mémoires*, 156.

Ayranci, K., Dashtgard, S. E., & MacEachern, J. A. (2014). A quantitative assessment of the neoichnology and biology of a delta front and prodelta, and implications for delta ichnology. *Palaeogeography, Palaeoclimatology, Palaeoecology*, 409, 114–134.

Baby, P., Rivadeneira, M., & Barragán, R. (2014). *La Cuenca Oriente Geología y Petróleo*, 144, 415.

Baby, P., Rivadeneira, M., Barragán, R., & Christophoul, F. (2013). Thick-skinned tectonics in the Oriente foreland basin of Ecuador. In: Nemčok, M., Mora, A., Codgrove, J.W. (Eds.), Thick-Skin-Dominated Orogens: From Initial Inversion to Full Accretion. *Geological Society, London, Special Publications*, 377, 59-76.

Baby, P., Rivadeneira, M., Christophoul, F., & Barragán, R. (1999). Style and timing of deformation in the Oriente basin of Ecuador. *Abstracts of the Fourth International Symposium on Andean Geodynamics*, Gottingen, 68-72.

Balkwill, H. R. (1995). Northern part of Oriente Basin, Ecuador; reflection seismic expression of structures. In Tankard, A.J., Suarez, R., and Welsink, H.J. (Eds.), *Petroleum Basin of South America: AAPG Memoir*, 62, 559.

Basan, P. B., & Scott, R. W. (1979). Morphology of *Rhizocorallium* and associated traces from the Lower Cretaceous Purgatoire Formation, Colorado. *Palaeogeography, Palaeoclimatology, Palaeoecology*, 28, 5–23.

Bhattacharya, J. P., & MacEachern, J. A. (2009). Hyperpycnal Rivers and Prodeltaic Shelves in the Cretaceous Seaway of North America. *Journal of Sedimentary Research*, 79, 184–209.

Boyd, R., Dalrymple, R. W., & Zaitlin, B. A. (2006). Estuarine and incised-valley facies models. In Posamentier, H.W., and Walker, R. (Eds.), Facies Models Revisited, *SEPM Special Publication*, 84, 175–240.

Bromley, R. G. (1996). *Trace Fossils: Biology, Taphonomy and Applications* (2nd ed.). Springer - Science.

Buatois, L. A., Gingras, M. K., MacEachern, J. A., Mángano, M. G., Zonneveld, J. P., Pemberton, S. G., Netto, R. G., Martin, A. J. (2005). Colonization of Brackish-Water Systems through Time: Evidence from the Trace-Fossil Record. *Palaios*, 20, 321–347.

Buatois, L. A., & Mángano, M. G. (1995). The paleoenvironmental and paleoecological significance of the lacustrine *Mermia* ichnofacies: An archetypical subaqueous nonmarine trace fossil assemblage. *Ichnos: An International Journal of Plant & Animal*, 4, 151–161.

Buatois, L. A., & Mángano, M. G. (2002). Trace fossils from Carboniferous floodplain deposits in western Argentina: Implications for ichnofacies models of continental environments. *Palaeogeography, Palaeoclimatology, Palaeoecology*, 183, 71–86.

Buatois, L. A., & Mángano, M. G. (2004). Animal-substrate interactions in freshwater environments: applications of ichnology in facies and sequence stratigraphic analysis of fluvio-lacustrine successions. In McIlroy, D. (Ed.), The Application of Ichnology to Palaeoenvironmental and Stratigraphic Analysis, *Geological Society, London, Special Publications*, 228, 311–333.

Buatois, L. A., & Mángano, M. G. (2007). Invertebrate ichnology of continental freshwater environments. In *Miller III, W., (Ed.), Trace Fossils: Concepts, Problems, Prospects, Amsterdam:* Elsevier, 285–323.

Buatois, L. A., & Mángano, M. G. (2011). *Ichnology Organism—Substrate Interactions in Space and Time* (University of Saskatchewan). Cambridge University Press.

Buatois, L. A., Mángano, M. G., Abdulrahman, A., & Timothy R., C. (2002). Sequence stratigraphic and sedimentologic significance of biogenic structures from a late Paleozoic marginal- to open-marine reservoir, Morrow Sandstone, subsurface of southwest Kansas, USA. *Sedimentary Geology*, 152, 99–132.

Buatois, L. A., Mángano, M. G., & Maples, C. (1997). The Paradox of Nonmarine Ichnofaunas in Tidal Rhythmites: Integrating Sedimentologic and Ichnologic Data from the Late Carboniferous of Eastern Kansas, USA. *Palaios*, 12, 467–481.

Buatois, L. A., Saccavino, L. L., & Zavala, C. (2011). Ichnologic Signatures of Hyperpycnal Flow Deposits in Cretaceous River-dominated Deltas, Austral Basin, Southern Argentina. In Slatt, R.M. and Zavala, C. (Eds.), Sediment Transfer from Shelf to Deep Water. Revisiting the Delivery System, *American Association of Petroleum Geologists Studies, Geology*, 61, 153–170.

Buatois, L. A., Santiago, N., Herrera, M., Plink-Björklund, P., Steel, R., Espin, M., & Parra, K. (2012). Sedimentological and Ichnological Signatures of Changes in Wave, River and Tidal Influence Along a Neogene Tropical Deltaic Shoreline. *Sedimentology*, 78, 458-479.

Buatois, L. A., Santiago, N., Parra, K., & Steel, R. (2008). Animal-Substrate Interactions in an Early Miocene Wave-Dominated Tropical Delta: Delineating Environmental Stresses and Depositional Dynamics (Tácata Field, Eastern Venezuela). *Journal of Sedimentary Research*, 78, 458–479.

Burgos, J. D. Z., Christophoul, F., Baby, P., Antoine, P. O., Soula, J. C., Good, D., & Rivadeneira, M. (2005). Dynamic evolution of Oligocene-Neogene sedimentary series in a retro-foreland basin setting: Oriente Basin, Ecuador. *6th International Symposium on Andean Geodynamics (ISAG 2005, Barcelona), Extended Abstracts*, 127–130.

Canale, N., Ponce, J. J., Carmona, N. B., & Drittanti, D. I. (2016). Ichnology of deltaic mouth-bar systems of the Lajas Formation (Middle Jurassic) in the Sierra de la Vaca Muerta, Neuquén Basin, Argentina. *Ameghiniana*, 53, 170–184.

Canfield, R., Bonilla, R., & Raymond, R. (1982). Sacha Oil Field of Ecuadorian Oriente. *The American Association of Petroleum Geologists Bulletin*, 66, 1076-1090.

Carbonel, P., & Moyes, J. (1987). Late Quaternary Paleoenvironmets of the Mahakam Delta (Kalimantan, Indonesia). *Palaeogeography, Palaeoclimatology, Palaeoecology*, 61, 265–284.

Carmona, N. B., Buatois, L. A., & Mángano, M. G. (2008). Ichnology of the Lower Miocene Chenque Formation, Patagonia, Argentina: Animal-substrate interactions and the modern evolutionary fauna. *Ameghiniana*, 45, 93–122.

Carmona, N. B., Buatois, L. A., Ponce, J. J., & Mángano, M. G. (2009). Ichnology and sedimentology of a tide-influenced delta, Lower Miocene Chenque Formation, Patagonia, Argentina: Trace-fossil distribution and response to environmental stresses. *Palaeogeography, Palaeoclimatology, Palaeoecology*, 273, 75–86.

Cattaneo, A., & Steel, R. J. (2003). Transgressive deposits: A review of their variability. *Earth Science Reviews*, 62, 42.

Catuneanu, O. (2006). *Principles of sequence stratigraphy* (1st ed). Elsevier.

Christophoul, F. (1999). Discrimination des influences tectoniques et eustatiques dans les basins liés à des zones de convergence: Exemples du bassin subandin d'Equateur. *Phd Thesis, Université Toulouse III, Paul Sabatier*, 184.

Christophoul, F., Baby, P., & Dávila, C. (2002). Stratigraphic responses to a major tectonic event in a foreland basin: The Ecuadorian Oriente Basin from Eocene to Oligocene times. *Tectonophysics*, 345, 281–298.

Curran, H. A., & Frey, R. W. (1977). Pleistocene trace fossils from North Carolina (U.S.A.), and their Holocene analogues. In Crimes, T.P., and Harper, J.C. (Eds.), Trace Fossils 2, *Geol. J. Special Issue*, 9, 139–162.

Dafoe, L. T., Gingras, M. K., & Pemberton, S. G. (2010). Wave-influenced deltaic bodies and offshore deposits in the Viking Formation, Hamilton Lake area, south-central Alberta, Canada. *Bull. Can. Pet. Geol.*, 58, 173–201.

Dalrymple, Robert W., & Choi, K. (2007). Morphologic and facies trends through the fluvial–marine transition in tide-dominated depositional systems: A schematic framework for environmental and sequence-stratigraphic interpretation. *Earth-Science Reviews*, 81, 135–174.

Dalrymple, R.W., Leckie, D. A., & Tillman, R. W. (2006). Incised-valleys in time and space: An introduction to the volume and an examination of the controls on valley formation and filling. In Dalrymple, R.W., Leckie, D.A., and Tillman, R.W. (Eds.), Incised Valleys in Time and Space, *Society for Sedimentary Geology Special Publications.*, 85, 5–12.

Dalrymple, R.W., Zaitlin, B. A., & Boyd, R. (1992). Estuarine Facies Models: Conceptual Basis and Stratigraphic Implications. *Journal of Sedimentary Petrology*, 62, 17.

Dasgupta, S., Buatois, L. A., & Mángano, M. G. (2016). Living on the Edge: Evaluating the Impact of Stress Factors on Animal–Sediment Interactions in Subenvironments of a Shelf-Margin Delta, the Mayaro Formation, Trinidad. *Journal of Sedimentary Research, 86*, 1034–1066.

Dasgupta, S., Buatois, L. A., Zavala, C., Mángano, M. G., & Törő, B. (2016). Ichnology of a subaqueously prograding clastic wedge, late Pliocene Morne L'Enfer Formation, Fullarton, Trinidad: Implications for recognition of autogenic erosional surfaces and delineation of stress factors on irregular echinoids. *Palaeogeography, Palaeoclimatology, Palaeoecology*, 459, 365–380.

Dashwood, M. F., & Abbotts, I. L. (1990a). Aspects of the petroleum geology of the Oriente Basin, Ecuador. In Brooks J., (Ed.), Classic petroleum provinces, *Geological Society, London, Special Publications*, 50, 89–117.

Dashwood, M. F., & Abbotts, I. L. (1990b). Aspects of the Petroleum Geology of the Oriente Basin, Ecuador. *Geological Society, London, Special Publications*, 50, 89–117.

Davis Jr, R. A., & Hayes, M. O. (1984). What is a wave-dominated coast?, *Marine Geology*, 60, 313–329.

Davis, R. A., & Dalrymple, R. W. (Eds.). (2012). *Principles of tidal sedimentology*. Springer.

Dawson, W. C. (1981). Secondary burrow porosity in quartzose biocalc-arenites, Upper Cretaceous, Texas: U.S.A. *VIII Congreso Geológico Argentino, San Luis (20-26 Septiembre, 1981)*, 637–649.

De Berc, S. B., Soula, J. C., Baby, P., Souris, M., Christophoul, F., & Rosero, J. (2005). Geomorphic evidence of active deformation and uplift in a modern continental wedge-top–foredeep transition: Example of the eastern Ecuadorian Andes. *Tectonophysics*, 399, 351–380.

Díaz, M., Baby, P., Rivadeneira, M., & Christophoul, F. (2004). El pre-Áptense de la cuenca Oriente ecuatoriana. In *La Cuenca Oriente: Geología y Petróleo. Travaux de l'Institut Francis es Etudes Andine, 144*, 23-44.

Dyer, K. R. (1998). The typology of intertidal mudflats. *Geological Society, London, Special Publications*, 139, 11–24.

Dyer, K. R., Christie, M. C., & Wright, E. W. (2000). The classification of intertidal mudflats. *Continental Shelf Research*, 22.

Estupiñan, J., Marfil, R., Scherer, M., Permanyer, A. (2010). Reservoir sandstones of the Cretaceous Napo formation U and T members in the Oriente Basin, Ecuador: links between diagenesis and sequence stratigraphy. *Journal of Petroleum Geology, 33*, 221-246.

Farrow, G. E. (1966). Bathymetric zonation of Jurassic trace fossils from the coast of Yorkshire, England. *Palaeogeogr Palaeoclimatol Palaeoecol*, 103–151.

Frey, R. W., Howard, J. D., & Pryor, W. A. (1978). *Ophiomorpha*: Its morphologic, taxonomic, and environmental significance. *Palaeogeogr Palaeoclimatol Palaeoecol*, 23, 199–229.

Frey, R. W., Pemberton, S. G., & Fagerstrom, J. A. (1984). Morphological, ethological, and environmental significance of the ichnogenera *Scoyenia* and *Ancorichnus*. *Journal of Paleontology*, 511–528.

Fürsich, F. T. (1974). Corallian (Upper Jurassic) trace fossils from England and Normandy. *Stuttg. Beitr. Naturkd. (B), 13*, 1-52.

Gani, M. R., Bhattacharya, J. P., & MacEachern, J. A. (2008). Using ichnology to determine relative influence of waves, storms, tides, and rivers in deltaic deposits: Examples from

Cretaceous Western Interior Seaway, U.S.A. In MacEachern, J.A., Bann, K.L., Gingras, M.K, and Pemberton, S.G. (Eds.), *Applied Ichnology.*, *S*EPM Short Course Notes, 52, 209–225.

Gerard, J. R. F., & Bromley, R. G. (2008). Ichnofabrics in clastic sediments-application to sedimentological core studies: A practical guide. *Jean R.F.*, 97.

Gibling, M. R. (2006). Width and Thickness of Fluvial Channel Bodies and Valley Fills in the Geological Record: A Literature Compilation and Classification. *Journal of Sedimentary Research*, 76, 731–770.

Gingras, M. K., Dashtgard, S. E., & MacEachern, J. A. (2008). Biology of shallow-marine ichnology: A modern perspective. *Aquatic Biol.*, 2, 255–268.

Gingras, M. K., MacEachern, J. A., & Pemberton, S. G. (1998). A comparative analysis of the ichnology of wave-and river-dominated allomembers of the Upper Cretaceous Dunvegan Formation. *Bulletin of Canadian Petroleum Geology*, 46, 51–73.

Giosan, L., & Bhattacharya, J. P. (2005) (Eds.). *River deltas: Concepts, models, and examples*, SEPM (Society for Sedimentary Geology), 83.

Gombojav, N., & Winkler, W. (2008). Recycling of Proterozoic crust in the Andean Amazon foreland of Ecuador: Implications for orogenic development of the Northern Andes. *Terra Nova*, 20, 22–31.

Gowland, S. (1996). Facies characteristics and depositional models of highly bioturbated shallow marine siliciclastic strata: An example from the Fulmar Formation (Late Jurassic), UK Central Graben. In Hurst., A, Johnson., H.D., Urley., D.B. (Eds.), Geology of the Humber Group: Central Graben and Moray Firth, UKCS, *Geological Society of London (Special Publications)*, 114, 185–214.

Greb, S. F., & Chesnut, D. R. (1994). Paleoecology of an estuarine sequence in the Breathitt Formation (Pennsylvanian), central Appalachian Basin. *Palaios*, 9, 388–402.

Gugliotta, M., Kurcinka, C. E., Dalrymple, R. W., Flint, S. S., & Hodgson, D. M. (2016). Decoupling seasonal fluctuations in fluvial discharge from the tidal signature in ancient deltaic deposits: An example from the Neuquén Basin, Argentina. *Journal of the Geological Society*, 173, 94–107.

Gutiérrez, G., Horton, B. K., Vallejo, C., Jackson, L. J., & George, S. W. M. (2019). Provenance and geochronological insights into Late Cretaceous-Cenozoic foreland basin development in the Subandean Zone and Oriente Basin of Ecuador. In Horton, B.K., and Folguera, A., (eds.), *Andean Tectonics*: Amsterdam, Elsevier, 237–268.

Hansen, C. D., & MacEachern, J. A. (2009). Application of the asymmetric delta model to along-strike facies variations in a mixed wave-and river-influenced delta lobe, Upper Cretaceous Basal Belly River Formation, central Alberta. In MacEachern, J.A., Bann, K.L., Gingras, M.K., and Pemberton, S.G. (Eds.), Applied Ichnology, *Society for Sedimentary Geology Short Course Notes*, 52, 1-16.

Haq, B. U., Hardenbol, J., & Vail, P. R. (1987). Chronology of fluctuating Sea levels since the Triassic. *Science*, 235, 1156–1167.

Hasiotis, S. T. (2002). Continental Trace Fossils: *SEPM Short Course Notes*, Tulsa, Oklahoma, 51, 134.

Hori, K., Saito, Y., Zhao, Q., & Wang, P. (2002). Architecture and evolution of the tide-dominated Changjiang (Yangtze) River delta, China. *Sedimentary Geology*, 146, 249–264.

Howard, J. D. (1972). Trace fossils as criteria for recognizing shorelines in stratigraphic record. In Rigby, J.K., and Hamblin. W.K., (Eds.), Recognition of Ancient Sedimentary Environments. *Society of Economic Paleontologists and Mineralogists Special Publication*, 16, 215–225.

Hubbard, S. M., MacEachern, J. A., & Bann, K. L. (2012). Slopes. In Knaust, D., and Bromley, R.G., (Eds.), *Trace Fossils as Indicators of Sedimentary Environments*, 64, 607–642.

Ichaso, A. A., & Dalrymple, R. W. (2009). Tide- and wave-generated fluid mud deposits in the Tilje Formation (Jurassic), offshore Norway. *Geol. Soc. Am.*, 37, 539–542.

Jaillard, E. (1997). Síntesis Estratigráfica y Sedimentológica del Cretáceo y Paleógeno de la Cuenca Oriental del Ecuador. *Informe Final del Convenio ORSTOM-PETROPRODUCCION*, 1-168.

Joseph, J. K., Patel, S. J., & Bhatt, N. Y. (2012). Trace fossil assemblages in mixed siliciclastic-carbonate sediments of the Kaladongar Formation (Middle Jurassic), Patcham Island, Kachchh, Western India. *J. Geol. Soc. India*, 80, 189–214.

Kennedy, W. J., & Sellwood, B. W. (1970). *Ophiomorpha nodosa* Lundgren, a marine indicator from the Sparnacian of south-east England. *Proceedings of the Geologists' Association*, 81, 99-110.

Knaust, D. (2012). Trace-fossil systematics. *In:* Knaust, D., Bromley, R.G. (Eds.) Trace Fossils as Indicators of Sedimentary Environments, *Developments in Sedimentology,* 64, 79–101.

Knaust, D. (2013). The ichnogenus *Rhizocorallium*: Classification, trace makers, palaeoenvironments and evolution. *Earth Science Reviews*, 126, 1–47.

Knaust, D. (2017). *Atlas of Trace fossils in Well Core: Appearance, Taxonomy and Interpretation*. Springer, New York, 1- 219.

Knaust, D. (2018). The ichnogenus *Teichichnus* Seilacher, 1955. *Earth-Science Reviews*, 177, 386–403.

Kotlarczyk, J., & Uchman, A. (2012). Integrated ichnology and ichthyology of the Oligocene Menilite Formation, Skole and Subsilesian nappes, Polish Carpathians: A proxy to oxygenation history. *Palaeogeography, Palaeoclimatology, Palaeoecology*, 331, 104–118.

1. Lambert, B. (2003). Micropaleontological investigations in the modern Mahakam delta, East Kalimantan (Indonesia). *Carnets de Géologie (Notebooks on Geology), Articles* 02, 1-21.

Lambiase, J. J., Riadi, R. S., Nirsal, N., & Husein, S. (2017). Transgressive successions of the Mahakam Delta Province, Indonesia. *Geological Society, London, Special Publications*, 444, 335–348.

Leithold, E. L., & Dean, W. E. (1998). Depositional processes and carbon burial on a Turonian prodelta at the margin of the Western Interior Seaway. In Dean, W.E., and. Arthur, M.A. (Eds.), Stratigraphy and Palaeoenvironments of the Cretaceous Western Interior seaway, USA, *Society for Sedimentary Geology Concepts in Sedimentology and Palaeontology,* 6, 189-200.

Litherland, M., Aspden, J. A., & Jemielita, R. A. (1994). The metamorphic belts of Ecuador. *Memoir of the British Geological Survey,* 11, 147.

Luzieux, L. D. A., Heller, F., Spikings, R., Vallejo, C. F., & Winkler, W. (2006). Origin and Cretaceous tectonic history of the coastal Ecuadorian forearc between 1°N and 3°S: Paleomagnetic, radiometric and fossil evidence. *Earth and Planetary Science Letters*, 249, 400–414.

MacEachern, J. A., & Bann, K. L. (2008). The role of ichnology in refining shallow marine facies models. In Hampson, G.J. (Ed.*), Recent Advances in Models of Siliciclastic Shallow-Marine Stratigraphy, SEPM Special Publication*, 90, 73–116.

MacEachern, J. A., Bann, K. L., & Bhattacharya, J. P. (2005). Ichnology of deltas: Organisms' responses to the dynamic interplay of rivers, waves, storms and tides. In Giosan, L., and. Bhattacharya, J.P (Eds.), River Deltas: Concepts, Models, and Examples, *SEPM Special Publication*, 83, 49–85.

MacEachern, J. A., Bann, K. L., & Gingras, M. K. (2012). The ichnofacies paradigm. In Knaust, D., Bromley, R.G. (Eds.), Trace Fossils as Indicators of Sedimentary Environments, *Developments in Sedimentology*, Elsevier: Amsterdam 64, 103–138.

MacEachern, J. A., Bann, K. L., Pemberton, S. G., & Gingras, M. K. (2007). The ichnofacies paradigm: High-resolution paleoenvironmental interpretation of the rock record, In MacEachern, J.A., Bann, K.L., Gingras, M.K., and Pemberton, S.G. (Eds.), Applied Ichnology. *SEPM (Society for Sedimentary Petrology) Short Course Notes*, 52, 27-64.

MacEachern, J. A., & Gingras, M. K. (2007). Recognition of brackish-water trace-fossil suites in the Cretaceous Western Interior Seaway of Alberta, Canada. In Bromley, R., Buatois, L.A., Mángano, M.G., Genise, J., and Melchor, R. (Eds.) Sediment–Organism Interactions: A Multifaceted Ichnology. *Society of Economic Paleontologists and Mineralogists (Society for Sedimentary Geology) Special Publications*, 88, 149-193.

MacEachern, J. A., & Pemberton, S. G. (1992). Ichnological Aspects of Cretaceous Shoreface Successions and Shoreface Variability in the Western Interior Seaway of North America. In Pemberton, S.G. (Ed.) Applications of Ichnology to Petroleum Exploration: A Core Workshop, *SEPM (Society for Sedimentary Geology)*, 17, 57-84.

MacEachern, J. A., & Pemberton, S. G. (1994). Ichnological aspects of incised-valley fill systems from the Viking Formation of the Western Canada Sedimentary Basin, Alberta, Canada. In Boyd, R., Zaitlin, B.A., and Dalrymple, R. (Eds.) Incised-valley Systems: Origin and Sedimentary Sequences, *SEPM Special Publication*, 51, 129-157.

Mángano, M. G., & Buatois, L. A. (2004a). Ichnology of Carboniferous tide-influenced environments and tidal fiat variability in the North American Midcontinent. In McIlroy, D. (Ed.) The Application of Ichnology to Paleoenvironmental and Stratigraphic Analysis, *Geological Society of London*, 228, 157–178.

Mángano, M. G., & Buatois, L. A. (2004b). Reconstructing Early Phanerozoic intertidal ecosystems: Ichnology of the Cambrian Campanario Formation in northwest Argentina. In Webby, B.D., Mángano, M.G., and Buatois, L.A. (Eds.), Trace Fossils in Evolutionary Palaeoecology, *Fossils and Strata*, 51, 17-38.

McAnally, W. H., Friedrichs, C., Hamilton, D., Hayter, E., Shrestha, P., Rodriguez, H., Sheremet, A., & Teeter, A. (2007). Management of Fluid Mud in Estuaries, Bays, and Lakes. I: Present State of Understanding on Character and Behavior. *Journal of Hydraulic Engineering*, 133, 9–22.

McGroder, M. F., Lease, R. O., & Pearson, D. M. (2015). Along-strike variation in structural styles and hydrocarbon occurrences, Subandean fold-and-thrust belt and inner foreland, Colombia to Argentina. *Geological Society of America Memoirs*, 212, 79–113.

McIIroy, D. (2004). Ichnofabrics and sedimentary facies of a tide-dominated delta: Jurassic lle Formation of Kristin Field, Haltenbanken, Offshore Mid-Norway. In McIlroy, D. (Ed.) The Application of Ichnology to Palaeoenvironmental and Stratigraphic Analysis, *Geological Society of London Special Publications*, 228, 237–272.

Mehta, A. J., & McAnally, W. H. (2002). Fine grained cohesive sediment transport. *Sedimentation Engineering*, 2, 75.

Melchor, R. N., Genise, J. F., & Buatois, L. A. (2012). Fluvial environments. In Knaust, D., Bromley, R.G. (Eds.), Trace fossils as indicators of sedimentary environments, *Sedimentology*, 64, 329–378.

Michels, K. H., Kudrass, H. R., Hübscher, C., Suckow, A., & Wiedicke, M. (1998). The submarine delta of the Ganges–Brahmaputra: Cyclone-dominated sedimentation patterns. *Marine Geology*, 149, 133–154.

Mikuláš, R. (2003). The *Mermia* ichnofacies across the fossilization barrier: A comparison of the Permian Krkonoe Piedmont Basin (Czech Republic) and modern flood sediments at Prague. *VII International Ichnofabric Workshop, Program, Abstracts*, 44-45

Miller, M. F., & Knox, L. W. (1985). Biogenic structures and depositional environments of a Lower Pennsylvanian coal-bearing sequence, northern Cumberland Plateau, Tennessee, U.S.A. *In:* Curran, H.A. (Ed.), Biogenic Structures: Their Use in Interpreting Depositional Environments, *SEPM Special Publication*, 35, 67–97.

Monaco, P., Caracuel M., J. E., Giannetti, A., Soria Mingorance, J. M., & Yébenes Simón, A. (2007). *Thalassinoides* and *Ophiomorpha* as cross-facies trace fossils of crustaceans from shallow-to-deep-water environments: Mesozoic and Tertiary examples from Italy and Spain. *3rd Symposium on Mesozoic and Cenozoic Decapod Crustaceans-Museo di Storia Naturale di Milano*, 80-82.

Moslow, T. F., & Pemberton, S. G. (1988). An integrated approach to the sedimentological analysis of some Lower Cretaceous shoreface and delta front sandstone sequences. In: James, D.P. & Leckie, D.A. (Eds.), Sequences, Stratigraphy, Sedimentology: Surface and Subsurface. *Canadian Society of Petroleum Geologist, Memoir 15*, 373-386.

Mulder, T., Syvitski, J. P. M., Migeon, S., Faugères, J.-C., & Savoye, B. (2003). Marine hyperpycnal flows: Initiation, behavior and related deposits. A review. *Marine and Petroleum Geology*, 20, 861–882.

Neto de Carvalho, C., & Rodrigues, N. P. (2003). Los *Zoophycos* del Bajociense-Bathoniense de la Praia da Mareta (Algarve, Portugal): Arquitectura y finalidades en régimen de dominancia ecológica. *Revista Española de Paleontología*, 18, 229–241.

Nickel, L. A., & Atkinson, R. J. A. (1995). Functional morphology of burrows and trophic modes of three thalassinidean shrimp species, and a new approach to the classification of thalassinidean burrow morphology. *Mar. Ecol. Prog. Ser.*, 128, 181–197.

Nittrouer, C. A., Kuehl, S. A., DeMaster, D. J., & Kowsmann, R. O. (1986). The deltaic nature of Amazon shelf sedimentation. *Geological Society of America Bulletin*, 97, 444–458.

Nix-Morris, W. M. (1996). *Biodeposition and organic carbon burial within an ancient prodeltaic environment of the Turonian Greenhorn Sea*. North Carolina State University. Thesis.

Nummedal, D., Hasan Sidi, F., & Posamentier, H. W. (2003). A Framework for Deltas in Southeast Asia. In, Sidi, F.H., Nummedal, D., Imbert, D., Darman, P., Posamentier, H.W. (Eds.), Tropical Deltas of Southeast Asia. *SEPM (Society for Sedimentary Geology)*, 76, 5-17.

Odin, G. S. (1988) (Ed.). Green Marine Clays: Oolitic Ironstone Facies, Verdine Facies, Glaucony Facies and Celadonite-Bearing Rock Facies-A Comparative Study. *Developments in Sedimentology,* Elsevier, 45, 445.

Ordoñez, M., Jiménez, N., & Suarez, J. (2006). *Micropaleontología Ecuatoriana* (Petroproducción).

Patruno, S., Hampson, G. J., Jackson, C., & Dreyer, T. (2015). Clinoform geometry, geomorphology, facies character and stratigraphic architecture of a sand-rich subaqueous delta: Jurassic Sognefjord Formation, offshore Norway. *Sedimentology*, 62, 350–388.

Patruno, S., & Helland-Hansen, W. (2018). Clinoforms and clinoform systems: Review and dynamic classification scheme for shorelines, subaqueous deltas, shelf edges and continental margins. *Earth-Science Reviews,* 185, 202–233.

Pearson, N. J., Mángano, M. G., & Buatois, L. A. (2013). Environmental variability of *Macaronichnus* ichnofabrics in Eocene tidal-embayment deposits of southern Patagonia, Argentina. *Lethaia*, 46, 341–354.

Pearson, T. H., & Rosenberg, R. (1978). Macrobenthic succession in relation to organic enrichment and pollution of the marine environment. *Oceanogr. Mar. Biol. Ann. Rev*, 16, 229–311.

Pemberton, S. G. (Ed.). (1992). *Applications of Ichnology to Petroleum Exploration*. SEPM (Society for Sedimentary Geology), 17.

Pemberton, S. G., Flach, P. D., & Mossop, G. D. (1982). Trace Fossils from the Athabasca Oil Sands, Alberta, Canada. *Science*, 217, 825–827.

Pemberton, S. G., & Frey, R. W. (1982). Trace Fossil Nomenclature and the *Planolites-Palaeophycus* Dilemma. *Journal of Paleontology*, 56, 843-881.

Pemberton, S. G., & Jones, B. (1988). Ichnology of the Pleistocene Ironshore Formation, Grand Cayman Island, British West Indies. *Journal of Paleontology*, 62, 495–505.

Pemberton, S. G., MacEachern, J. A., & Dashtgard, S. E. (2012). Shorefaces. In Knaust, D., Bromley, R.G. (Eds.), Trace Fossils as Indicators of Sedimentary Environments. *Developments in Sedimentology*, 64, 563–604.

Pemberton, S. G., Spila, M., Pulham, A. J., Saunders, T., MacEachern, J. A., Robbins, D., & Sinclair, I. K. (2001). Ichnology & sedimentology of shallow to marginal marine systems. *Geol. Assoc. Can., Short Course*, 15, 343.

Pemberton, S. G., & Winghtman, D. M. (1992). Ichnological characteristics of brackish water deposits. In Pemberton, S.G. (Ed.), Application of Ichnology to Petroleum Geology, A core workshop. *SEPM Core Workshop*, 17, 141–167.

Peng, Y., Steel, R. J., & Olariu, C. (2018). Amazon fluid mud impact on tide- and wave-dominated Pliocene lobes of the Orinoco Delta. *Marine Geology*, 406, 57–71.

Perkins, E. J. (1975). The biology of estuaries and coastal waters. *Limnology and Oceanography*, *20*, 684–685.

Pollard, J. E., Goldring, R., & Buck, S. G. (1993). Ichnofabrics containing *Ophiomorpha*: Significance in shallow-water facies interpretation. *Journal of the Geological Society*, 150, 149–164.

Posamentier, H., Allen, D., & Tesson, M. (1992). Forced regressions in a sequence stratigraphic framework: Concepts, examples, and exploration significance. *AAPG Bulletin*, 76, 1687–1709.

Posamentier, H., & Vail, P. R. (Eds.). (1988). Eustatic Controls on Clastic Deposition II-Sequence and Systems Tract Models. In Wilgus, C.K., Hastings, B.S., Kendall, C.G, Posamentier, H.W.,

Ross, C.A., Van Wagoner, J.C. (Eds.), Sea Level Changes: An Integrated Approach. *SEPM (Society for Sedimentary Geology) Special Publication*, 42, 125-154.

Postma, D. (1982). Pyrite and siderite formation in brackish and freshwater swamp sediments. *American Journal of Science*, 282, 1151–1183.

Potter, P. E., Maynard, J. B., & Depetris, P. J. (2005). *Mud and mudstones: Introduction and overview*. Berlin: Springer Science & Business Media.

Prantl, F. (1945). Two new problematic trails from the Ordovician of Bohemia. *Academie Tcheque Des Sciences. Bulleting International, Classe des Sciences Mathematiques et Naturelles et de la Mèdecine,* 46, 49-59.

Raharimahefa, T., & Kusky, T. M. (2010). Environmental monitoring of Bombetoka bay and the Betsiboka estuary, Madagascar, using multi-temporal satellite data. *Journal of Earth Science*, 21, 210–226.

Ranger, M. J. & Pemberton, S. G., (1992). The Sedimentology and Ichnology of Estuarine Point Bars in the McMurray Formation of the Athabasca Oil Sands Deposit, North-Eastern Alberta, Canada. In Pemberton, S.G. (Ed.), Applications of Ichnology to Petroleum Exploration: A Core Workshop, *SEPM (Society for Sedimentary Geology)*, 17, *401-421*.

Raynaud, J. F., Bouroullec, J., Homewood, P., & Villanova, M. (1993). Equateur, Basin de l'Oriente: Etude palynologique d'un intervalle Crétacé supérieur sur 20 puits. Etude sédimentologique des grés M-1. *Informe Inédito*, 99.

Reineck, H. E. (1958). Wühlbau-Gefüge in Abhängigkeit von sediment-umlagerungen. *Senckenbergiana Lethaea*, 39, 1–14.

Reineck, H. E. (1967). Layered sediments of tidal flats, beaches, and shelf bottoms of the North Sea. In Lauff, G.H (Ed.), Estuaries, *American Association for the Advancement of Science Special Publication*, 83, 191-206.

Reineck, H., & Wunderlich, F. (1968). Classification and Origin of Flaser and Lenticular Bedding. *Sedimentology*, 11, 99–104.

Roberts, H. H., & Sydow, J. (2003). Late Quaternary stratigraphy and sedimentology of the offshore Mahakam delta, east Kalimantan (Indonesia). In Sidi, H., and Nummedal, D. (Eds.), Tropical deltas of the Southeast Asia, Sedimentology, stratigraphy, and petroleum geology: *SEPM Special Publication*, 76, 125-145.

Roddaz, M., Hermoza, W., Mora, A., Baby, P., Parra, M., Christophoul, F., Brusset, S., & Espurt, N. (2010). Cenozoic sedimentary evolution of the Amazonian foreland basin system. In Hoorn, C., and Wesselingh, F.P. (Eds.), Amazonia, Landscape and Species Evolution: A Look into the Past, *Wiley-Blackwell, UK*, 61–88.

Romeuf, N., Aguirre, L., Soler, P., Feraud, G., Jaillard, E., & Ruffet, G. (1995). Middle Jurassic volcanism in the northern and central Andes. *Andean Geology*, 22, 245–259.

Rosero, J. (1997). Estructuras y etapas de deformación de la Zona Subandina en el Nororiente Ecuatoriano (entre 0°10'S y 0°50'S). *Master's Thesis, Escuela Politécnica Nacional*, 88.

Ruiz, G. M., Seward, D., & Winkler, W. (2007). Evolution of the Amazon Basin in Ecuador with special reference to hinterland tectonics: Data from zircon fission-track and heavy mineral analysis. *Developments in Sedimentology*, 58, 907–934.

Salahuddin, & Lambiase, J. J. (2013). Sediment Dynamics and Depositional Systems of the Mahakam Delta, Indonesia: Ongoing Delta Abandonment on A Tide-Dominated Coast. *Journal of Sedimentary Research*, 83, 503–521.

Sassi, M. G., Hoitink, A. J. F., de Brye, B., Vermeulen, B., & Deleersnijder, E. (2011). Tidal impact on the division of river discharge over distributary channels in the Mahakam Delta. *Ocean Dynamics*, 61, 2211–2228.

Savrda, C. E. (1995). Ichnologic applications in paleoceanographic, paleoclimatic, and sea-level studies. *Palaios*, 10, 565–577.

Schlirf, M. (2011). A new classification concept for U-shaped spreite trace fossils. *Neues Jahrbuch für Geologie and Paläontologie Abhandlungen*, 260, 33–54.

Schlirf, M., & Uchman, A. (2005). Revision of the ichnogenus *Sabellarifex* Richter, 1921 and its relationship to *Skolithos* Haldeman, 1840 and *Polykladichnus* Fürsich, 1981. *Journal of Systematic Palaeontology*, 3, 115–131.

Seilacher, A. (1955). Spuren und Fazies im Unterkambrium: Akademie der Wissenschaften und der Literatur zur Mainz. *Mathematisch-Naturwissenschaftliche Klasse, Abhandlungen*, 10, 373–399.

Shchepetkina, A., Gingras, M. K., Mángano, M. G., & Buatois, L. A. (2019). Fluvio-tidal transition zone: Terminology, sedimentological and ichnological characteristics, and significance. *Earth-Science Reviews*, 192, 214–235.

Shepherd, M. (2009). Oil Field Production Geology. Memoir 91. *The American Association of Petroleum Geologists*, 359.

Solórzano, E. J., Buatois, L. A., Rodríguez, W. J., & Mángano, M. G. (2017). From freshwater to fully marine: Exploring animal-substrate interactions along a salinity gradient (Miocene Oficina Formation of Venezuela). *Palaeogeography, Palaeoclimatology, Palaeoecology*, *482*, 30–47.

Soyinka, O. A., & Slatt, R. M. (2008). Identification and micro-stratigraphy of hyperpycnites and turbidites in Cretaceous Lewis Shale, Wyoming: Hyperpycnites and turbidites. *Sedimentology*, 55, 1117–1133.

Spikings, R., Cochrane, R., Villagomez, D., Van der Lelij, R., Vallejo, C., Winkler, W., & Beate, B. (2015). The geological history of northwestern South America: From Pangaea to the early collision of the Caribbean Large Igneous Province (290–75 Ma). *Gondwana Research*, 27, 95–139.

Stanistreet, I. G., Le Blanc Smith, G., & Cadle, A. B. (1980). Trace fossils as sedimentological and paleoenvironmental indices in the Ecca Group (Lower Permian) of the Transvaal. *Transactions of the Geological Society of South Africa*, 83, 333–344.

Stanton, R. J., & Dodd, J. R. (1984). *Teichichnus pescaderoensis*—New ichnospecies in the Neogene shelf and slope sediments, California. *Facies*, 11, 219–227.

Steel, R. J., Carvajal, C., Petter, A., & Uroza, C. (2008). Shelf and Shelf-Margin Growth in Scenarion of Rising and Falling Sea Level. In Hampson, G.J., Steel, R.J., Burgess, P.M., and Dalrymple, R.W. (Eds.), Recent Advances in Models of Siliciclastic Shallow-Marine Stratigraphy. *SEPM (Society for Sedimentary Geology*), 90, 47-71.

Swinbanks, D. D., & Luternauer, J. L. (1987). Burrow distribution of thalassinidean shrimp on a Fraser Delta tidal flat, British Columbia. *Journal of Paleontology*, 61, 315–332.

Taylor, A. M., & Goldring, R. (1993). Description and analysis of bioturbation and ichnofabric. *Journal of the Geological Society*, 150, 141–148.

Tchoumatchenco, P., & Uchman, A. (2001). The oldest deep-sea *Ophiomorpha* and *Scolicia* and associated trace fossils from the Upper Jurassic–Lower Cretaceous deep-water turbidite deposits of SW Bulgaria. *Palaeogeography, Palaeoclimatology, Palaeoecology*, 169, 85–99.

Tonkin, N. S. (2012). Deltas. In Knaust, D., Bromley, R.G. (Eds.), Trace Fossils as Indicators of Sedimentary Environments., *Developments in Sedimentology*, 64, 507–528.

Tschopp, H. (1953). Oil Explorations in the Oriente of Ecuador. *Bulletin of the American Association of Petroleum Geologists*, 37, 45.

Uchman, A., & Wetzel, A. (2012). Deep-sea fans. In Knaust, D., Bromley, R.G. (Eds.) Trace fossils as indicators of sedimentary environments. *Developments in Sedimentology*, 64, 643–671.

Vallejo, C., Hochuli, P. A., Winkler, W., & Von Salis, K. (2002). Palynological and Sequence Stratigraphic Analysis of the Napo Group in the Pungarayacu 30 well, Sub-Andean Zone, Ecuador. *Cretaceous Research*, 23, 845–859.

Vallejo, C., Spikings, R., Luzieux, L., Winkler, W., Chew, D., & Page, L. (2006). The early interaction between the Caribbean Plateau and the NW South American Plate. *Terra Nova*, 18, 264–269.

Vallejo, C., Tapia, D., Gaibor, J., Steel, R., Cardenas, M., Winkler, W., Valdez, A., Esteban, J., Figuera, M., Leal, J., & Cuenca, D. (2017). Geology of the Campanian M1 Sandstone Oil Reservoir of Eastern Ecuador: A Delta System Sourced from the Amazon Craton. *Marine and Petroleum Geology*, 86, 1207–1223.

Vossler, S. M., & Pemberton, S. G. (1988). *Skolithos* in the Upper Cretaceous Cardium Formation: An ichnofossil example of opportunistic ecology. *Lethaia*, 21, 351–362.

Walker, R. G., & James, N. P. (eds.). (1992). Facies models: Response to sea level change (8. print), *Geological Association of Canada,* 407.

Wetzel, A. (1984). Bioturbation in deep-sea fine-grained sediments: Influence of sediment texture, turbidite frequency and rates of environmental change. In Stow, D.A.V., and Piper, D.J.W. (Eds.), Fine-grained sediments: processes and facies, *Geological Society, London, Special Publications,* 15, 595–608.

White, H. J., Skopec, R. A., Ramirez, F. A., Rodas, J. A., & Bonilla, G. (1995). Reservoir Characterization of the Hollin and Napo Formations, Western Oriente Basin, Ecuador. In Tankard, A.J., Suárez. S. R., and Welsink, H.J. (Eds.), Petroleum basins of South America: *AAPG Memoir,* 62, 573-596.

Wignall, P. B. (1991). Dysaerobic trace fossils and ichnofabric in the Upper Jurassic Kimmeridge Clay of southern England. *Palaios*, 6, 264–270.

Wolaver, B. D., Coogan, J. C., Horton, B. K., Bermudez, L., Sun, A. Y., Wawrzyniec, T. F., Zhang, T., Shanahan, T. M., Dunlap, D. B., & Costley, R. A. (2015). Structural and hydrogeologic evolution of the Putumayo basin and adjacent fold-thrust belt, Colombia. *AAPG Bulletin*, 99, 1893–1927.

Zaitlin, B. A. (1994). The Stratigraphic Organization of Incised-Valley Systems Associated with Relative Sea-Level Change. In Dalrymple, R.W., & Boyd, R. (Eds.), Incised-Valley Systems: Origin and Sedimentary Sequences. *SEPM Society for Sedimentary Geology*, 45-60.

Zavala, C., Arcuri, M., Di-Meglio, M., Diaz, H., & Contreras, C. (2011). A Genetic Facies Tract for the Analysis of Sustained Hyperpycnal Flow Deposits. In Slatt, R.M., Zavala, C. (Eds.), Sediment Transfer from Shelf to Deep Water: Revisiting the Delivery System, *American Association of Petroleum Geologists,* Studies in Geology 61, 31–51.

Zavala, C., & Pan, S. (2018). Hyperpycnal flows and hyperpycnites： Origin and distinctive characteristics. *Lithologic Reservoirs,* 30, 27.

Zavala, Carlos, Ponce, J. J., Arcuri, M., Drittanti, D., Freije, H., & Asensio, M. (2006). Ancient lacustrine hyperpycnites: A depositional model from a case study in the Rayoso Formation (Cretaceous) of west-central Argentina. *Journal of Sedimentary Research*, 76, 41–59.

Zonneveld, J. P., Bartels, W. S., & Clyde, W. C. (2003). Stratal Architecture of an Early Eocene Fluvial-Lacustrine Depositional System, Little Muddy Creek Area, Southwestern Green River Basin, Wyoming. In Raynolds, R.G., Flores, R.M. (Eds.) Cenozoic systems of the Rocky Mountain region: Rocky Mountain Section, *SEPM (Society for Sedimentary Geology)*, 253-287.